

## Investigating the impact of protein products on the gut microbiome using the SIFR® technology

#### Administrative details

Our reference: 0443/P0140

Date of report: 12-Aug-24

Project Manager: Lien Van den Bossche

Scientists: Jonas Poppe, Lam Dai Vu, Pieter

Van den Abbeele

Contract and invoicing: Ingmar van Hengel

Chris Chen

**Angel Yeast** 

Cheng Dong Avenue 168

443003 Yichang

China

#### Key conclusions of the study

The aim was to assess the impact of three non-animal protein products (yeast protein (YP), whey protein isolate (WPI) and soy protein isolate (SPI)) on the gut microbiota of 50-65y male adults. The high throughput of the ex vivo SIFR® technology allowed including 6 subjects in the design. These subjects covered the spectrum of interpersonal differences in microbial composition that occurs in vivo, in line with the concept of enterotypes, thus ensuring representative findings.

Combined community modulation score (CMS) First, all products strongly increased production of health-related SCFA acetate, propionate, butyrate, valerate (thus, total SCFA), as well as isobutyrate, isovalerate (thus, total bCFA). This was in line with the observation that all products (especially SPI/YP) promoted microbial diversity (according to the community modulation score (CMS)).

While various gut microbes were similarly boosted by all products, different product-specific effects on microbial composition were uncovered, thus explaining product-specific effects on SCFA production:

100-Increased microbial diversity

YP.

Our reference: 0443/P0140

- Acetate/propionate-producing Bacteroidaceae members:
  - WPI/SPI > YP → highest acetate/propionate for WPI/SPI
  - All products promoted following **Bacteroidaceae** species, yet remarkable product-specific effects were noted:
    - SPI → Bacteroides uniformis 🗠
    - WPI → Phocaeicola vulgatus/massili<u>ensi</u>s
    - $YP \rightarrow Bacteroides thetaiotaomicron$

All products also promoted Parabacteroides (succinate producers) and Acidaminococcaceae spp.

Bifidogenic effects (= stimulation of health-related Bifidobacterium adolescentis): SPI > YP/WPI → highest acetate and butyrate (via cross-feeding) for SPI

(succinate-converting, propionate producers), contributing to propionate increases for all products.

Stimulation of different **butyrate** producers belonging to the **Bacillota\_A** phylum:

Cryptobiotix SA VAT BE 0762.565.104 Technologiepark-Zwijnaarde 82, 9052 Ghent, Belgium



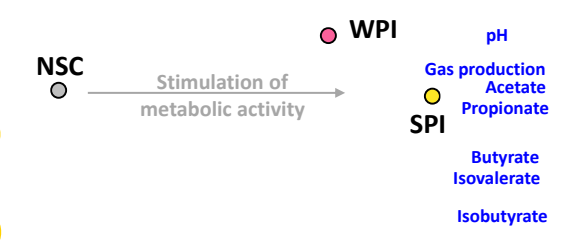
- Key butyrogenic species stimulated by SPI: Fuecalibacterium and Agathobaculum spp. → highest butyrate for SPI
- Compared to WPI, YP generally displayed stronger stimulation of most butyrate producers
   → higher butyrate production for YP > WPI
- YP most strongly stimulated the versatile SCFA producing Anaerotignum faecicola

In summary, at the same dose of 40 g/L:

- <u>SPI</u> most strongly enhanced acetate, propionate, butyrate
- WPI: more acetate, propionate compared to YP
- <u>YP</u>: more butyrate, valerate, isobutyrate, isovalerate compared to <u>WPI</u>

Interestingly, YP resulted in significantly less gas production (even when normalized per mol of SCFA produced) 

potentially higher tolerability of YP.



**Key fermentation parameters** 

O YP

Next, metabolomics analysis revealed additional metabolites promoted by the protein products (well beyond SCFA), including several metabolites that have previously been linked with anti-inflammatory effects or improvement of gut barrier function, such as extracted amino acids, aromatic lactic acids, indole-3-propionic acid, 2-hydroxyisocaproic acid, acetylated polyamines among others.

Finally, host-microbiota interaction assays demonstrated that the production of health-related metabolites by specific microbes translated in beneficial effects on host cells for all test products:

- Enhanced gut barrier integrity for all products
   (especially YP), both under non-stressed (no LPS) and
   stressed (+ LPS) conditions
- Anti-inflammatory effects: increased antiinflammatory cytokine IL-10 and decreased proinflammatory markers (IL-1β, TNF-α, CXCL10)

Pro-inflammatory **IL-8** was significantly increased **only by WPI** 

→ Overall, these effects resulted in a positive antiinflammatory index (higher for SPI/YP > WPI). Importantly, a positive correlation was established

TEER (30h)

Anti-inflammatory index

Anti-infl

Gut barrier integrity (TEER) and anti-inflammatory index

between SCFA production and enhanced gut barrier function/anti-inflammatory activity, suggesting the importance of SCFA in health promoting effects.

In summary, colonic fermentation of the protein products resulted in pronounced changes in microbial composition that correlated with increased production of SCFA and led to stimulation of additional health-related metabolites. This stimulated production of health-related metabolites likely explains the observed enhanced gut barrier function as well as anti-inflammatory effects. In addition, the protein products also displayed a positive impact on microbial diversity. Altogether, the findings in the study suggested a series of potential health benefits for the host upon supplementation with the protein products.



## Contents

1	Intro	duction
	1.1	Ex vivo gastrointestinal simulation – SIFR® technology
	1.2	Scientific evidence for the SIFR® technology
	1.2.1	Biorelevance in the SIFR®: technology
	1.2.2	Biorelevance in the SIFR®: biology
	1.2.3	In vivo validation of SCFA production predicted by SIFR®
	1.2.4	In vivo validation of compositional shifts predicted by SIFR®
	1.2.5	Applications of the SIFR® technology
	1.2.6	Importance of biorelevance for metabolomics analysis
	1.2.7	Error aversion and high reproducibility of SIFR® technology
2	Rese	arch aim
3	Mate	rials and methods
	3.1	Test products
	3.2	Experimental design SIFR® incubations
	3.2.1	Oral, gastric and small intestinal simulation
	3.2.2	SIFR® colonic incubations
	3.3	Key fermentation parameters
	3.4	Metagenomics
	3.5	Metabolomics
	3.6	Gut barrier and immune modulation
	3.7	Data analysis
4	Resu	ts – Key fermentation parameters
	4.1	Quality Control
	4.2	High-level observations
	4.3	In-depth analysis of treatment effects
	4.4	Predicted <i>in vivo</i> SCFA production
5	Resu	lts – Microbial composition1
	5.1	Donor characterization (0h)
	5.2	Quality control: SIFR® technology = an accurate <i>ex vivo</i> gut microbiome testing platform 18
	5.3	Cell density and α-diversity



	5.4	Exploratory data analysis	21				
	5.5	In-depth analysis of treatment effects	22				
6	Meta	abolomics	30				
	6.1	Quality control	30				
	6.2	In-depth analysis of treatment effects	30				
7	Resu	ts – Host-microbe interactions					
	7.1	Gut barrier integrity					
	7.2	Immune modulation	47				
8	Discu	ussion and conclusions	51				
9	Refe	erences	54				
1(	О Арре	endix	64				
	10.1	Supplementary files	64				
	10.2	New diversity score: community modulation score (CMS)	65				
10.2.1		.1 Diversity indices: problem statement	65				
	10.2.	.2 CMS: towards more accurate diversity estimations	66				
	10.3	Supplementary Tables	67				
	10.4	Supplementary Figures	70				



#### 1 Introduction

#### **1.1** Ex vivo gastrointestinal simulation – SIFR® technology

Traditional microbiological research struggles reconciling biorelevance with the increasing need for throughput. The latter is critical for statistically robust study designs and comparative analysis of products and product combinations. Moreover, due to the increasing awareness of interpersonal differences in gut microbiota composition<sup>1</sup> and how this impacts the response to interventions<sup>2</sup>, addressing interindividual differences among human subjects is a prerequisite to ensure representative outcomes. Cryptobiotix was founded with the aim to push the boundaries of preclinical gastrointestinal research on both throughput and biorelevance, shifting the current paradigm from limited data generation with labour-intensive, complex models, towards extensive data generation with high-throughput and more biorelevant models. With this novel approach, Cryptobiotix aims to accelerate product development cycles by implementing its proprietary SIFR® ("cipher") technology. SIFR® stands for Systemic Intestinal Fermentation Research. The technology addresses operational and analytical bottlenecks to increase experimental throughput, while continuously ameliorating biorelevance (elaborated in section 1.2).

The versatility and biorelevance of the SIFR® makes it an ideal tool for both the early (screening) and late (in-depth) preclinical R&D during product characterisation and development. The SIFR® can be implemented to simulate a wide range of host organisms (human and animal) and conditions (age groups, well vs unwell, IBD, pathogen infections...) according to published state-of-the-art protocols and is compatible with virtually all kind of actives, from naked actives, API and food components like antibodies, pre-/pro- or synbiotics, to formulated products and whole food.

#### 1.2 Scientific evidence for the SIFR® technology

#### **1.2.1** Biorelevance in the SIFR®: technology

A first key aspect of the SIFR® technology is that it involves the **use of sets of small individual bioreactors** that are handled in a **custom-built processing device** allowing for temperature control as well as headspace control and monitoring. The realised **increase in throughput** allows the SIFR® technology to **overcome limitations of popular microtiter plate (MTP) approaches** to high throughput. The advantages are numerous:

- Gas measurement: individually sealed bioreactors retaining gases in headspace allow for observation of effects of produced gases as well as measurement of gas production
  - $\leftrightarrow$  gases produced in MTP typically evaporate through the seal.
- Absence of cross-contamination: each bioreactor is sterilised and processed individually, so no contamination across reactors can occur.

 $\Leftrightarrow$  elevated risk of contamination across wells in MTP approaches due to processing in non-sterile, anaerobic chamber, close proximity of neighbouring wells, contamination risk via seal, ...

- <u>Suitable sampling capacity</u>: millilitre-to-centilitre-range bioreactor volumes generate more than enough samples for both fundamental and advanced analyses
  - $\label{eq:microliter-to-millilitre-range} \ \textit{well bioreactors in MTP limit the scope of downstream analyses}$



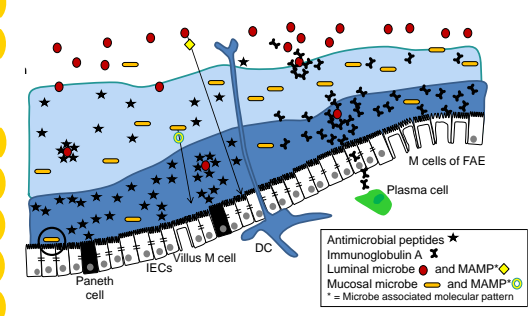
#### 1.2.2 Biorelevance in the SIFR®: biology

A key focus of Cryptobiotix has been to implement procedures that minimise the bias in microbiota composition between the *in vivo*-derived microbiota and the one colonising the bioreactors during SIFR® studies. Optimisations were guided by metrics that quantify such *in vitro* bias and involved an interplay of (i) <u>inoculum</u> preparation, (ii) <u>anaerobicity</u>, (iii) <u>medium composition</u> and (iv) <u>pH control</u>. Specific protocols have been developed for human adults, infants and several animal species (poultry and swine). A generic protocol is used for simulation of other host species (e.g., cats and dogs).

Overall, as recently published for human adults<sup>3</sup>, the minimal bias in microbiota composition during SIFR® studies is in contrast to consistent *in vitro* biases that have been observed for <u>traditional long-term in vitro models</u> (5 days – several weeks)<sup>4–6</sup>. Such bias is even more pronounced in the <u>recently developed short-term models</u><sup>7–10</sup>, where a limited amount of taxa (often belonging to *Proteobacteria*, *Enterococcaceae*, *Streptococcaceae* and/or *Veillonellaceae*) almost exclusively dominate the *in vitro* 

microbiota within 1 day upon initiation of the tests. In contrast, the SIFR® studies adhere more to *ex vivo* than *in vitro* principles.

A final aspect increasing the biorelevance of the SIFR® technology is that, when relevant for a given research question, a mucosal microbiota can be simulated in the bioreactors to provide an increased granularity on the interplay of actives with both luminal and mucosal microbial niches <sup>3</sup>.



#### 1.2.3 In vivo validation of SCFA production predicted by SIFR®

A key function of the gut microbiome consists in the fermentation of carbohydrates in the colon, resulting in the production of short-chain fatty acids (SCFA)<sup>11</sup>, mainly including acetate, propionate and butyrate, each related with particular health benefits<sup>12–15</sup>. As a result, the predictivity of the SIFR® technology in terms of SCFA production was assessed against high-quality *in vivo* data of SCFA production upon intake of the reference prebiotic inulin<sup>16</sup>. It followed that the predicted SCFA production by the SIFR® technology corresponds well to the actual *in vivo* SCFA production, particularly in terms of the total SCFA (Figure 1).

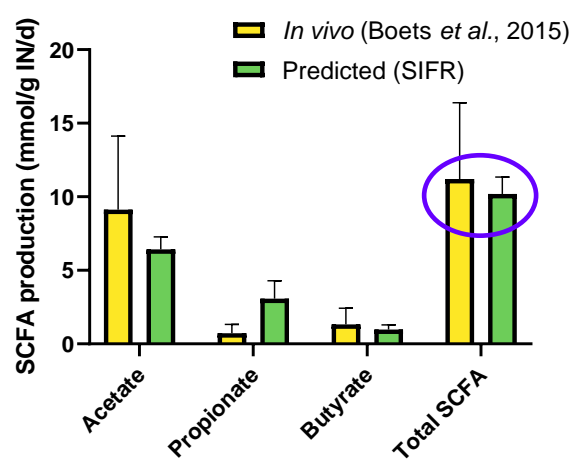


Figure 1. Predicted (SIFR® technology) and in vivo SCFA production (Boets et al., 2015<sup>16</sup>) (mmol/g inulin/day).



#### 1.2.4 In vivo validation of compositional shifts predicted by SIFR®

As recently published<sup>3</sup>, the SIFR technology has been validated by studying the **impact of three structurally different carbohydrates** (inulin, 2'fucosyl-lactose and resistant dextrin) for which clinical data is available<sup>17–20</sup>. Interestingly, it followed that **changes observed in the SIFR® technology within 24-48h** corresponded with *in vivo* **observations upon repeated daily intake** of the aforementioned carbohydrates **over weeks** (2-6 weeks), down to species level (shallow-shotgun sequencing). *l.e.* **resistant dextrin** specifically increased *Parabacteroides distasonis*<sup>20</sup>, **2'FL** specifically increased *Bifidobacterium adolescentis* and *Anaerobutyricum hallii*<sup>18,19</sup>, while **inulin** increased *Bifidobacteriaceae*<sup>17</sup>. These validation studies also demonstrated that, unlike working with a single or pooled inoculum (n = 6), including 6 different donors (n = 1) provided **representative insights** that support **mode-of-action**, via the strong correlations between metabolic and compositional datasets<sup>3</sup>.

#### 1.2.5 Applications of the SIFR® technology

Besides being validated to provide **predictive insights** for clinical findings **upon long-term prebiotic intake**<sup>3</sup>, other applications of the SIFR® technology are related to, amongst others, (i) the **development of synbiotics to boost butyrate** production<sup>21</sup>, (ii) scoping of **prebiotic potential of serum-derived immunoglobulins**<sup>22</sup>, (iii) development of **age-specific functional ingredients**<sup>23</sup>, (iv) investigation of the **specificity by which prebiotics** impact the gut microbiota<sup>24</sup>, or (v) effects of **probiotics** when supplied to a **small intestinal microbiota**<sup>25</sup>.

#### 1.2.6 Importance of biorelevance for metabolomics analysis

As mentioned above, a key focus of Cryptobiotix has been to minimise the bias in microbiota composition between *in vivo*-derived microbiota and the one colonising the bioreactors during SIFR® studies. While this is already important when investigating the impact on microbial composition, this is even of greater importance when performing metabolomics studies given that altered ratios among species greatly impact the metabolic output. As an example, during a recent study<sup>26</sup>, upon its introduction in a traditional *in vitro* gut model for breast-fed infants, a major increase of *Veillonellaceae* was observed upon cultivation over several weeks (> 80%). This contrasts with the *in vivo* microbiota of breast-fed infants that contains <1% *Veillonellaceae* and >98% *Bifidobacteriaceae*. As a result, metabolite production in such models was not mainly acetate/lactate (produced by *Bifidobacteriaceae*) but rather acetate/propionate (metabolites of *Veillonellaceae*)<sup>26</sup>. By avoiding bias in microbial composition, the SIFR® technology allows for more representative observations.

#### 1.2.7 Error aversion and high reproducibility of SIFR® technology

A final strength of the SIFR® technology comes from standardisation and automation. Whereas traditional preclinical models rely on complex and intensive manual work that contribute to variations in the output, the SIFR® technology relies on automation and identical processing of bioreactors to minimise the error rate and maximise the **technical reproducibility across replicates.** The variability observed on key fermentation parameters (pH, gas production, SCFA levels) is typically around 1-3%, demonstrating that the entire pipeline from SIFR® implementation to sample to result is highly robust. Consequently, the SIFR® technology is a very sensitive platform to scope for potential treatment effects on the gut microbiota, even if minimal.



#### 2 Research aim

The research objective of the study was to characterise the impact of **three non-animal protein products** (yeast protein, whey protein isolate and soy protein isolate) on the gut microbiota of **50-65y male human adults**. Using the *ex vivo* SIFR® technology, the impact of the test products **on metabolite production** (key fermentation parameters (pH, gas, SCFA, bCFA) and metabolomics) and **microbial composition** (quantitative shallow-shotgun sequencing) of the gut microbiota of **6 different test subjects** was assessed along with the subsequent **impact on the host** (host-microbiota interaction assay).

#### 3 Materials and methods

#### 3.1 Test products

Three protein products, i.e., yeast protein (YP), whey protein isolate (WPI), soy protein isolate (SPI), were tested against were tested at 40 g/L (Table 1). The products were tested against a no-substrate control (NSC).

Table 1. Study arms, test products, respective test doses along with abbreviations that were used to refer to the study arms along the report.

#	Study arm/test product	Dose [g/L]	Terminology
1 Blank (No Substrate Control)		N/A	NSC
2	2 Yeast protein		YP
3	Whey protein isolate	40	WPI
4	Soy protein isolate	40	SPI

#### 3.2 Experimental design SIFR® incubations

#### 3.2.1 Oral, gastric and small intestinal simulation

A simulation of the oral phase and upper gastrointestinal tract was performed according to the INFOGEST 2.0 consensus method, published in Nature Protocols by Brodkorb *et al.* <sup>27</sup>. It elaborates on the condensed knowledge of numerous world experts, upgrading the digestion method published in 2014 by Minekus *et al.* <sup>28</sup>. Among improvements, a first one of particular interest is the **use of more biorelevant enzymes** such as human salivary amylase (essential for starch digestion) and rabbit gastric lipase (superior *versus* microbial-derived lipases due to the correct specificity and pH activity – essential for fat digestion). Given their high cost and required concentrations, these enzymes are however often not applied in conventional, more voluminous *in vitro* models. A second improvement pertains to the implementation of a **quality control on the secretions added**. To ensure that **results obtained during the current project performed by Cryptobiotix are in line with protocol of Brodkorb** *et al.* **<sup>27</sup> (with demonstrated** *in vivo-in vitro* **correlation), Cryptobiotix applied <b>six enzyme assays** (amylase, pepsin activity, lipase, trypsin, chymotrypsin) together with an assay to quantify **bile acids**. To render the aforementioned digestion method compatible with colonic fermentation experiments, **Cryptobiotix additionally implemented (i) the removal of oxygen** along the small intestinal incubation and (ii) a **simulation of the small intestinal absorption** via the use of dialysis membranes.



#### 3.2.2 SIFR® colonic incubations

An *ex vivo* SIFR® study was performed, simulating the colonic fermentation of test products by the gut microbiota derived from healthy, male human adults  $(n = 6)^1$ . The simulation parameters were as follows (Figure 2):

- Study arms = 4:
  - No substrate control (NSC) = background medium + microbiota (no product)
  - o Three test products
- Time points = 0h (only NSC), 24h

As a remark, the NSC at 24h was run in technical triplicate per donor to demonstrate the high reproducibility of the SIFR® technology.

#### Timeline and analyses (Figure 3):

- **Key fermentation parameters:** pH, gas production, SCFA (acetate, propionate, butyrate and valerate), bCFA (isobutyrate, isovalerate) at 0h (only NSC) and 24h (all test arms)
- Microbial composition analysis (shallow shotgun sequencing) at 0h (NSC), 24h (all test arms)
- Metabolomics (untargeted LC-MS/MS semi-polar analysis) at 0h (only NSC), 24h (all test arms)
- Host-microbiome interaction (Caco-2/THP-1 co-culture) at 24h for all study arms:
  - Transepithelial electrical resistance (TEER) analysis for gut permeability
  - $\circ$  Cytokine/chemokine measurement: (pro-/anti-)inflammatory targets IL-6, IL-8, IL-10, IL-1 $\beta$ , CXCL10 and TNF- $\alpha$  on the basolateral side
  - O NF-κβ measurement: total and phosphorylated

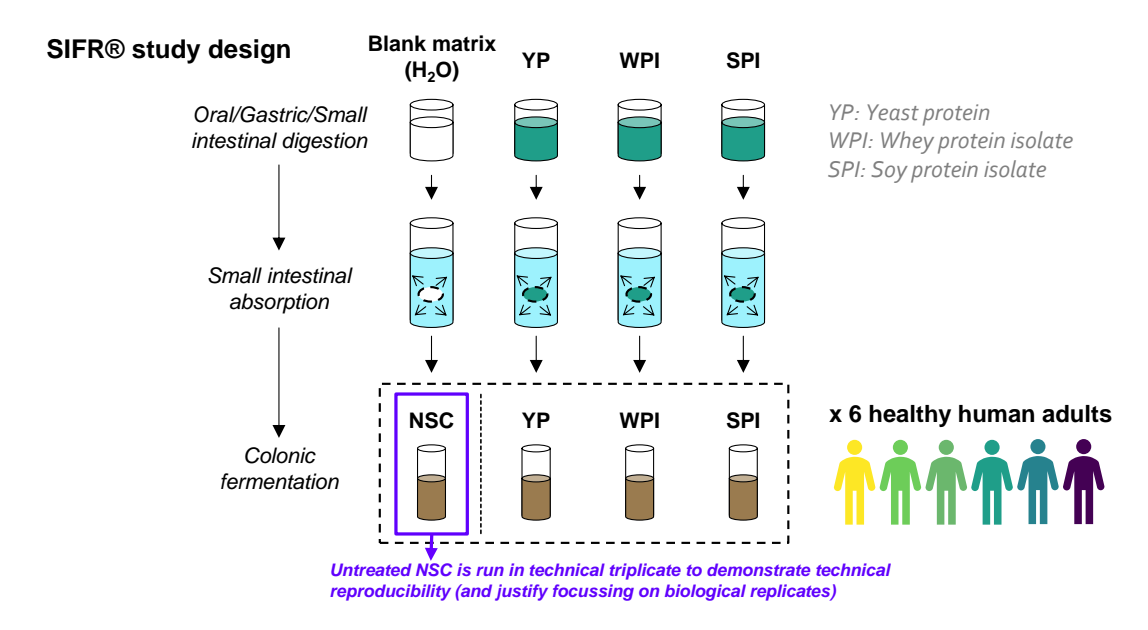


Figure 2. Schematic overview of the reactor design of the project during which the SIFR® technology was used to assess the impact on metabolite production and composition by the gut microbiota of 50-65y male human adults (n = 6) upon treatment with protein products.

-

<sup>&</sup>lt;sup>1</sup> Faecal samples were collected according to a procedure approved by Ethics Committee of the University Hospital Ghent (reference number BC-09977). The selection criteria for donors were as follows: male, age 50-65y, no antibiotic use in the past 3 months, no gastro-intestinal disorders (cancer, ulcers, IBD), no use of probiotic, non-smoking, alcohol consumption < 3 units/d and BMI < 30.



#### Timeline and analysis

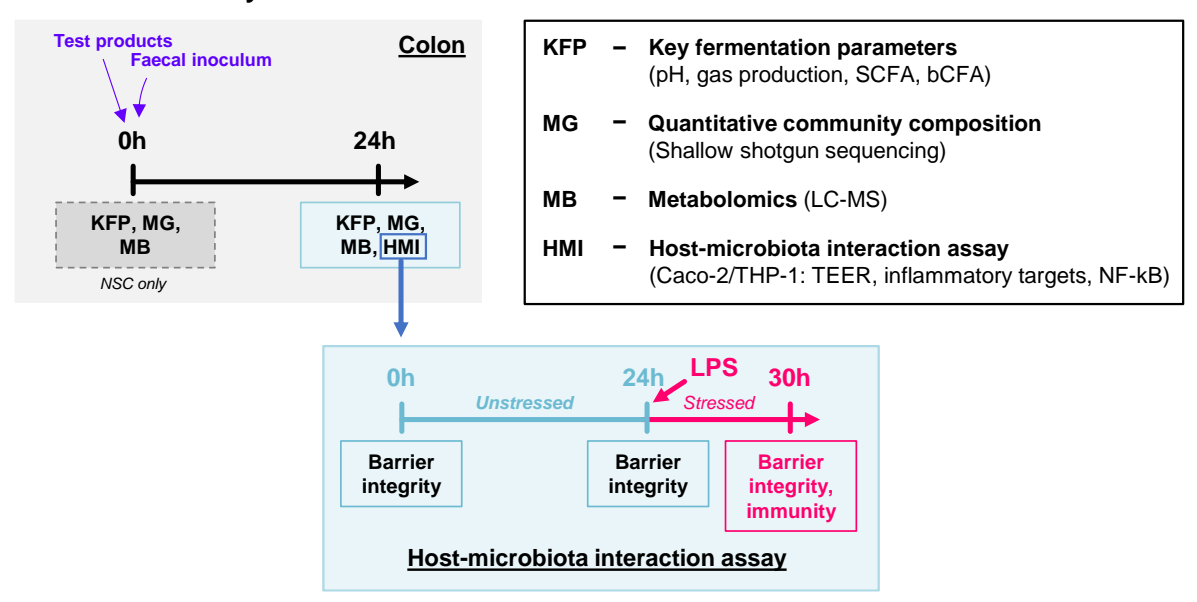


Figure 3. Schematic of the timeline and analyses of the project during which the SIFR® technology was used to assess the impact on metabolite production and composition by the gut microbiota of 50-65y male human adults (n = 6) upon treatment with protein products. The sub-panel (blue) indicates the timeline and the analysis of the host-microbiota interaction assay.

## 3.3 Key fermentation parameters

During the current study, acetate, propionate, butyrate (summed as total short-chain fatty acids (SCFA)), valerate, as well as isobutyrate, isovalerate (summed as total branched chain fatty acids (bCFA)) were determined via a GC-FID approach. Further, also pH and gas production were measured as key markers for microbial metabolic activity.

## 3.4 Metagenomics

Upon **DNA extraction**, standardized **Illumina library preparation** was performed followed by **3M total DNA sequencing**. Results were analysed at different **taxonomic levels** (species, family and phylum level). For taxonomic analysis, the proportional data derived from sequencing (%) were corrected for the total amount of cells present in each sample (detected via **flow cytometry**), allowing to obtain more representative insights in the impact of interventions on the gut microbiota<sup>29</sup>.

#### 3.5 Metabolomics

The **LC-MS** analysis was carried out using a Thermo Scientific Vanquish LC coupled to Thermo Q Exactive HF MS. An electrospray ionization interface was used as ionization source. Analysis was performed in negative and positive ionization mode. The UPLC was performed using a slightly modified version of the protocol described by Doneanu *et al.*<sup>30</sup>. Peak areas were extracted using Compound Discoverer 3.1 (Thermo Scientific). In addition to the automatic compound extraction by Compound Discoverer 3.1, a manual extraction of compounds included in an in-house library was performed using Skyline 21.1 (MacCoss Lab Software)<sup>31</sup>.

**Identification of compounds were performed at three levels;** Level 1: identification by retention times (compared against in-house authentic standards), accurate mass (with an accepted deviation of



3ppm), and MS/MS spectra, Level 2a: identification by retention times (compared against in-house authentic standards), accurate mass (with an accepted deviation of 3ppm). Level 2b: identification by accurate mass (with an accepted deviation of 3ppm), and MS/MS spectra. Level 3: identification by accurate mass alone (with an accepted deviation of 3ppm).

#### 3.6 Gut barrier and immune modulation

The timeline of the experiment is presented in Figure 3. Briefly, this involved appropriate differentiation periods for both Caco-2 (= epithelial cells) and THP1-cells (immune cells) after which the co-culture experiment was performed during which the *in vivo* gut wall was recreated by covering the THP-1 cells with the epithelial layer in a transwell system. The actual experiment consisted of (i) a 24h treatment period during which test products were applied on the apical side of the epithelial cells allowing to evaluate the impact on gut barrier integrity and (ii) a subsequent 6h LPS challenge of THP-1 cells at the basal side to evaluate the impact of the test products on immune functioning.

Caco-2 cell lines obtained from the ATCC were cultured in MEM media supplemented with 1X NEAA and 1mM Sodium Pyruvate with 10% FBS. 24-well trans-well inserts were coated with Collagen I Rat Tail Protein and 1 x  $10^5$  Caco-2 cells seeded onto the apical chambers. The basal chambers were filled with  $\mu$ l culture media and plates incubated in a 5% CO2 humidified incubator for **14 days**. During the differentiation process, media were changed every other day. The TEER was measured to ensure that only transwells with a TEER of more than  $300 \, \Omega$ .cm<sup>2</sup> were selected for the main experiment.

**THP-1 cells** were cultured in RPMI-1640 supplemented with 10% FBS, 1mM sodium pyruvate and 10 mM HEPES at 37°C with 5% CO2. Cultures were initially inoculated at a density of 3 x  $10^5$  cells/ml and split once density had reached 1 x  $10^6$  cells/ml. To differentiate THP-1 cells into macrophages, THP-1 cells were centrifuged and resuspended in cell culture medium containing 100 ng/ml PMA. The PMA-treated THP-1 cells were seeded (5 x  $10^5$  cells) on transwell-suitable 24-well plates and incubated at 37°C 5% CO2 to induce **differentiation**. After **48 hours**, Caco-2 bearing inserts were moved to the transwell-suitable 24-well plates containing the PMA differentiated THP-1 cells.

At the start of the **main experiment**, culture media in the apical chamber were replaced with samples derived from the SIFR® incubations, diluted in cell medium. Upon measuring **TEER**, plates were incubated for **24h** after which the **TEER** was again measured and 500 ng/ml of **LPS** was added to the basal chamber of the transwells containing the THP-1 cells. Upon a **6h LPS challenge** to boost cytokine/chemokine production, TEER was measured and samples from both apical and basal compartments were collected and subjected to cytokine/chemokine analysis using Multiplex Luminex® Assay kit on the MAGPix® analyser (IL-6, CXCL10, IL-10, IL-1β, TNF-α) or ELISA (IL-8).

#### 3.7 Data analysis

For **exploratory evaluation** of the obtained results, a series of **principle component analysis (PCA)** was performed. The two principal components with the largest eigenvalues were plotted.

For the statistical evaluation of the treatment effects on key fermentation parameters, cell counts, microbial diversity (4 indices) and microbial composition (phylum level), TEER and cytokines/chemokines across 6 different donors, a repeated measures ANOVA analysis was performed (~ based on paired t-testing, thus accounting for fact that values are compared between samples of a given donor). The statistical significance of the potential treatment effects was determined via Benjamini-Hochberg *post hoc* testing<sup>32</sup>. The latter involves that a correction for multiple comparisons



was implemented where p-values were adjusted by multiplying them with the total number of comparisons divided by the rank of each original p-value (across all p-values). In this specific case, 6 comparisons were considered (= 3 comparisons between NSC vs. 3 treatments), 3 cross-product comparisons) (Figure 4). In practice, this means that while the largest obtained p-value remained uncorrected (i.e., multiplied 1), the **lowest p-value was multiplied with 6**, thus strongly decreasing the chance of type 1 errors (i.e. false positives). In addition, the **resulting series of adjusted p-values** was rendered **non-decreasing** (i.e., when an adjusted p-value was higher than any of the subsequent adjusted p-values, its value was equalled to this lowest value). This generates a **false discovery rate threshold** allowing to **estimate** and **control the chance of type 1 errors** (i.e., false **positives**).

Statistical differences were visualized via:

- \*  $(0.1 < p_{adjusted} < 0.2)$ , \*\*  $(0.05 < p_{adjusted} < 0.1)$  or \*\*\*  $(p_{adjusted} < 0.05)$  for treatment vs NSC
- \$ (0.1 <  $p_{adjusted}$  < 0.2), \$\$ (0.05 <  $p_{adjusted}$  < 0.1) or \$\$\$ ( $p_{adjusted}$  < 0.05) for WPI/SPI vs YP
- & (0.1 < p<sub>adjusted</sub> < 0.2), && (0.05 < p<sub>adjusted</sub> < 0.1) or &&& (p<sub>adjusted</sub> < 0.05) for SPI vs WPI

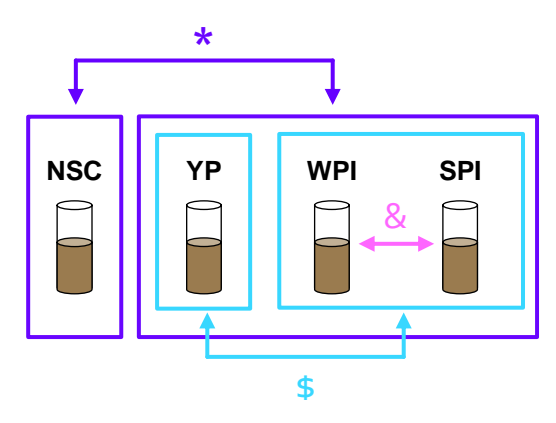


Figure 4. Overview of the statistical comparisons that were performed during the project.

For the **statistical evaluation** of the **treatment effects** on **microbial composition** (family and species level) and **metabolite production** (metabolomics), the **Benjamini-Hochberg correction was applied within each comparison** (NSC vs. 3 test products), given the large number of features analysed.

As a remark, for statistical analysis of the quantitative shallow shotgun sequencing, a value below the **limit of quantification** (LOQ) was equalled to the LOQ. Then, statistics was performed based on log-transformation of the absolute values (to render the data normally distributed).

To illustrate the most representative change for each taxon or metabolite, **fold changes against the NSC were calculated for individual donors**. Subsequently, **log<sub>2</sub>-transformation** was performed on the **geometric mean** of these fold changes. **Geometric mean** was used since it is **more accurate and representative** than the often-used arithmetic mean, especially for positively skewed data which is often the case for microbial composition and metabolomic data (due to interpersonal variances).

Further, **regularized Canonical Correlation Analysis** (rCCA) was performed to highlight **correlations** between **metabolites** and **compositional data** (at family and species level). Regarding compositional data, log-transformed, absolute phylogenetic data was used as input. rCCA was executed using the mixOmics package with the shrinkage method for estimation of penalisation parameters in R (https://www.r-project.org/)<sup>33</sup>.



## 4 Results - Key fermentation parameters

Background on the key fermentation parameters that will be discussed below.

The **key function of the gut microbiota** is to ferment carbohydrates (and to lesser extent proteins), resulting in the formation of **short-chain fatty acids (SCFA)**<sup>11</sup>. Acetate, propionate and butyrate are SCFA that have each been related with particular **health benefits** as reviewed by Rivière *et al.* <sup>12</sup>. Besides exerting anti-inflammatory effects, SCFA also decrease the **pH** of the colonic lumen which for instance increases mineral absorption and inhibits growth of pathogens. **Acetate** is a minor energy source for epithelial cells but reaches the portal vein after which it is metabolized in various tissues. Like acetate, **propionate** reaches the portal vein after which it is taken up by the liver. Health effects related to propionate include that it promotes satiety, lowers blood cholesterol, decreases liver lipogenesis and improves insulin sensitivity. **Butyrate** on the other hand is the preferred energy source of epithelial cells and plays a protective role against colon cancer and colitis. As a result, treatments preferable stimulate acetate, propionate and butyrate production. Further, while **valerate** is much less studied than the other SCFA, it has also been demonstrated to decrease growth of cancer cells<sup>34</sup> or to exert antipathogenic effects against *C. difficile*<sup>35</sup>.

In contrast to aforementioned SCFA, **bCFA** are indicative for proteolytic fermentation <sup>36</sup>, which is associated with formation of metabolites such as phenol and indole that exert **detrimental health effects** <sup>37,38</sup>. On the other hand, there is also evidence that bCFA can be oxidized when butyrate is not available, thereby contributing to **health benefits** <sup>39</sup>. In addition, Boudry *et al.* (2013) showed that a mix of bCFA (isobutyrate and isovalerate) was able to prevent gut permeability induced by proinflammatory cytokines in the Caco-2 cell line model <sup>40</sup>.

Finally, while fermenting colonic substrates, the main **gases** that are produced are H<sub>2</sub> and CO<sub>2</sub>. They can be further converted to other gases (CH<sub>4</sub>, H<sub>2</sub>S) but also to acetate. While fermentation by gut microbes (except Bifidobacteria) inevitably results in gas production, excessive gas production should be avoided as this can lead to abdominal pain or bloating.

#### 4.1 Quality Control

On top of the core experimental design, additional incubations were run for the sole purpose of quality control. This considered that **NSC** incubations at **24h** were run in technical triplicate. Based on the analysis of pH and levels of three main SCFA (acetate, propionate and butyrate) for these replicates, it followed that the **coefficient of variation** (= standard deviation/average) was as low as **0.89%**. This variation is very low since it includes all variation the preparation of the media/reactors up to final sample analysis via GC-FID/pH probes. The **high reproducibility of the SIFR® platform** makes it a very sensitive tool to unravel the impact of test ingredients on the gut microbiome.

Upon analysing **key fermentation parameters** (pH, gas production, SCFA and bCFA) at the **end of the untreated NSC incubations** (24h), it followed that **microbial communities derived from each of the 6 donors** resulted in **diverse metabolic profiles** (Table 2). The production of butyrate, produced by strictly anaerobic gut microbes further confirmed that the **SIFR® experiment** was performed under optimal conditions. While technical reproducibility was 0.89%, **biological variation across the 6 human adults was 10.47%,** reflecting interpersonal differences across human population.



Table 2. Average values (± SD) of key fermentation parameters as averaged across all test subjects, at the end of the untreated NSC incubations, following inoculation with a faecal microbiota of 50-65y male human adults (n = 6).

	NSC				
рН	6.65	±	0.04		
Gas production	171	±	16		
Acetate	18.5	±	1.8		
Propionate	5.59	±	0.49		
Butyrate	3.99	±	0.91		
Valerate	1.07	±	0.12		
total SCFA	30.9	±	1.5		
Isobutyrate	0.67	±	0.02		
Isovalerate	1.10	±	0.04		
total bCFA	1.77	±	0.06		

#### 4.2 High-level observations

A PCA based on key fermentation parameters<sup>2</sup>, as averaged across the 6 test subjects, provided comprehensive insight in overall treatment effects since the first two components explained 96.2% of variation of the dataset (Figure 5A). All parameters correlated negatively with PC1, indicating that samples with enhanced microbial activity positioned to the left side.

First, when focusing on the **impact of time**, there was a **marked differential clustering of 0h and 24h samples**. As the incubation progressed, samples moved from the top right to the lower left side, suggesting enhanced production of **gases/acetate/propionate/butyrate/isobutyrate/isovalerate**.

Next, an **additional PCA** was made for **24h only** and thus removed the effects of time from 0h to 24h (Figure 5B) and demonstrated **marked treatment effects at 24h**:

- **All 3 test products** positioned to the right side of NSC and related to higher production of **gases, acetate, propionate, butyrate, isobutyrate** and **isovalerate**, thus stimulating microbial metabolite production
- SPI shifted the furthest to the right, indicating the strongest stimulatory effects on metabolic activity and relating to higher pH, and enhanced production of gases, acetate, propionate, butyrate, and isovalerate compared to WPI and YP
- WPI positioned upward from YP along PC2 and related to higher pH and higher production of gases, acetate, propionate
- On the other hand, YP related to higher levels of butyrate, isobutyrate and isovalerate

Finally, a PCA based on the individual values of each of the 6 donors at 24h (Figure 5C) demonstrated that there were some **interindividual differences** (~ spread of samples within each treatment group). Interestingly, the interpersonal differences observed for NSC were enlarged by treatment with the protein products, especially **WPI** (~ largest spread of samples for WPI). Nevertheless, treatment effects were consistent for the 6 test subjects (~ treatment groups hardly overlap).

<sup>&</sup>lt;sup>2</sup> The PCA was based on values of pH, gas production, acetate, propionate, butyrate, isobutyrate and isovalerate. Total SCFA and total bCFA were not included as the individual SCFA and bCFA used to calculate the total SCFA levels are already included. Valerate were also not included as it was produced at low levels so that it would disproportionally contribute to the PCA (based on standardized data (mean = 0, standard deviation = 1) *versus* the highly abundant SCFA.



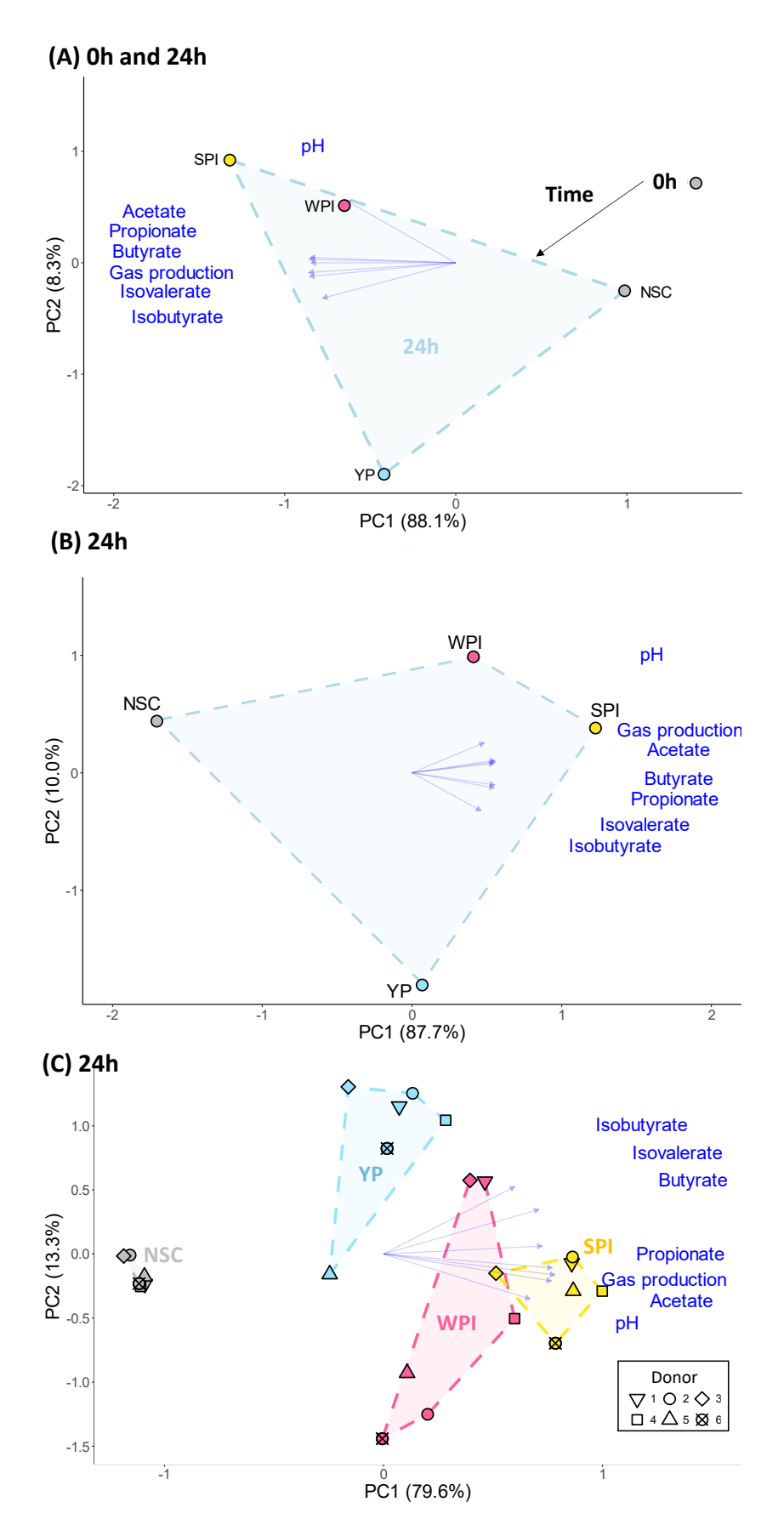


Figure 5. Principal component analysis (PCA) summarizing the impact on microbial metabolite production by 50-65y male human adults' gut microbiota, based on key fermentation parameters. PCA calculated based on the average across the 6 different donors (A) at 0h and 24h and (B) at 24h only or (C) based on individual values of the 6 donors (at 24h).



## 4.3 In-depth analysis of treatment effects

In order to fully grasp the **treatment effects at 24h**, **dedicated figures** were made per **fermentation parameter** (Figure 6). To understand which test product most strongly impacted a specific parameter, average values across donors were ranked, with 1 corresponding to the highest value (highlighted with yellow dot), and 4 corresponding to the lowest value (highlighted with purple dot). While '\*/\*\*/\*\*\*' indicate the extent of the <u>significance of a potential treatment effect versus the NSC</u>, '\$/\$\$/\$\$\$' on the other hand, indicate a potential <u>significant difference of WPI/SPI versus YP</u> and '&/&&/&&/ a potential <u>significant difference of SPI versus WPI</u>. Finally, additional graphs were generated to visualize the effects of each test product on the key fermentation parameter as % of change compared to NSC, as averaged across all donors (Table 3, Figure 7).

Upon simulation of a single intake, the protein products strongly **stimulated microbial metabolic activity** and **promoted the production of different metabolites** (Figure 6):

- Increased pH (significantly for WPI/SPI, SPI > WPI > YP)
- Significantly increased gas production (SPI > WPI > YP)
- Significantly increased the production of acetate (SPI > WPI > YP), propionate (SPI/WPI > YP),
   butyrate (SPI > YP > WPI) → significantly increased total SCFA levels (SPI > WPI > YP)
- Significantly increased valerate production (SPI > YP > WPI)
- Significantly increased **isobutyrate** and **isovalerate** (thus, **total bCFA**) (SPI/YP > WPI)

→ Overall, **SPI** exerted the **strongest stimulatory effects** on metabolite production. When comparing WPI and YP, WPI exerted stronger effects on acetate/propionate production, while YP stimulated more butyrate/valerate/bCFA production.

Table 3. The impact of the test products on the key fermentation parameters, represented as % change from NSC, averaged across six donors. The data is visualized in Figure 7.

	Gas	Acetate	Propionate	Butyrate	Total SCA	Valerate	bCFA	Isobutyrate	Isovalerate
ΥP	89.2	119.0	334.2	320.2	232.3	295.0	850.2	745.2	914.7
WPI	150.5	189.6	536.2	272.7	286.4	107.9	641.9	334.7	830.4
SPI	151.6	239.9	547.7	465.0	374.1	473.2	955.4	711.9	1104.9



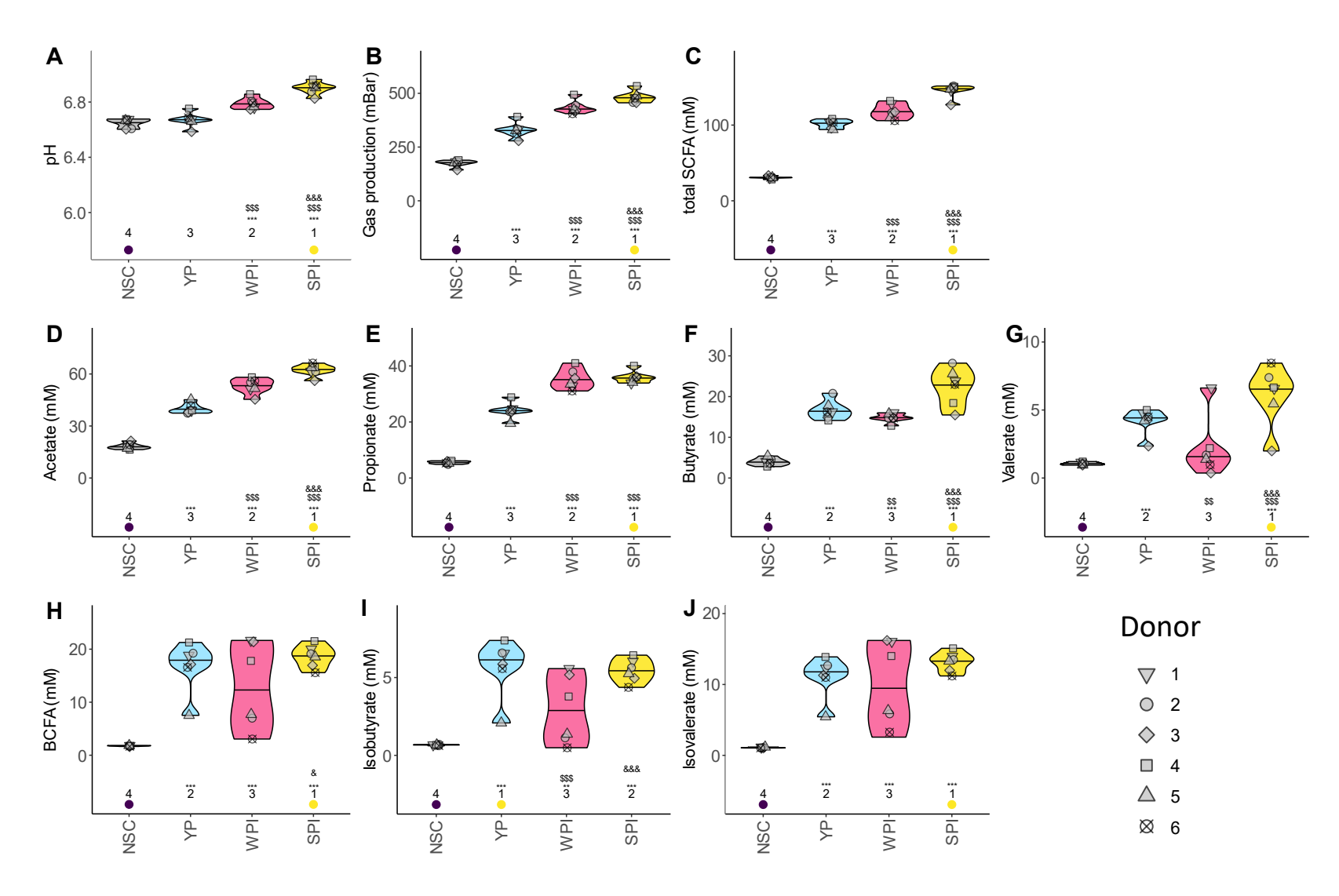


Figure 6. The impact of the test products on (A) pH, (B) gas production, (C) total SCFA, (D) acetate, (E) propionate, (F) butyrate, (G) valerate, (H) bCFA, (I) isobutyrate and (J) isovalerate for 50-65Y male human adults at 24h. Statistical differences between NSC and the individual treatments are visualized via \* (0.1 < padjusted < 0.2), \*\* (0.05 < padjusted < 0.1) or \*\*\* (padjusted < 0.05). Significant differences between WPI/SPI vs. YP are indicated via \$/\$\$/\$\$\$, and between SPI vs. WPI via &/&&/&&. The rank of the average values per treatment are indicated at the bottom of the figure, with the lowest average being indicated purple, and the highest value in yellow.



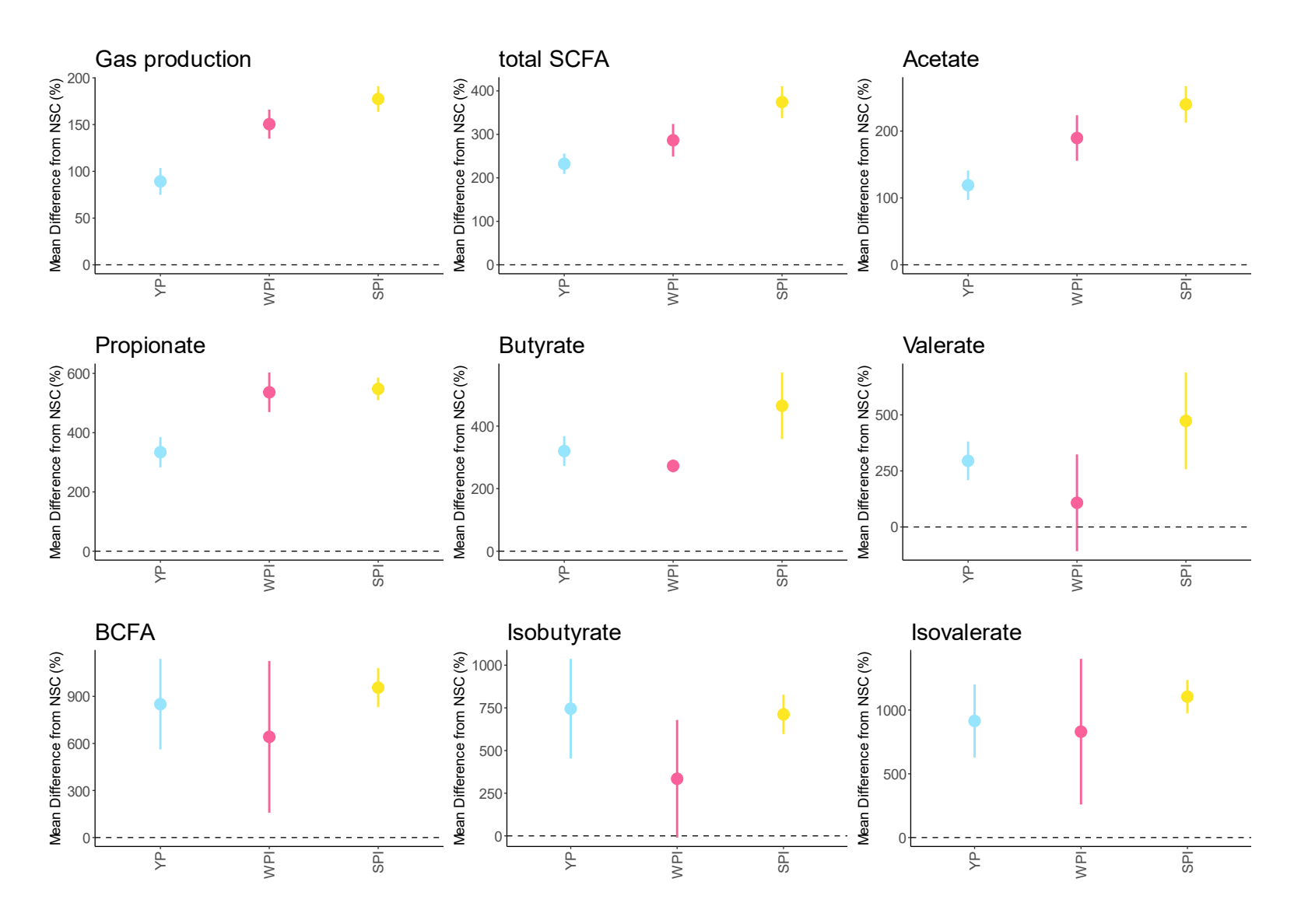


Figure 7. Comparison of the effects of test products on gas production, total SCFA, acetate, propionate, butyrate, valerate, total bCFA, isobutyrate and isovalerate against the no-substrate control (NSC). The effects are presented as % of increase (positive values) or decrease (negative values) from NSC (dashed line), as averaged across 6 d onors. Standard deviation is indicated by vertical lines.



## 4.4 Predicted in vivo SCFA production

While the test products can exert health benefits via other mode-of-actions than via stimulating SCFA production, SCFA stimulation could be an important mode of action. In order to understand whether the aforementioned stimulation of SCFA production by the protein products could be biologically meaningful, the predicted *in vivo* total SCFA production was calculated, similar as during the *in vitro-in vivo* validation study with the SIFR® technology (elaborated in section 1.2.3). Upon comparing these values with *in vivo* reference values³, following findings were made (Figure 8):

- As the daily production of SCFA for human adults is in the range of 200-600 mmol/day<sup>4</sup>, dosing the proteins at 40 g/day would respectively result in up to 53.5% (YP), 65.8% (WPI) and 86.0% (SPI) of the total daily SCFA production. At these levels, the protein products could potentially exert an impact on host health.
- Several studies with pigs, the best proxy for the human host across animal models, demonstrated that beneficial effects could even follow from doses that are considerably lower. Following daily doses of SCFA are proposed to be effective (conversion was done according to Nair et al.<sup>41</sup>, assuming human adult body weight of 60 kg):

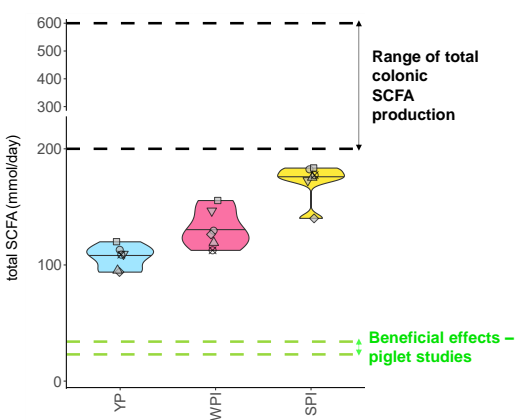


Figure 8. <u>Predicted in vivo SCFA production</u> (mmol/day) for <u>human adults</u> based on the outcomes of the current SIFR® study (at 24h) and comparison with literature data.

- o **34 mmol/day**<sup>5</sup> (Jiao *et al.*, 2018)<sup>44</sup> → attenuated fat deposition via inhibiting feed intake via reducing lipogenesis and enhancing lipolysis of different tissues.
- o **23 mmol/day**<sup>6</sup> (Fang *et al.*, 2014)<sup>45</sup>  $\rightarrow$  decreased diarrhoea incidence, higher serum IgG levels and increased efficiency of nitrogen utilization, overall decreasing the weaning and strengthening intestinal mucosa.
- → This range of daily SCFA production at which beneficial effects on the host are observed is well below the SCFA production upon intake of 40 g of the protein products per day. Thus, at such doses, YP/WPI/SPI likely exert health benefits for human adults via the production of SCFA.

<sup>&</sup>lt;sup>3</sup> While many studies have attributed beneficial effects to SCFA upon their production after the intake of prebiotic substrates, such studies are no good comparators as it is unsure how much SCFA were exactly produced *in situ*. Therefore, for the current research question, one focussed on **studies where SCFA were orally administered**, thus allowing to attribute a health effect to an exact amount of SCFA. As such studies have often been done in animal models, conversion factors were applied according to Nair *et al.* <sup>41</sup>.

<sup>&</sup>lt;sup>4</sup> The **total daily colonic SCFA production** for **human adults** was first estimated by McNeil *et al.* (1984) to be between 500-600 mmol/day assuming 50-60 g carbohydrates entering the colon<sup>42</sup>. Stephen *et al.* reviewed the actual fibre consumption (main source of colonic carbohydrates) across different geographical locations showing that the daily intake of fibres is rather in the range of 20 g/day, thus corresponding with an estimated daily SCFA production in the range of 200 mmol/day<sup>43</sup>.

 $<sup>^{5}</sup>$  0.2L \* 32.64 mM \* 60kg body weight/8.3 kg piglet weight \* 0.73 (conversion factor micro pig to human)

 $<sup>^6</sup>$  0.56\* kg feed/day \* 1g butyrate/kg feed \* 1/87 g/mol (MM butyrate) \*1000 mmol/mol \* 60kg body weight/12 kg piglet weight (average of initial/final weight reported during this study) \* 0.73 (conversion factor micro pig to human)



#### 5 Results - Microbial composition

#### Background on key phyla/families/species of the human gut microbiome.

The **Actinobacteria** phylum mainly consists of *Bifidobacteriaceae* and *Coriobacteriaceae*. The *Bifidobacteriaceae* family contains many known health-related species, able to produce acetate and lactate<sup>46</sup>. *Collinsella* species are on the other hand the most abundant *Coriobacteriaceae* members and produce H<sub>2</sub> gas, formate, acetate and lactate. The **Bacteroidetes** phylum contains versatile glycanfermenting members. Key families are the *Bacteroidaceae* and *Prevotellaceae*, two families considered to be main differentiators between the so-called enterotypes<sup>29</sup>. *Bacteroides* species produce acetate and propionate and doing so also succinate (as intermediate of propionate production)<sup>47</sup>. Other families are *Rikenellaceae*, *Tannerellaceae* and *Porphyromonadaceae*. Further, the **Firmicutes** phylum contains a diverse series of phyla including, amongst others:

- Acidaminococcaceae: a key species of this family is *Phascolarctobacterium faecium*, an abundant colonizer<sup>48</sup> that is able to convert succinate into propionate<sup>49</sup>
- Erysipelotrichaceae (e.g. Eubacterium biforme) and Christensenellaceae (e.g. C. minuta)
- Lachnospiraceae: contains several important butyrate-producing species such as Anaerobutyricum hallii<sup>50</sup>, Anaerostipes<sup>51</sup>, Butyrivibrio, Coprococcus, Eubacterium rectale, Roseburia. Further, Lachnospiraceae are among the first to be established in the gastrointestinal tract, with Ruminococcus gnavus being the exclusive representative of this family in 2-months old breast-fed infants<sup>52</sup>. Further, this family also contains Dorea spp., which is a major gas producer (H<sub>2</sub>/CO<sub>2</sub>) related to IBS <sup>53</sup>.
- Ruminococcaceae: several important butyrate-producing species such as Butyricicoccus pullicaecorum, Gemmiger formicilis<sup>54</sup>, Faecalibacterium prausnitzii<sup>55</sup> and Subdoligranulum variable.
- Selenomonadaceae: Megamonas species
- Veillonellaceae: lactate-converting, acetate/propionate/H<sub>2</sub>-producing species such as Veilonella
- As a remark, Enterococcaceae, Lactobacillaceae and Streptococcaceae are Firmicutes families
  containing lactic acid producing member that typically colonize the upper GIT but to much lower
  extent the colon.

While **Proteobacteria** mainly contain opportunistic pathogens (e.g. *Escherichia coli*), **Verrucomicrobia** has the health-related, mucin-degrading, acetate/propionate-producing *Akkermansia muciniphila* as its main representative. Finally, besides bacteria, there are also **Archaea** such as *Methanobrevibacter smithii* colonize the human gut. *M. smithii* converts H<sub>2</sub>/CO<sub>2</sub> to CH<sub>4</sub>. Other H<sub>2</sub> and/or CO<sub>2</sub> consumers are acetogens (*Blautia hydrogenotrophica*; *Lachnospiraceae* member) and sulfate reducers (*Desufovibrio piger*: Proteobacteria member that converts H<sub>2</sub>/SO<sub>4</sub> to H<sub>2</sub>S).



## 5.1 Donor characterization (0h)

A PCA at **genus level** (explaining a large portion of the variation (84.2%)) demonstrated that there were **marked differences in microbial composition between the 6 donors at baseline** (Figure 9).

The stratification of donors was in line with the **stratification of human gut microbiota according to the concept of enterotypes**<sup>56–58</sup>. Most of the variation was explained along PC1 (67.4%) and differentiated donors with high abundances of *Prevotella* (left: **donors 1/4/5**), a marker of *Prevotella* enterotype, from the others. Further, **donor 5/6** exhibited higher levels of *Bacteroides* and *Phocaeicola*, a marker for *Bacteroides* enterotype. Further, **donor 2/3** exhibited some characteristics of the **Firmicutes** enterotypes, as evidenced by higher levels of genera within the phylum **Firmicutes**, i.e., *Faecalibacterium* as well as *Ruminococcus\_E* (donor 2) and *Blautia\_A* (donor 3). Other interpersonal differences were noted for high abundances of *Bifidobacterium* for **donor 1/3**, *Collinsella* for **donor 3/4/6** as well as the *Alistipes* for **donor 2/4/6**.

Overall, these first findings stress that the 6 human adults covered the broad range of microbiota composition that occurs *in vivo*, thus ensuring representative findings.

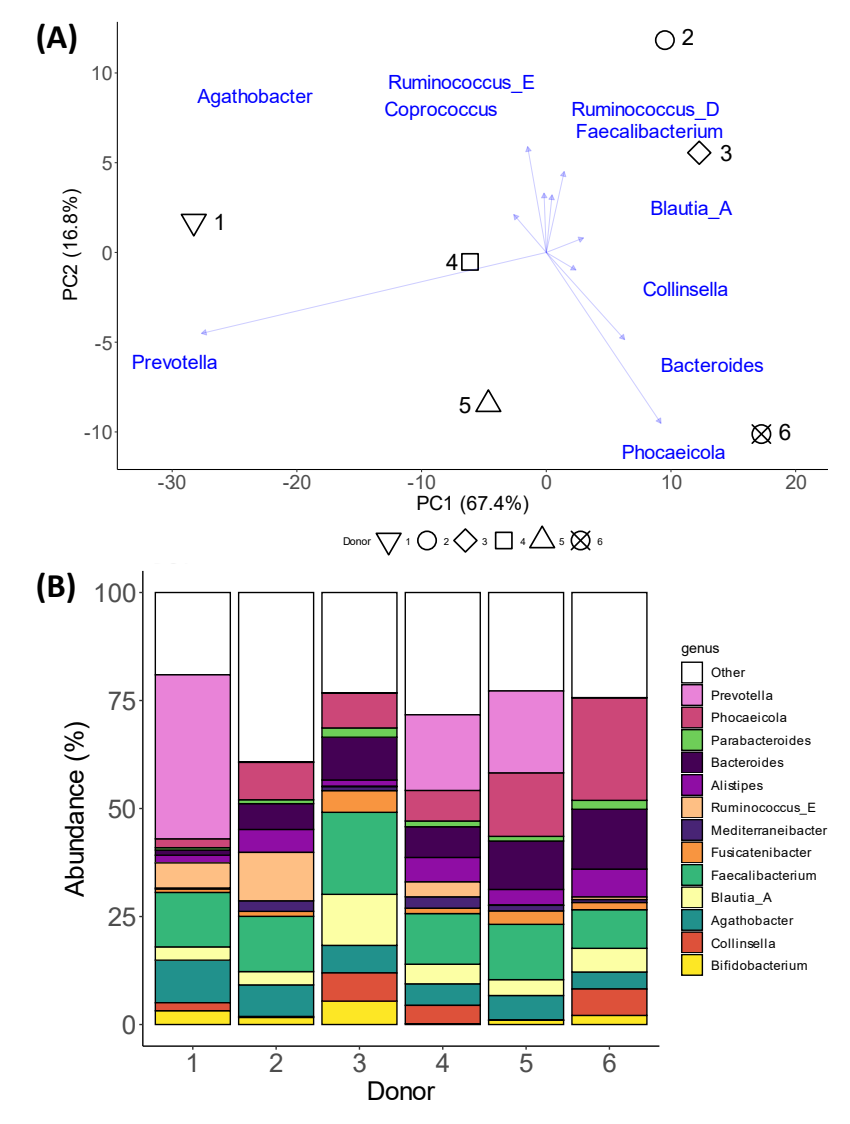


Figure 9. (A) Principal component analysis (PCA) summarizing the <u>microbial community composition</u> of the 6 human adults that provided a faecal donation for the current SIFR® study. The PCA was calculated based on the (centred) <u>abundances (%) of the microbial genera</u>, as quantified via shallow shotgun sequencing. (B) Abundances (%) of the key families of the different faecal microbiota.



# 5.2 Quality control: SIFR® technology = an accurate *ex vivo* gut microbiome testing platform

The **preservation of the** *in vivo*-derived microbiota and thus the minimal bias in microbiota composition during SIFR® studies is in contrast to consistent *in vitro* biases that have been observed for traditional long-term *in vitro* models <sup>4-6</sup> and in recently developed short-term *in vitro* models <sup>7-10</sup>, given that SIFR® studies adhere to *ex vivo* rather than *in vitro* simulation principles.

This was also confirmed during **the current study** upon comparing the original sample and the same sample incubated for 24h using the SIFR® technology. First, a diverse range of *in vivo*-derived gut microbes endured the procedure over the 24h incubation period, **maintaining** the **microbial diversity**, both in terms of species richness (Figure 10A/B) and evenness (Figure 10C/D). Under control conditions (NSC), the **total cell numbers increased** from 0h (INO) to 24h with a factor of 2.06 ( $\pm$  0.72) (Figure 10E). Importantly, at the **end of the 24h NSC incubation**, **microbial composition reflected** the **original inoculum** (INO) (Figure 10F).

This accurate preservation of *in vivo*-derived microbiota for the entire duration of the experiment classifies the application of SIFR® technology as an *ex vivo* study, which is a study that uses an artificial environment outside the human body with minimum alteration of natural conditions. Such sustained similarity is fundamentally different from consistent biases observed for the current generation of *in vitro* gut models<sup>7</sup>.

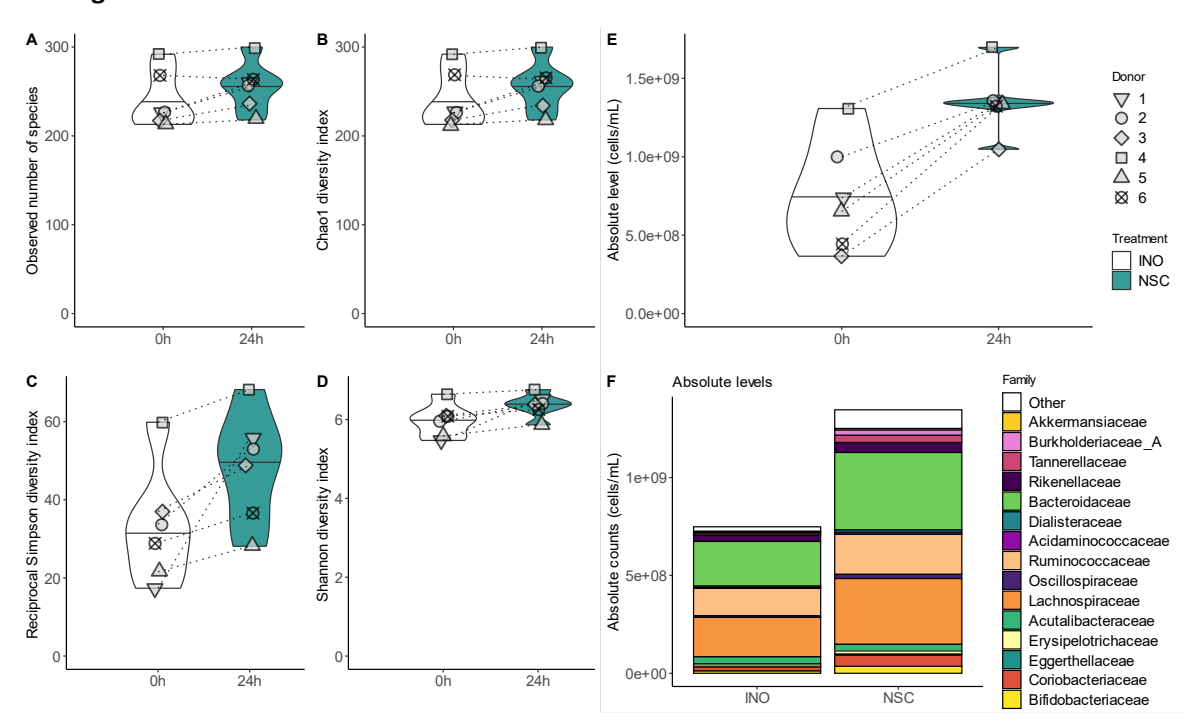


Figure 10. (A/B/C/D) Microbial diversity, (E) bacterial cell density (cells/mL) and (F) average microbial composition at family level (cells/mL) of the *in vivo*-derived inocula (INO) and upon 24h of incubation in the SIFR technology in absence of a treatment (NSC) (n = 6).

<sup>&</sup>lt;sup>7</sup> A key limitation of the current in vitro/ex vivo models is the drastic alteration of in vivo-derived microbial composition towards an in vitro-adapted one. This is highly pronounced for short-term models where, within a timeframe as short as 24h, fast-growing, aerotolerant taxa dominate the communities that contain e.g., 50% Enterobacteriaceae <sup>59</sup>, 75-80% Proteobacteria <sup>8</sup>, 75% Veillonellaceae <sup>10</sup>, or 60-70% Escherichia-Enterococcus-Streptococcus <sup>9</sup>. Similarly, the current generation of long-term gut models, aiming to simulate an average human individual, impose defined nutritional and environmental conditions, thus enriching taxa that thrive under these specific conditions <sup>4,5</sup>, as quickly as within three days <sup>60</sup>.



## 5.3 Cell density and $\alpha$ -diversity

Analysis of the total cell numbers across the different samples demonstrated that all three test products significantly increased total bacterial cell density (SPI > WPI/YP) (Figure 11A).

Given these differences in cell numbers across study arms, it was of key importance to **correct the proportional data** obtained via sequencing (%) with the **total cell counts** in order to obtain insights into the **true changes in microbial composition**<sup>8</sup>. The **conversion of sequencing data using flow cytometry** data is **visualized** at **phylum level** (Figure 11B/C). Subsequent data processing at species and family level was thus performed based on the quantitative results.

This exploratory data visualisation of <u>microbial composition at phylum level</u> showed that Actinomycetota, Bacteroidota, Bacillota, and Pseudomonadota were the main phyla. Interestingly, all three test products promoted the levels of these four phyla, suggesting that they support a broad diversity of gut microbes. Product-specific effects were noted for Actinomycetota (SPI>YP>WPI), Bacteroidota (SPI/WPI>YP), Bacillota (SPI/YP>WPI) and Pseudomonadota (SPI> WPI>YP).

Overall, in contrast to **WPI** that rather **specifically stimulated Bacteroidota**, **SPI** and **YP** exerted stimulatory effects on a **broader range of families** (with YP exerting milder effects compared to SPI).

For more details and statistical underpinning of these findings at phylum level, violin plots were generated based on quantitative data of the phyla for the individual donors. They are reported as part of the supplementary information of this report (Supplementary Figure 32).

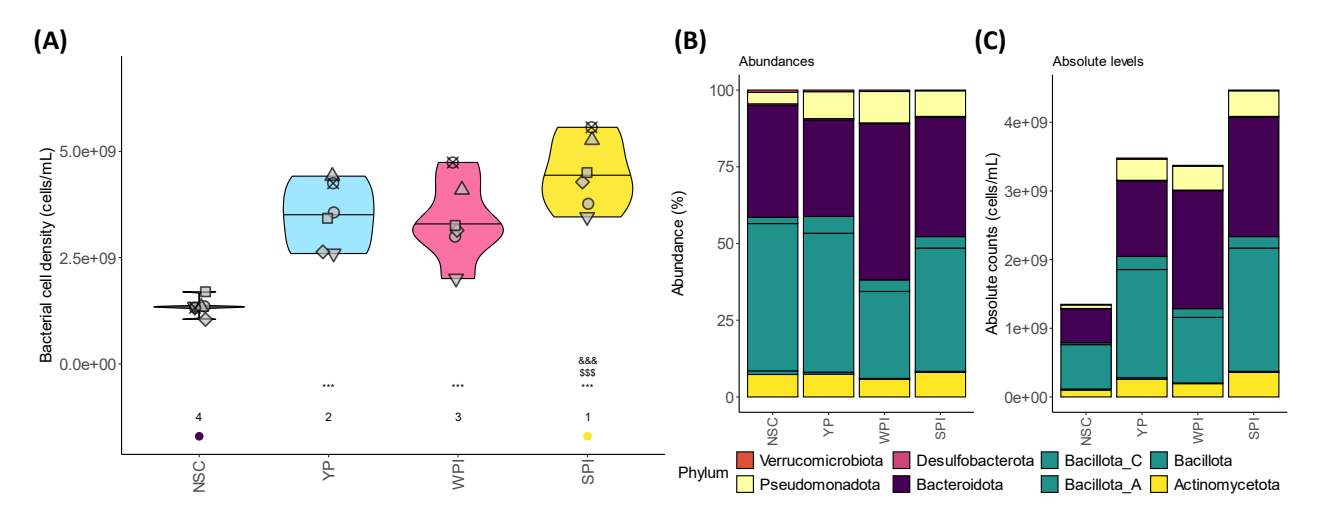


Figure 11. (A) The impact on total bacterial cell counts of the test products compared to an untreated control (NSC). Samples were collected after 24h of simulated colonic incubations. Statistical differences between NSC and the individual treatments are visualized via \* (0.1 < padjusted < 0.2), \*\* (0.05 < padjusted < 0.1) or \*\*\* (padjusted < 0.05). Significant differences between WPI/SPI vs. YP are indicated via \$/\$\$/\$\$, and between SPI vs. WPI via &/&&/&&. The rank of the average values per treatment are indicated at the bottom of the figure, with the lowest average being indicated purple, and the highest value in yellow. (B/C) The impact of the test products on microbial composition at phylum level as averaged over simulations for 6 human adults via the SIFR® technology platform, presented both as (B) proportional (%) and (C) absolute values (cells/mL).

\_

<sup>8</sup> Imagine a microbial community that consists of two bacteria, A and B, each present at 1\*10° cells/mL. Sequencing of such community would provide following results at baseline: 50%/50% (proportional data) 1\*10°/1\*10° cells/mL (quantitative data). When a given treatment would increase the levels of bacteria A from 1\*10° cells/mL up to 3\*10° cells/mL, proportional levels of the overall community would become 75%/25%. This not only suggests that bacteria A increased upon treatment but erroneously also suggests that bacteria B decreased upon treatment. By accounting for the flow cytometry data (4\*10° cells/mL would be detected upon treatment), the conclusion would be that upon treatment, bacteria A is present at 3\*10° cells/mL and bacteria B is present at 1\*10° cells/mL. This allows to make the true conclusion that bacteria A is decreased upon treatment while bacteria B is unaffected.



Four diversity indices were calculated to obtain optimal insights into microbial diversity (Figure 12).

First, a **new diversity score**, i.e. **the community modulation score** (**CMS**), was recently developed by Cryptobiotix<sup>61</sup> (Figure 12A). This index removes great part of the noise that is introduced when assessing diversity using traditional indices (for background information, see Appendix, section 10.2). Calculation of the CMS demonstrated that **all three test products**, especially **YP and SPI**, **strongly enhanced microbial diversity**.

Next, traditional diversity indices were also calculated: while the **Chao1** diversity index is a measure of species richness (Figure 12B), the reciprocal Simpson diversity index/Shannon diversity index reflect also species evenness (Figure 12C/D). In contrast to the CMS, these indices (likely due to their limitations; section 10.2) failed to show the diversity-promoting effect of the three test products. In contrast, the traditional indices demonstrated that all the three protein products, especially WPI, significantly decreased microbial diversity, both in terms of species richness and species evenness. The marked decrease in species evenness with WPI is in line with aforementioned observation of the rather specific increase of Bacteroidota members.

Overall, in contrast to the conventional diversity indices, the CMS score demonstrated that **all three test products**, especially **YP and SPI**, **positively impacted microbial diversity**.

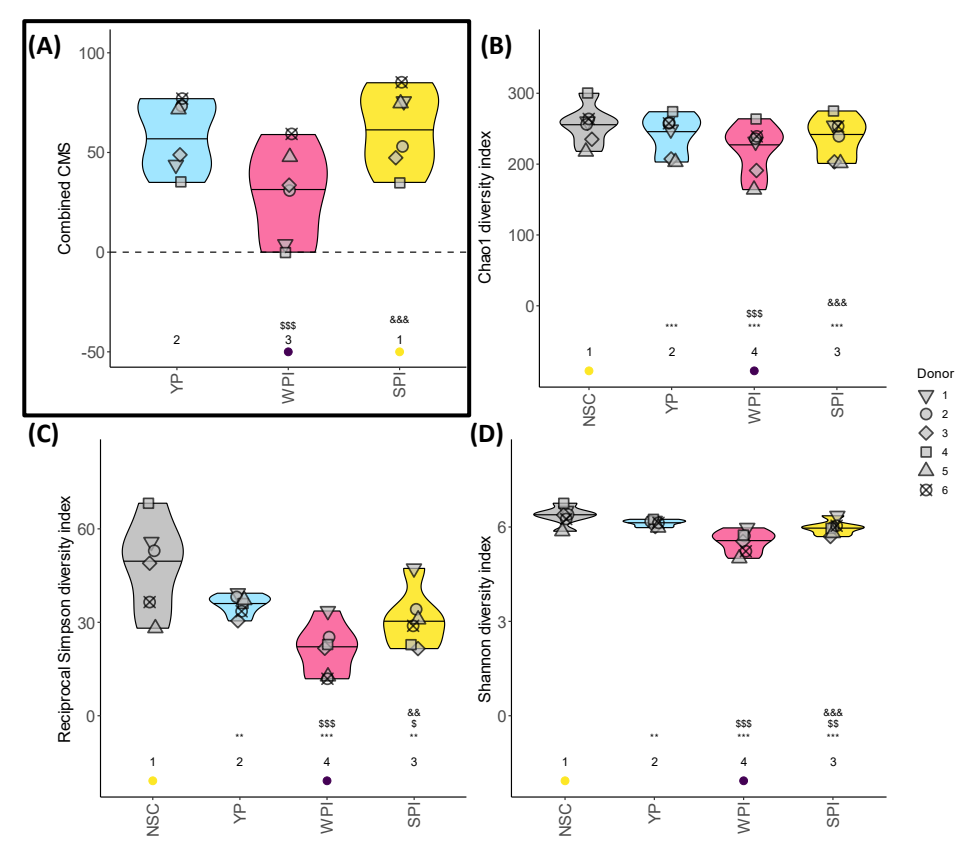


Figure 12. The impact on (A) the combined community modulation score (CMS), (B) the Chao1 diversity index, (C) the reciprocal Simpson diversity index and the (D) Shannon diversity index, for the test products, compared to a no substrate control (NSC). Samples were collected after  $\underline{24h}$  of incubation. Statistical differences between NSC and the individual treatments are visualized via \* (0.1 <  $p_{adjusted}$  < 0.2), \*\* (0.05 <  $p_{adjusted}$  < 0.1) or \*\*\* ( $p_{adjusted}$  < 0.05). Significant differences between WPI/SPI vs. YP are indicated via \$/\$\$,\$\$, and between SPI vs. WPI via &/&&/&&&. The rank of the average values per treatment are indicated at the bottom of the figure, with the lowest average being indicated purple, and the highest value in yellow.



## 5.4 Exploratory data analysis

To focus on treatment effects, PCA analysis was conducted based on the average results across the 6 test subjects at 24h. For optimal insights, the PCA was made at high phylogenetic resolution, i.e. based on centered average levels of the most abundant families and species <sup>9</sup> (Figure 13A/B). The resulting PCA demonstrated pronounced impact of the test products on the microbial composition (mostly observed along PC1) in a product-specific manner (observed along PC2).

At both phylogenetic levels, the **test products** shifted to the right side of the NSC and related to **increased levels of a wide range of families and species**, i.e., the SCFA-producing taxa **Anaerotignaceae** (including **Anaerotignum faecicola**), **Butyricicoccaceae** (including **Agathobaculum** spp.), **Acidaminococcaceae** (including **Acidaminococcus intestini**), **Dialisteraceae**. Other taxa relating to the treatment effects that are noted on the species-level PCA (Figure 13B) were the **butyrate producing Roseburia hominis**, a cluster of **Copromonas** species and a cluster of **propionogenic species** within the phylum Bacteroidota including **Alistipes putredinis**, **Phocaeicola vulgatus**, **Odoribacter splanchnicus**. Importantly, there were also **differences in how WPI/SPI/YP affected these taxa**, which were mainly observed along PC2. **WPI** for instance strongly related with **Phocaeicola vulgatus**.

To statistically support these findings, the data was further processed at two phylogenetic levels, i.e., family and species level (next sections).

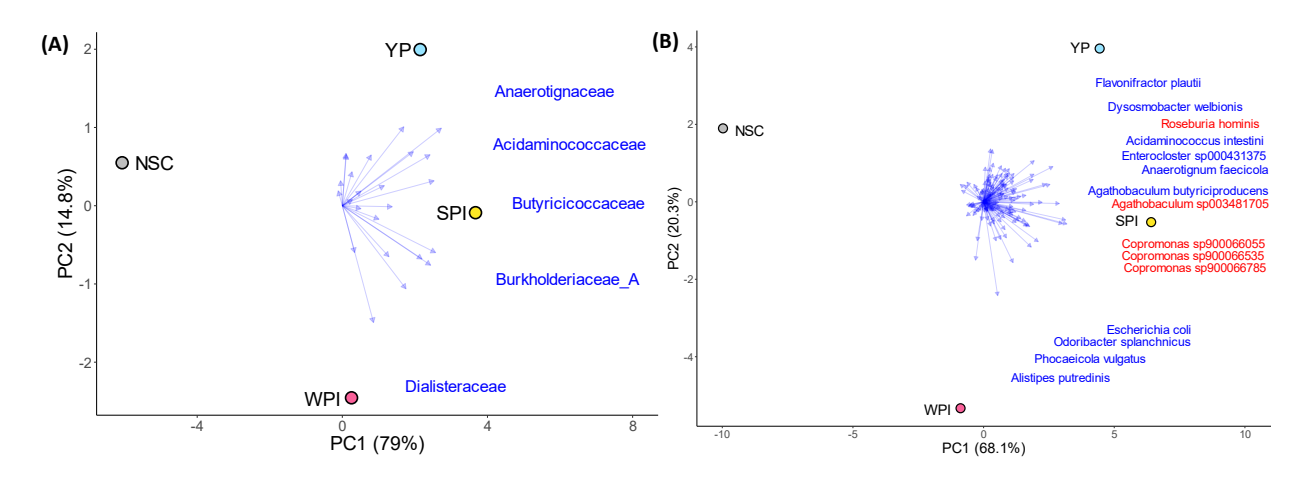


Figure 13. Principal component analysis (PCA) summarizing the impact of the test products on the gut microbial composition of human adults (n = 6), compared to a no substrate control (NSC), as tested via the SIFR® technology. The PCA was calculated based on the log 2-transformation of centred average levels of (A) the top 24 most abundant families and (B) the top 150 most abundant species, as quantified via shallow shotgun sequencing combined with flow cytometry (cells/mL), at 24h of incubation. (A) highlighted top 5 bacterial families and (B) top 15 species (with top 5 highlighted in red) that exhibited the largest variances in the PCAs.

\_

<sup>&</sup>lt;sup>9</sup> The threshold for inclusion was based on the highest abundance (%) reached in at least 1 sample. The cut-off for inclusion was that a species needed to be at least in 1 sample above 0.63 %. This selection of 150 species accounted for, on average, 89.69% of the total abundances of a sample. When applying the same threshold at family and phylum level, 24 families and 8 phyla were retained covering on average respectively 99.66% and 99.92% of the total microbiota.



## 5.5 In-depth analysis of treatment effects

To gain insight in treatment effects at **family** and **species level**, all taxa that were **significantly** (p<sub>adjusted</sub> < 0.20) and **non-significantly but consistently**<sup>10</sup> affected were displayed in a heat map based on the **average ratios versus the NSC** (Figure 14A and Figure 15). Top 5 families and species with the largest variations among the treatments (Figure 13A/B) were also included in the heat maps. A selection of relevant families/species will be highlighted along the text below via **dedicated figures** based on **log<sub>2</sub>(fold change of treatment vs. NSC)**. Further, **absolute abundances (cells/mL)** of the **most abundant families/species** are presented in Supplementary Files 1-2 (section 10.1)<sup>11</sup>.

Further, at both taxonomic levels, a rCCA was performed to highlight correlations between key fermentation parameters and specific taxa (Figure 14B and Figure 16). In addition, pairwise correlation analysis using Kendall rank correlation coefficient were also performed with significant correlations also being highlighted in the figures. Owing to interpersonal differences and treatment effects, correlations could be established between specific metabolites and certain taxa, in line with known metabolic capabilities of these taxa. As published recently, such approach allows to build hypothesis on mode-of-action<sup>3</sup>. Following interesting correlations were established (significant correlations are indicated by black dots):

- Acetate ~ the major acetate producer Bifidobacterium adolescentis<sup>46</sup> as well as other acetogenic species Alistipes putredinis<sup>62</sup> (mostly WPI/SPI), Parabacteroides distasonis<sup>63</sup> (mostly YP), Odoribacter splanchnicus<sup>64</sup> (mostly WPI/SPI) along with specific Bacteroidaceae species depending on the product (Bacteroides caccae, Bacteroides stercoris, Phocaeicola massiliensis)
- **Propionate** ~ propionate producers **Phascolarctobacterium faecium**<sup>49</sup>, **Odoribacter splanchnicus**<sup>64</sup> (mostly YP) as well as **Parabacteroides distasonis** which produces **succinate** a precursor of **propionate**<sup>65</sup>
- Butyrate ~ butyrate producers Agathobaculum butyriciproducens<sup>66</sup>, Eubacterium\_I ramulus<sup>67</sup>, Roseburia hominis<sup>47</sup>, Faecalibacterium spp.<sup>51</sup> as well as Bifidobacterium adolescentis which produces acetate/lactate that can be converted into butyrate via cross-feeding <sup>68,69</sup>

\_

<sup>&</sup>lt;sup>10</sup> Families/species that insignificantly but consistently increased/decreased for at least 4 donor and were not affected for the other donors were included in the heat map to also grasp treatment effects on taxa that were not present in all donors (which obscures observation of statistical differences).

<sup>&</sup>lt;sup>11</sup> The added value of figures based on absolute values is that they show the marked differences in absolute levels of a given microbial taxon between different donors. This is of interest as findings of more abundant taxa are more likely to impact metabolite levels (e.g. SCFA). In contrast, such figures based on absolute levels thus also mostly visualize findings for the donor(s) for which a given taxon is most abundant, thus obscuring findings for donors where levels of a specific taxon are lower. Therefore, to optimally focus on treatment effects, the main description of the report mostly includes fold change-based figures (that better visualize treatment effects for all donors), while supplementary files contain figures based on absolute levels.



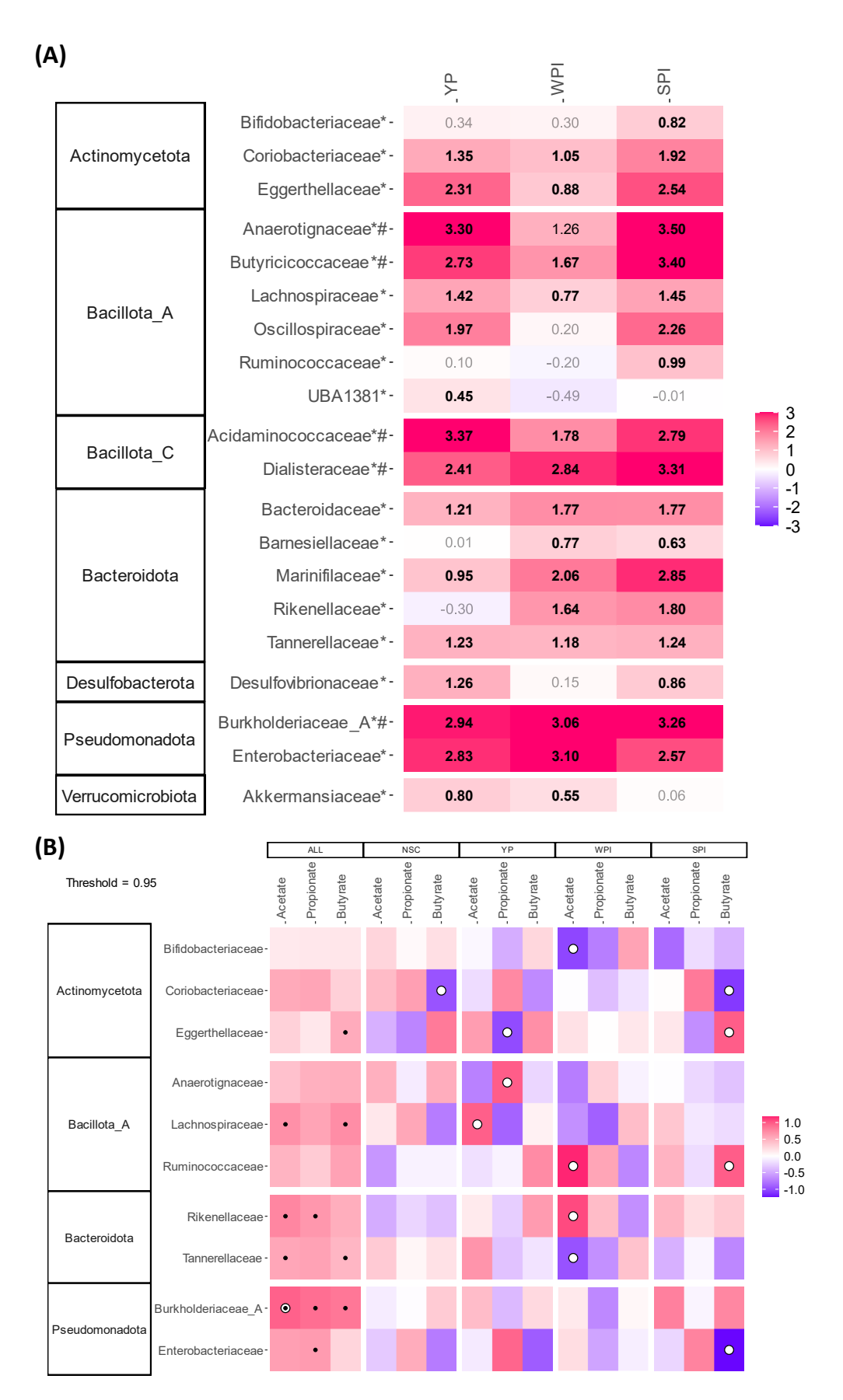


Figure 14. (A) The impact of the test products on bacterial families that were significantly (padjusted < 0.20, indicated by \*) and/or consistently affected by any of the treatments, expressed as log<sub>2</sub> transformation of abundance treatment/abundance NSC ratios (log<sub>2</sub>FC), averaged across all 6 donors. Log<sub>2</sub>FC was indicated in bold where statistical significance or consistent increase/decrease occurred. Top 5 families with the largest variations among the treatments (Figure 13A) were also included in the heat map and indicated with #. (B) Regularized Canonical Correlation Analysis (rCCA) to highlight correlations between fundamental fermentation parameters and microbial composition (families) in all study arms or in the NSC and individual treatment arms (threshold > 0.95). The white circles indicate values larger than the threshold and black dots indicate statistical significance (p < 0.05) in the individual correlations between the SCFA and the families based on Kendall rank correlation coefficient.



			Ϋ́	WPI	SPI	
	Bifidobacteriaceae	Bifidobacterium adolescentis *-	0.42	0.42	1.04	
Actinomycetota	Comphant	Collinsella aerofaciens_G*-	1.02	0.76	1.62	
	Coriobacteriaceae	_	1.17 1.06	0.66	1.62 1.34	
Collinsalla perofeciens C*	3.34	1.61	2.94			
			2.47	1.56	2.95	
	Butylicicoccaceae	Agathobaculum sp003481705*#-	2.99	1.89	3.93	
		· ·	1.27	0.60	0.52	
			1.08 0.24	-0.04 -1.60	0.24 0.29	
			2.38	0.87	0.75	
			2.09	1.14	1.93	
			1.80 0.74	<b>0.99</b> -0.74	1.72 0.74	
			1.01	0.06	1.08	
			1.23	-0.14	0.97	
		_ ·	0.73 1.22	-0.15 0.20	0.99 0.76	
			0.65	-0.49	0.56	
			0.92	-0.34	0.72	
			1.06 1.59	-0.43 1.55	0.87 1.94	
			0.74	-0.36	-0.11	
			1.27	0.37	1.04	
	Lachnosniraceae		1.69 1.06	0.67 -0.44	1.43 1.16	
	Lacinospiiaceae		2.96	2.37	4.49	
		Copromonas sp900066535*#-	3.17	2.66	4.48	
			2.82 1.15	2.40 1.14	4.36 1.58	
DIII :			2.33	2.32	2.13	
Bacillota_A		Dorea_A longicatena_B*-	2.24	2.27	2.07	
			1.13 1.78	0.81 <b>1.07</b>	0.49 1.48	
			3.36	1.64	2.64	
		Eubacterium_I ramulus*-	2.26	2.29	2.25	
			0.15	-0.57	-0.07	
			0.42	0.16	0.35 -0.02	
			0.34	-0.07	0.48	
			2.74	0.52	3.42	
			1.50 1.78	0.05	0.95 1.13	
			1.23	0.56	0.76	
		Dysosmobacter welbionis * -	2.31	0.56	2.29	
	Oscillospiraceae		1.21	-0.20	1.45	
		· ·	2.21 -1.41	0.03 <b>0.86</b>	<b>2.31</b> 0.49	
			0.36	-0.46	1.38	
		Faecalibacterium prausnitzii_A*-	0.13	-1.70	0.20	
			-1.01	-1.34	-0.74	
	Ruminococcaceae		0.28 -0.97	-0.68 - <b>1.29</b>	<b>1.30</b> <b>-</b> 0.24	
			-0.05	-1.23	0.37	
		-	0.35	-0.30	1.20	
			0.57 0.89	-0.39 - <b>0.64</b>	1.01 0.03	
	UBA1381	_	0.45	-0.49	-0.01	
			2.66	1.02	2.06	
Bacillota C	Acidaminococcaceae		1.52	1.66	1.65	
Daomota_0	Dialisteraceae		1.97	1.92	2.08	
Bacillota_C	<del> </del>		1.17 0.56	1.09	1.46 0.54	
Bacillota_C			1.46	0.81	1.33	
		Bacteroides faecis*	1.12	0.29	0.48	
			1.71	0.79	1.37	
	Bacteroidaceae		0.43 <b>1.56</b>	1.11 0.27	1.48 -0.35	
			1.87	1.21	2.67	
			1.00	0.83	1.65	
			0.69 0.90	1.75 2.52	0.71 1.96	
Bacteroidota	Barnesiellaceae	*	0.00	0.75	0.64	
			0.92	1.88	3.24	
		· ·	-1.15	0.42	0.38	
		Alistipes onderdonkii*-	0.28	1.34	1.29	
	Rikenellaceae		-1.31 0.28	1.96	2.24	
	]		0.28 -1.66	1.25 -1.74	<b>1.71</b> -0.86	
			1.58	1.63	1.82	
		Parabacteroides distasonis *-				
	Tannerellaceae	Parabacteroides johnsonii*	0.50	0.65	0.42	
	Tannerellaceae	Parabacteroides johnsonii*- Parabacteroides merdae*-	1.02	1.05	0.96	
		Parabacteroides johnsonii*- Parabacteroides merdae*- Parasutterella excrementihominis*-	1.02 1.94	1.05 1.53	0.96 2.07	
<sup>2</sup> seudomonadota	Tannerellaceae  Burkholderiaceae_A	Parabacteroides johnsonii*- Parabacteroides merdae*-	1.02	1.05	0.96	
Pseudomonadota		Parabacteroides johnsonii*- Parabacteroides merdae*- Parasutterella excrementihominis*- Parasutterella sp900552195*-	1.02 1.94 1.55	1.05 1.53 1.33	0.96 2.07 1.57	

Figure 15. (A) The impact of the test products on species that were significantly ( $p_{adjusted} < 0.20$ , indicated by \*) and/or consistently affected by any of the treatments, expressed as  $log_2$  transformation of abundance treatment/abundance NSC ratios, averaged across all 6 donors.  $log_2$ FC was indicated in bold where statistical significance or consistent increase/decrease occurred. Top 5 species with the largest variations among the treatments (Figure 13B) were also included in the heat map and indicated with #.



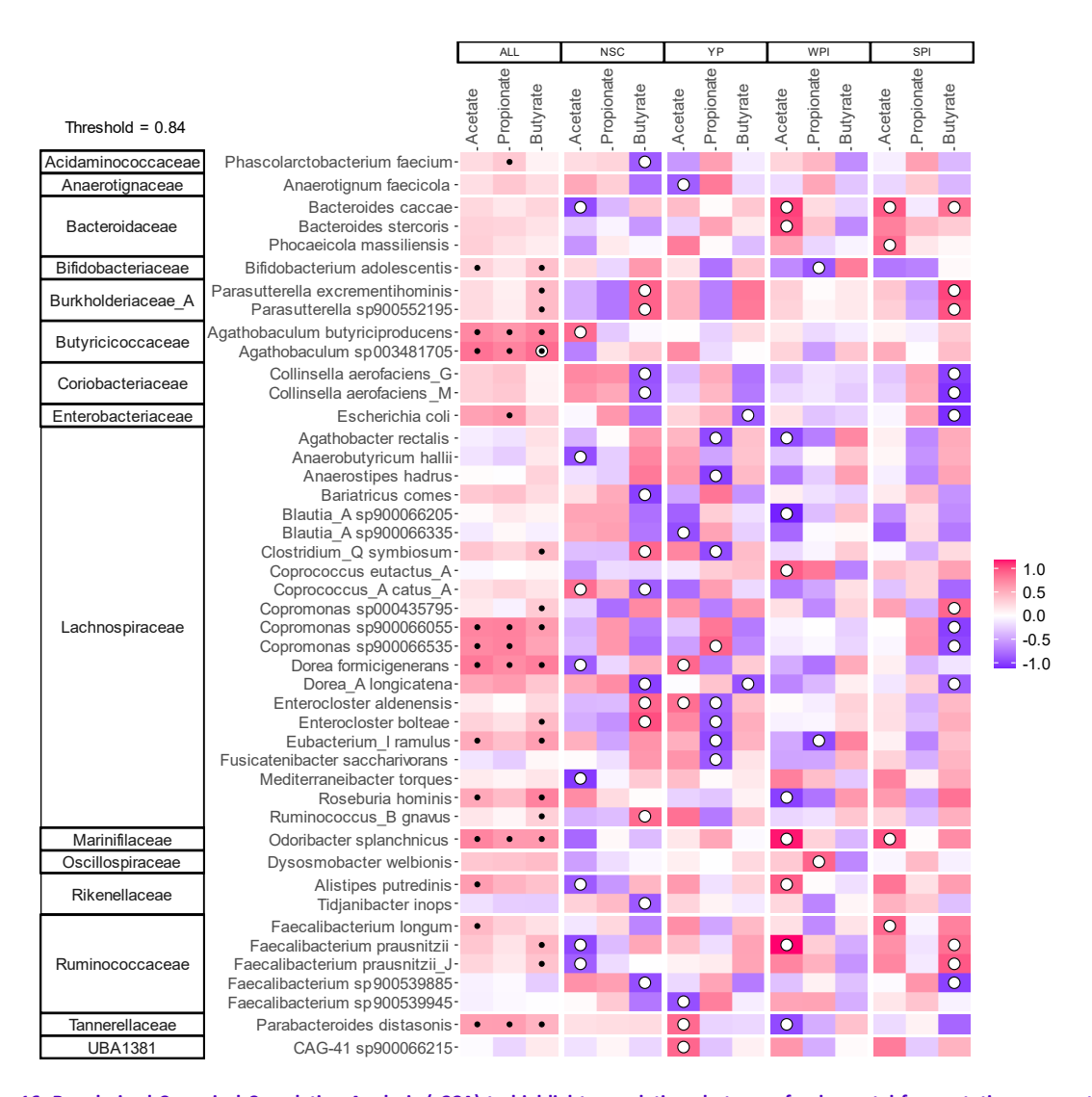
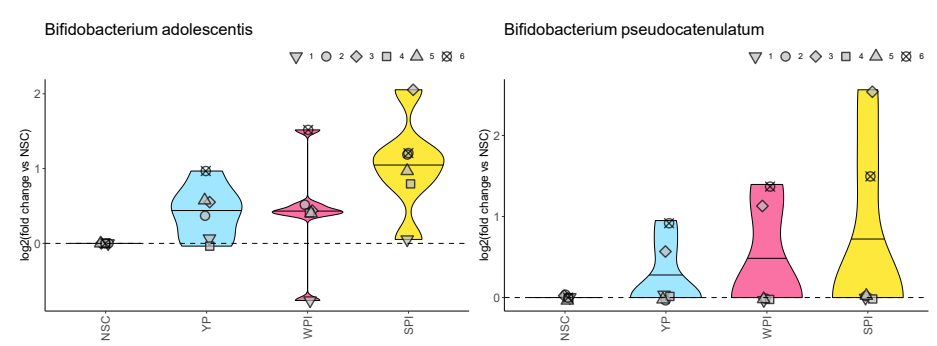


Figure 16. Regularized Canonical Correlation Analysis (rCCA) to highlight <u>correlations</u> between fundamental fermentation parameters and microbial composition (species) upon fermentation in all study arms or in the NSC and individual treatment arms (threshold > 0.84). The white circles indicate values larger than the threshold and black dots indicate statistical significance (p < 0.05) in the individual correlations between the SCFA and the families based on Kendall rank correlation coefficient.

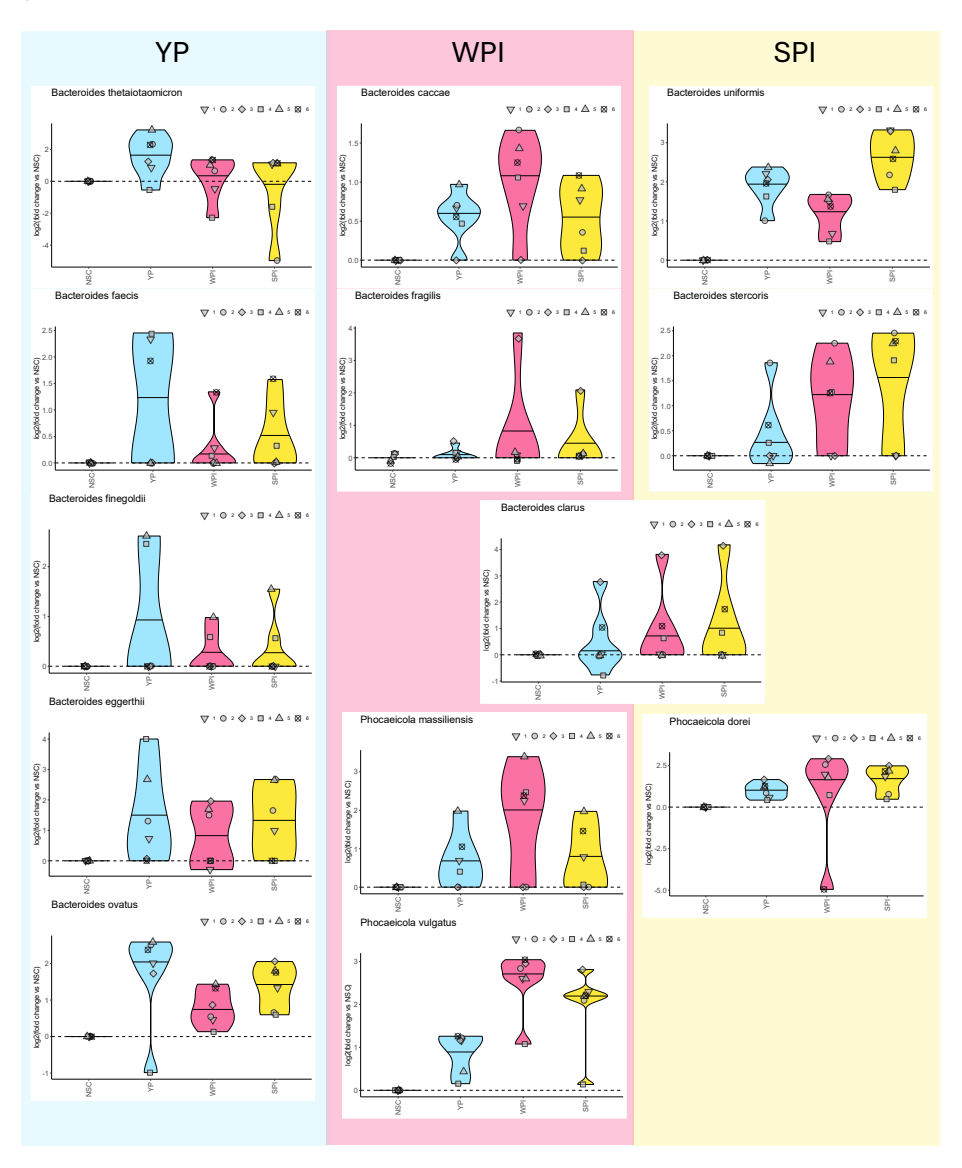
First, fermentation of all test products, especially SPI, resulted in bifidogenic effects (= increased levels of health-related *Bifidobacteriaceae*), due to increased levels of *B. adolescentis* and *B. pseudocatenulatum* (no significant effects due to detectable levels in only 2 donors). *Bifidobacterium* species produce acetate/lactate and can also promote butyrate production via cross-feeding with butyrate producers<sup>68,69</sup> (acetate/lactate are precursors for butyrate). This aligned with significant positive correlations between *B. adolescentis* and acetate/butyrate across all study arms (Figure 16).





Next, adding the protein products increased a wide range of species in the family *Bacteroidaceae*, some of which have been shown to display proteolytic activity in past studies<sup>22,70</sup>. Further, some members of this family are prominent acetate/propionate producers of the gut microbiota<sup>47</sup>. Importantly, while all treatments generally stimulated each species, strongest increases were highly product-specific for different species (most abundant species with in the gut microbiome are indicated by underlining):

- YP: <u>Bacteroides thetaiotaomicron</u>, B. faecis, B. finegoldii, B. eggerthii, B. ovatus
- WPI: B. caccae, B. fragilis, Phocaeicola vulgatus, P. massiliensis
- SPI: B. uniformis, B. stercoris, P. dorei
- WPI/SPI : B. clarus



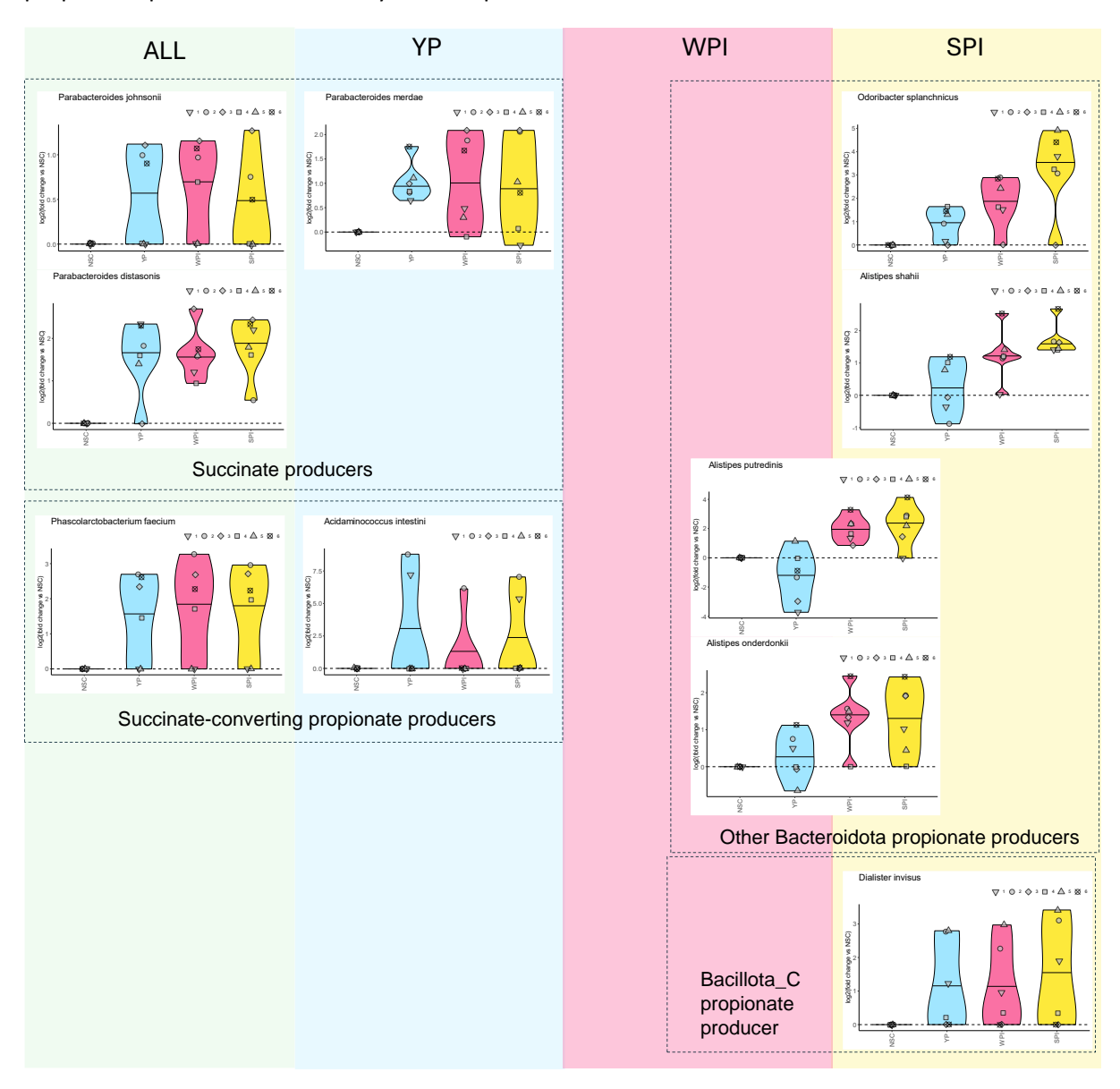
Besides *Bacteroidaceae*, the test products also increased the abundances of propionogenic species belonging to other *Bacteroidota* families with the highest specificity observed for:

- **SPI**: Odoribacter splanchnicus<sup>64</sup>, Alistipes shahii<sup>62</sup>
- SPI/WPI: A. putredinis, A. onderdonkii<sup>62</sup>



Additionally, the test products, especially **SPI**, also increased the abundance of the **Bacillota\_C** propionate producer *Dialister invisus*<sup>47</sup>.

In addition to the aforementioned propionate producers, *Parabacteroides* species in the family *Tannerellaceae* are capable of producing a large quantity of succinate, a precursor of propionate biosynthesis. Succinate can then be converted into propionate by other propionate producers<sup>65</sup>, notably by the members of *Acidaminococcaceae* (phylum Bacillota\_C) which use succinate as the main energy source. Interestingly, both *Parabacteroides* species and two members of *Acidaminococcaceae* (*Phascolarctobacterium faecium*, *Acidaminococcus intestini*) were promoted by all test products, suggesting cross-feeding between these taxa as a mechanism contributing to the propionate production induced by the test product<sup>71</sup>.

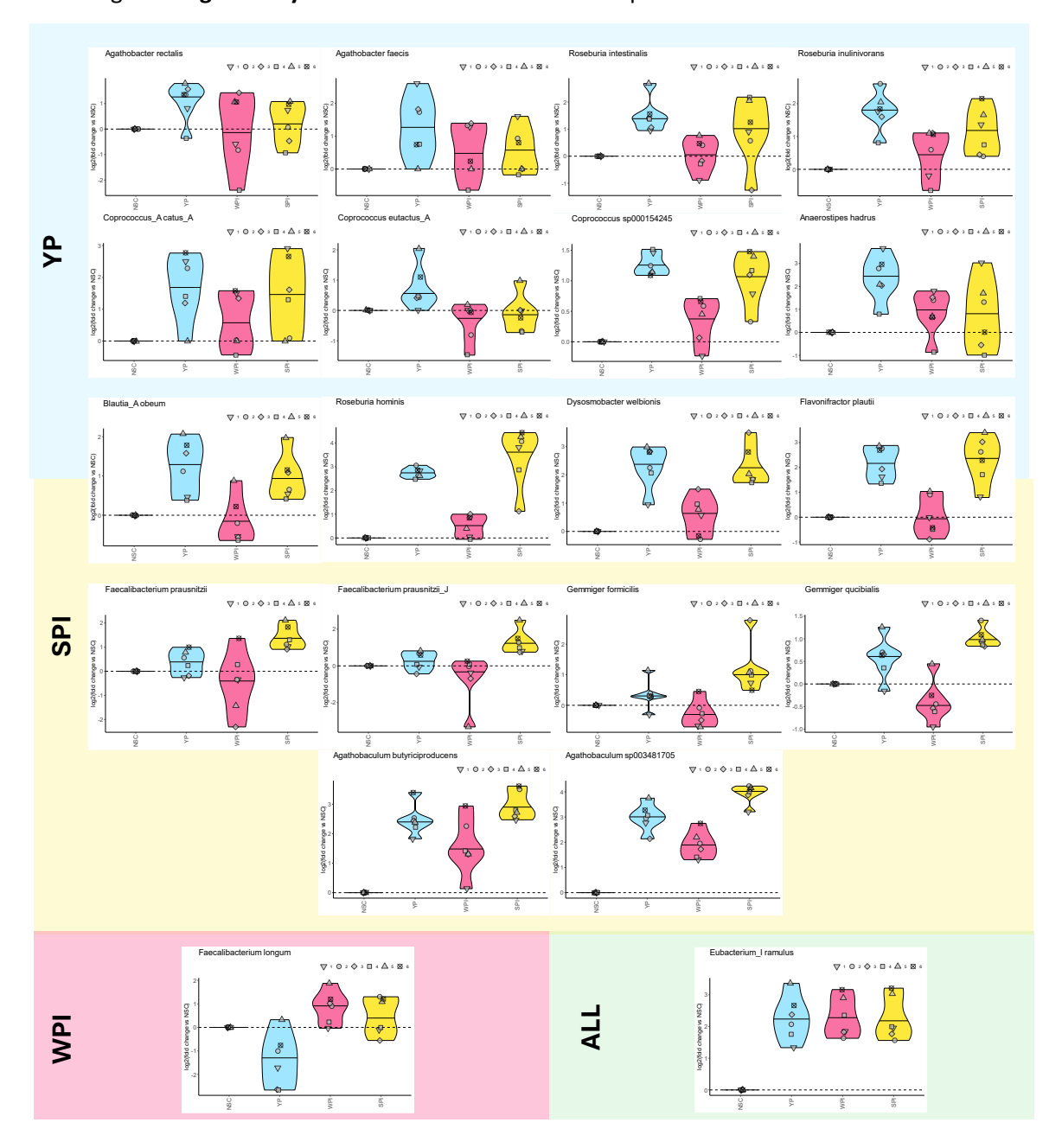


Further, the test products exerted product-specific stimulatory effects on different species belonging to families within the phylum Bacillota\_A, i.e., *Lachnospiraceae*, *Butyricicoccaceae*, *Oscillospiraceae* and *Ruminococcaceae*, which contain major butyrate producers of the gut microbiota<sup>47</sup>. Especially, each protein product again exerted product-specific effects on certain butyrate producers:



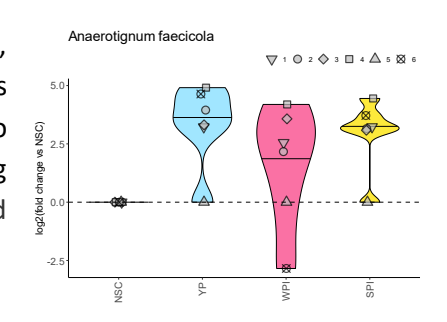
- **YP**: Agathobacter rectalis, A. faecis<sup>47</sup>, Roseburia intestinalis, R. inulinivorans<sup>47</sup>, Coprococcus spp.<sup>47</sup>, Anaerostipes hadrus<sup>47</sup>
- **SPI**: Faecalibacterium prausnitzii, Faecalibacterium prausnitzii\_J<sup>51</sup>, Gemmiger formicilis<sup>54</sup>, G. qucibialis, Agathobaculum spp.<sup>72</sup>
- YP/SPI: Blautia spp., R. hominis<sup>47</sup>, Dysosmobacter welbionis<sup>73</sup>, Flavonifractor plautii<sup>74</sup>
- WPI: Faecalibacterium longum<sup>75</sup>
- All test products: Eubacterium\_I ramulus<sup>47</sup>

→ Considering the prevalence of *Faecalibacterium* and *Agathobaculum* (Figure 9), the stimulatory effects of **SPI** on species within these genera may contribute to the **higher butyrate** production observed for **SPI** compared to YP/WPI. This is also evidenced by the significant positive correlations between butyrate production and *Agathobaculum* spp. as well as *F. prausnitzii*. In addition, **YP** generally displayed stronger stimulation of most butyrate producers (except *F. longum*), thus correlating with **higher butyrate levels** observed for **YP** compared to **WPI**.

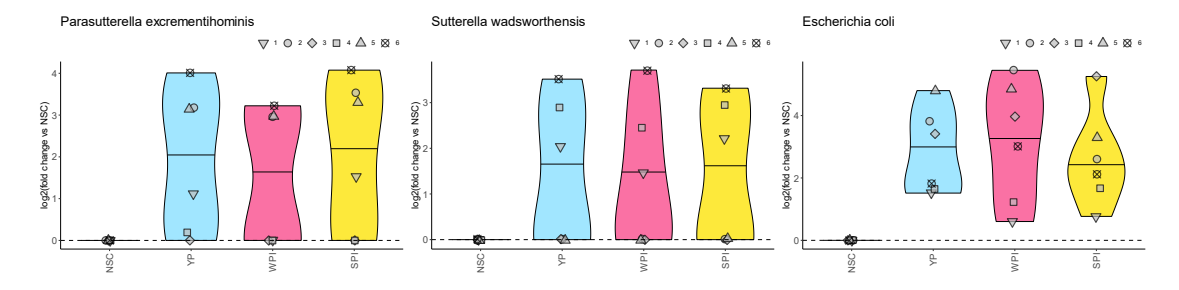




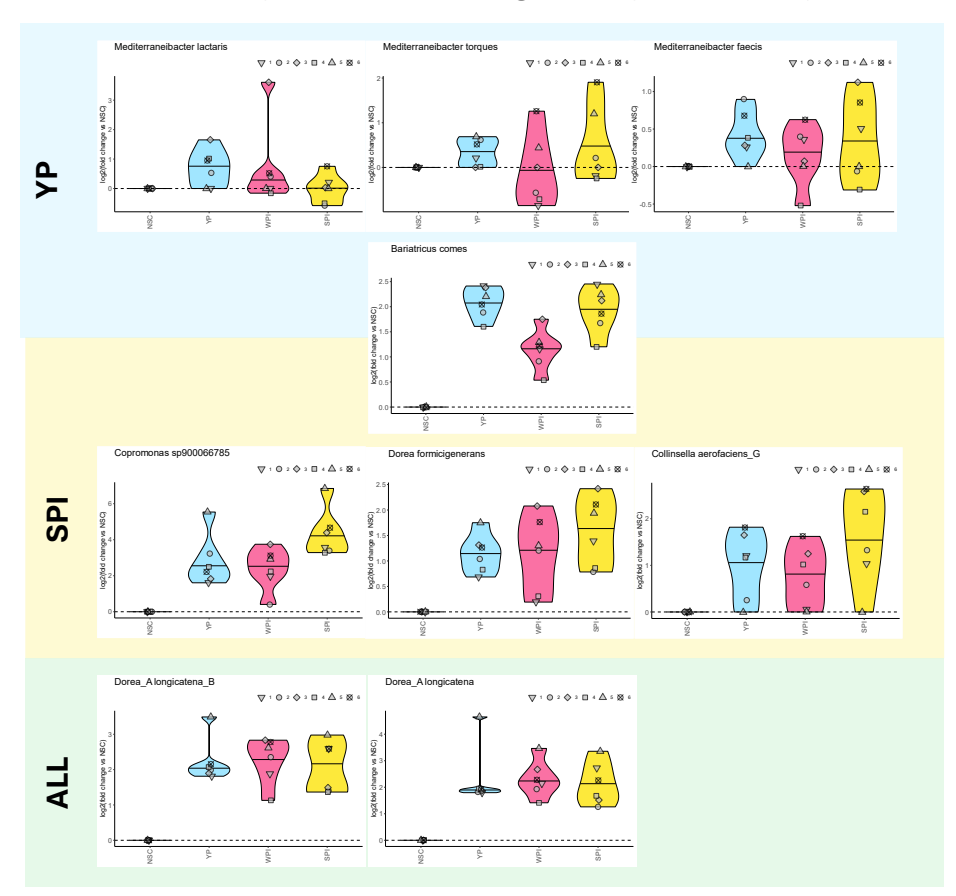
Another notable SCFA-producing species within Bacillota\_A, i.e., *Anaerotignum faecicola*, were also strongly increased by **YP/SPI**, with less consistent effects also observed for WPI. *A. faecicola* is closely related to amino acid-decomposing *A. aminivorans*<sup>76</sup> which is capable of producing acetate, propionate from L-alanine and L-serine, as well as propionate and butyrate from L-threonine<sup>77</sup>.



In addition, increased proteolytic activity of the gut microbiota was also evidenced by the increased of multiple species within the phylum **Pseudomonadota** (formerly known as **Proteobacteria**), i.e., **Parasutterella excrementihominis**, **Sutterella wadsworthensis**, **Escherichia coli**.



Finally, following species with less known implications on SCFA production and host health were also promoted by the protein products: *Mediterraneibacter* spp. (higher/more consistent increase for YP), *Copromonas* spp., *Dorea formicigenerans*, *Collinsella* spp. (higher increase for SPI), *Bariatricus comes* (higher increase for both YP/SPI) as well as *Dorea longicatena* (all treatments).





#### 6 Metabolomics

#### 6.1 Quality control

A total of **592 compounds** was detected upon the **LC-MS** metabolomics analysis. As elaborated in materials and methods, the **identification of compounds was performed at three levels**, i.e., level 1 (retention time, accurate mass and MS/MS spectra), level 2 (2a: retention times and accurate mass - 2b: accurate mass and MS/MS spectra) and level 3 (accurate mass). **352** metabolites were annotated on **level 3**, **108** on **level 2b**, **90** on **level 2a**, and **42** on **level 1**. Given the higher degree of certainty of correct annotation at level 1 and 2a, the report mostly focusses on level 1/2a metabolites.

A quality control was performed by analysing a QC sample, created by taking a small aliquot from each sample, with regular intervals throughout the analysis sequence. As followed from the PCA based on the level 1/2a-annotated metabolites, these 9 QC samples grouped tightly together indicating that the biological variance (represented by the spread of the samples) largely exceeded the analytical variance (represented by the spread of QC samples) (Figure 17). The high reproducibility of both the SIFR® incubations as well as the metabolomics analysis warrants that observed differences are truly due to a treatment and not due to technical variation.

Further, when focusing on the effects of time, there was a marked differential clustering of 0h and 24h samples (Figure 17A). As the incubation progressed, samples moved from the top left to the lower right of the PCA, suggesting consumption of nutrients/production of specific metabolites between 0h (INO) and 24h.

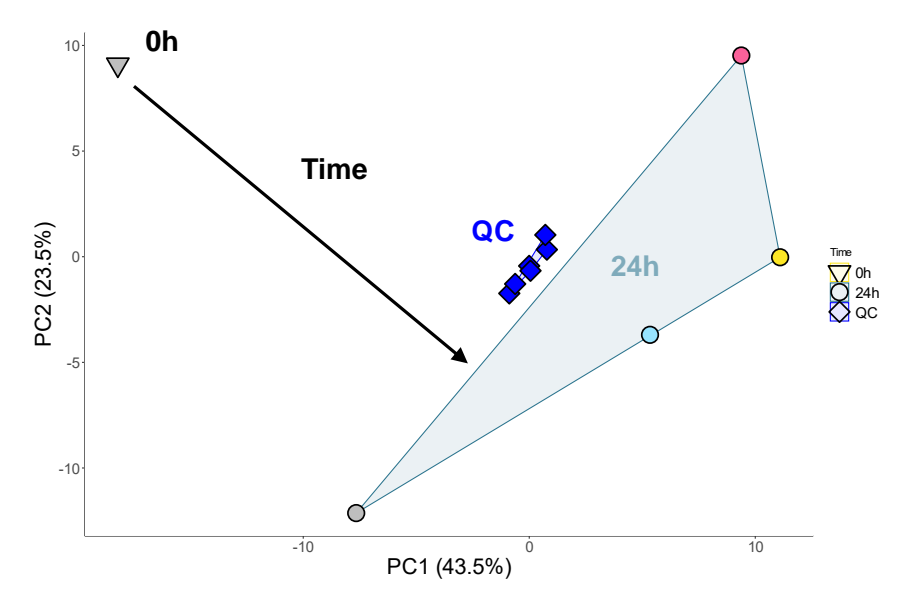


Figure 17. Principal component analysis (PCA) summarizing the impact on microbial metabolite production by the gut microbiota of human adults (n = 6) upon treatment with the test products compared to a parallel untreated no substrate control (NSC). The PCA was calculated <u>based on standardized average values of metabolites annotated at level 1/2a</u> as quantified via untargeted LC-MS, at 0h and 24h of colonic incubations.

#### 6.2 In-depth analysis of treatment effects

While the data was statistically processed at each annotation level, the current report focuses on 132 level 1/2a metabolites (ensuring correct annotation) and given that these metabolites have previously been linked with the gut microbiome (as nutrient or metabolite) often in the context of



health or disease (Supplementary Table 4). Out of these **132** metabolites, **the levels of 91 metabolites increased in at least 4 donors** along 24h incubations<sup>1</sup>. This could be attributed to their **production by the gut microbes** or **their presence in one of the test products**. Further, **78** out of **91** aforementioned metabolites (FDR = 0.20) were significantly affected by any of the test products.

To better grasp treatment effects at 24h, an additional PCA was made (Figure 18), based on the average values of the 78 aforementioned metabolites across 6 donors at 24h only (thus omitting differences between 0-24h that were already represented in Figure 17). Similar to treatment effects on the key fermentation parameters and microbial composition, the resulting PCA demonstrated pronounced impact of the test products (mostly observed along PC1), relating to the increased levels of a wide range of microbial metabolites. Further, it also demonstrated the differences across the test products (observed along PC2) with the largest differences between YP and WPI.

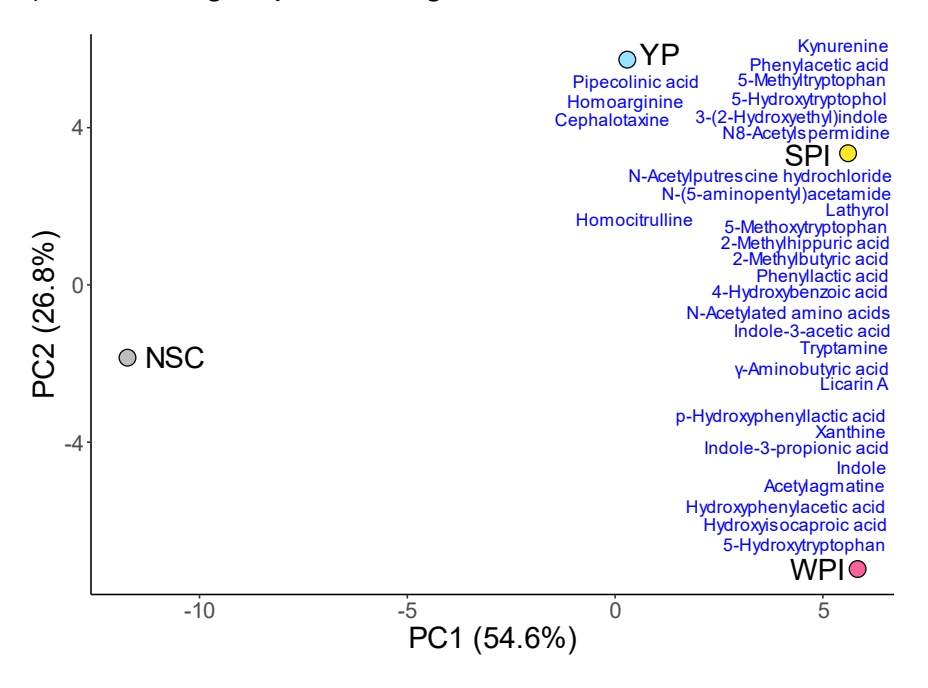


Figure 18. Principal component analysis (PCA) summarizing the impact on microbial metabolite production by the gut microbiota of 50-65y male human adults (n = 6) as tested via the SIFR® technology, upon simulated ingestion of the test products. The PCA was calculated based on the standardized average values across the six donors tested for 91 'produced' metabolites annotated at level 1/2a, quantified via untargeted LC-MS, at 24h upon initiation of the colonic incubations. Several notable significantly affected metabolites discussed in the text below are highlighted in the PCA.

To refine the insights, the **78** significantly affected metabolites were presented in a heat map (based on the log<sub>2</sub> ratios versus the NSC; Figure 19). Notable metabolites related to health or diseases will be discussed further in the text below. The absolute levels of the significantly affected metabolites can be found in **Supplementary File 3** (section 10.1). In addition, in order to **link the production of specific metabolites to specific microbial taxa**, a **correlation analysis** was again performed between these significantly affected metabolites and compositional data (at family level (Figure 20) and species level (Figure 21)). This revealed that **correlations** could be established between the presence of **specific taxa and the production of specific metabolites**.

-

<sup>&</sup>lt;sup>1</sup> The increase of a metabolite along the 24h incubation was defined by a higher value in at least one test condition at 24h compared to the initial concentration in the blank for at least 4 out of 6 donors.



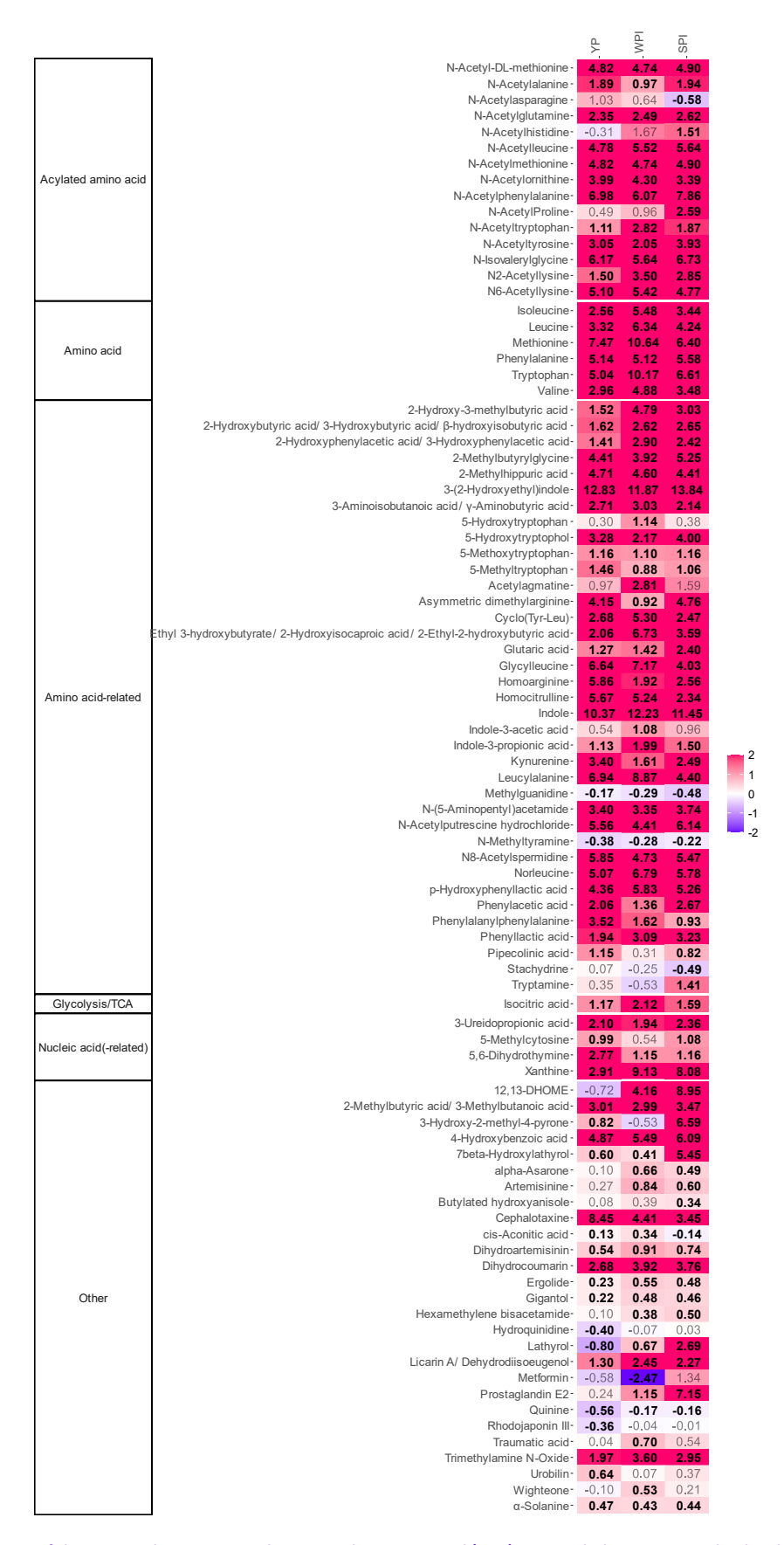


Figure 19. The impact of the test products compared to a no substrate control (NSC) on <u>metabolites annotated at level 1/2</u> as quantified via untargeted LC-MS after 24h of incubation, tested via the SIFR® technology for <u>human adults (n = 6)</u>. The metabolites were <u>significantly affected</u> by any of the treatments (FDR = 0.20). Significant differences are indicated by bold of the average  $log_2$ (abundance treatment/abundance NSC).



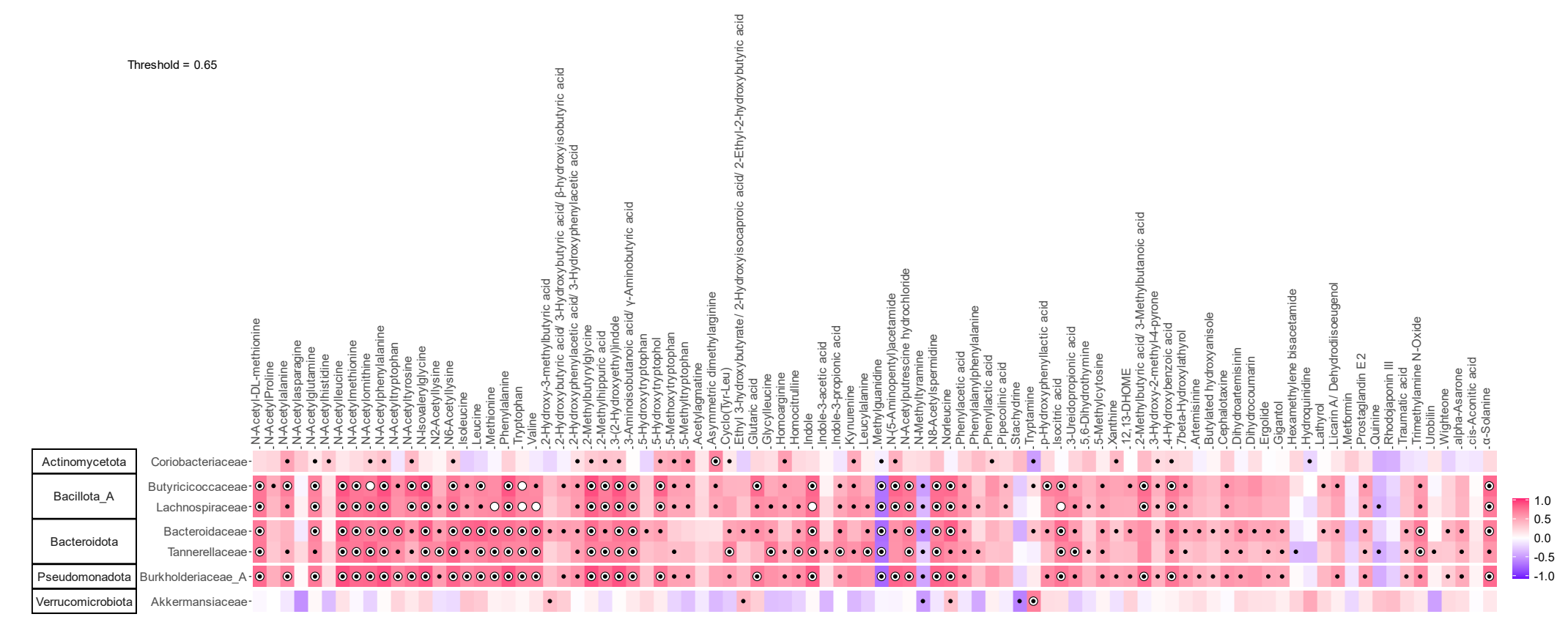


Figure 20. Regularized Canonical Correlation Analysis (rCCA) to highlight correlations between specific <u>significantly affected metabolites</u> (shown in Figure 19) and <u>significantly/consistently affected families</u> (shown in Figure 14A) upon simulated ingestion of the test products (threshold > 0.65). The white circles indicate values larger than the threshold and black dots indicate statistical significance (p < 0.05) in the individual correlations between the metabolites and the families based on Kendall rank correlation coefficient.

Report reference: 0443/P0140



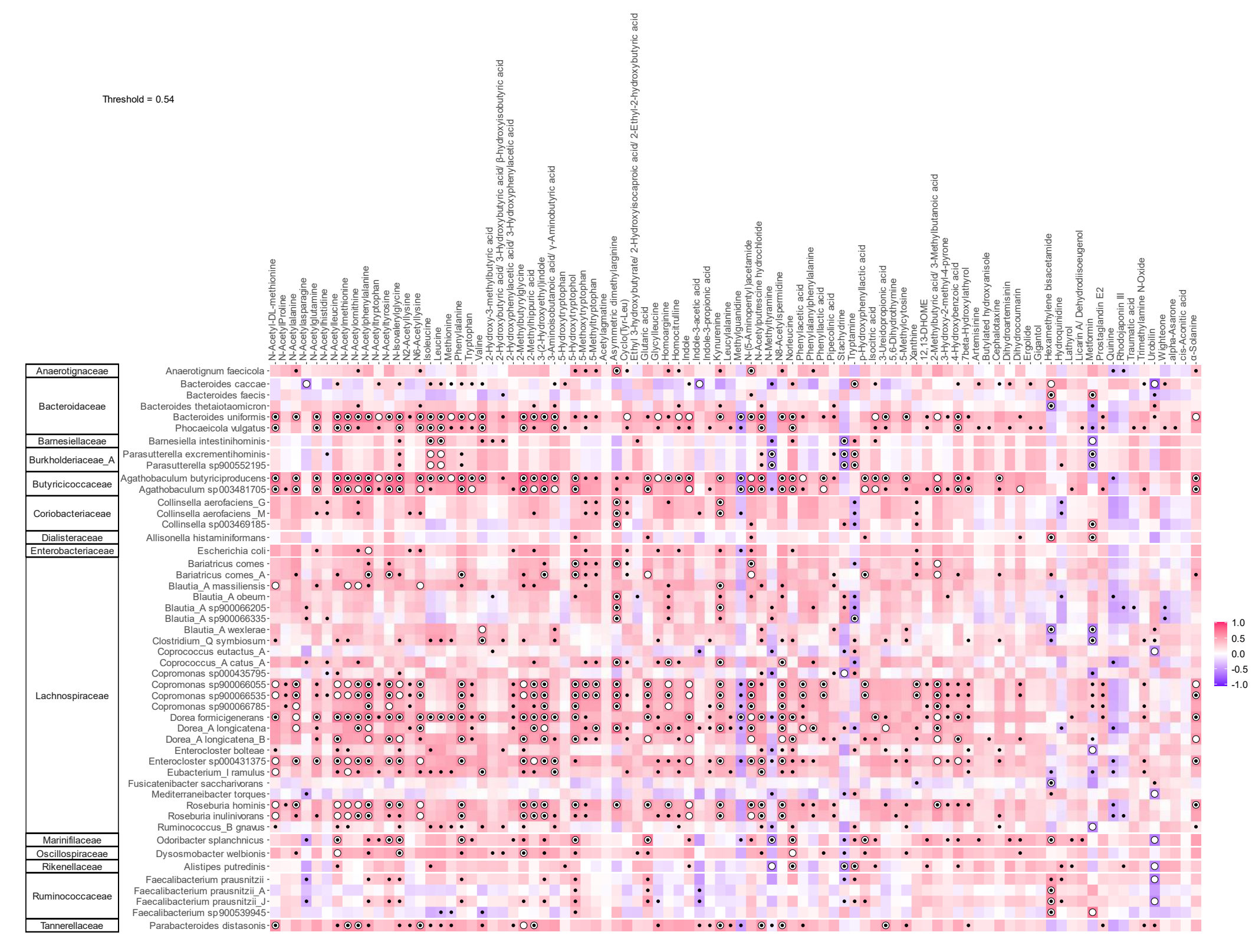
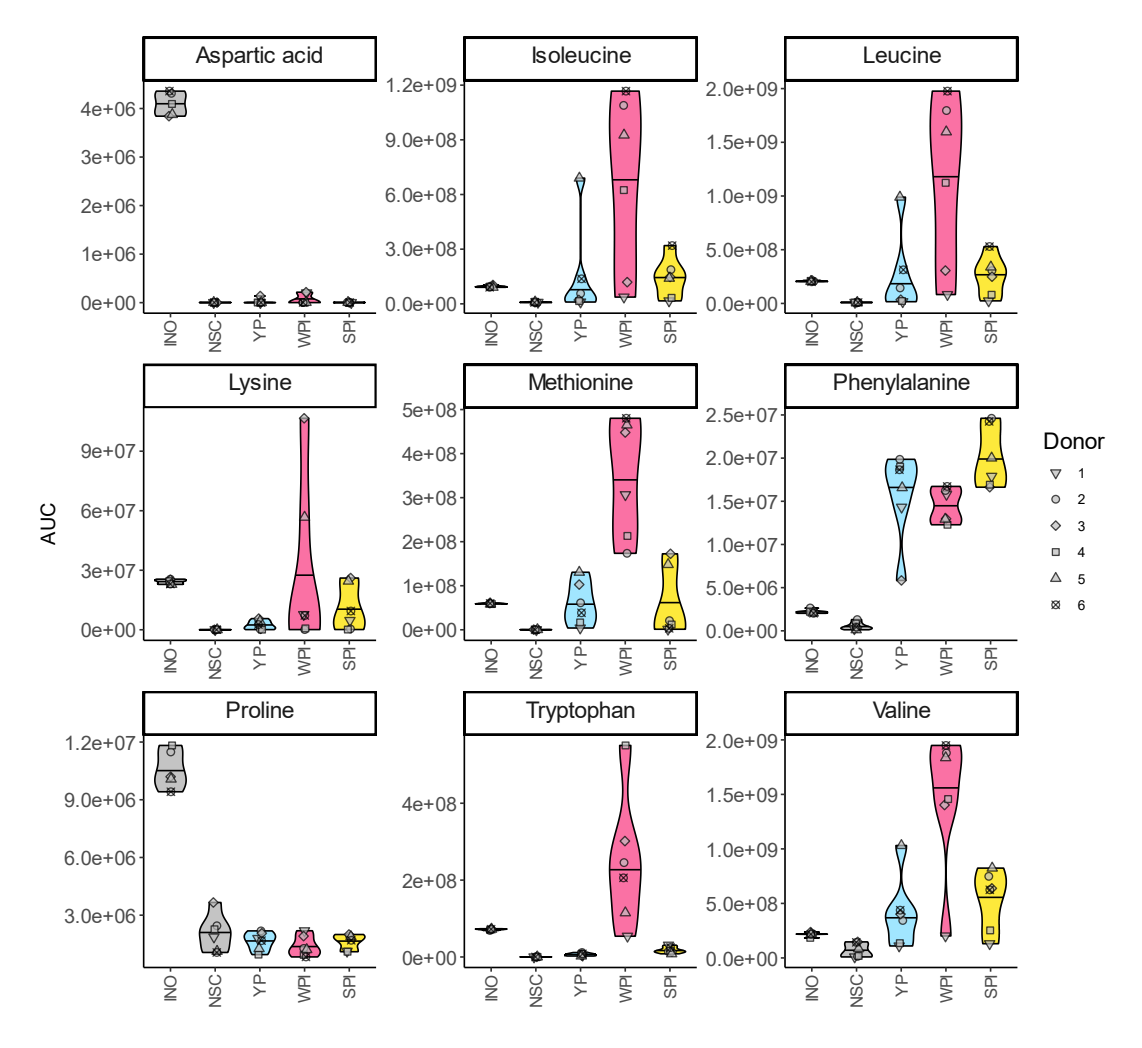


Figure 21. Regularized Canonical Correlation Analysis (rCCA) to highlight correlations between specific <u>significantly affected metabolites</u> (shown in Figure 19) and significantly/consistently affected species shown in Figure 15) upon simulated ingestion of the test products (threshold > 0.54). The white circles indicate values larger than the threshold and black dots indicate statistical significance (p < 0.05) in the individual correlations between the metabolites and the species based on Kendall rank correlation coefficient.



First, upon 24h of colonic fermentation, the protein products still elevated the levels of **all essential amino acids** detected (isoleucine, leucine, lysine, methionine, phenylalanine, tryptophan and valine) compared to NSC, indicating the **test products** are a **rich source of these amino acids**. Moreover, despite the simulation of **digestion/absorption along the upper GIT** and **fermentation by bacteria along the colon** (processes that likely strongly decreased amino acid levels), part of the amino acids was thus still present in the colonic environment, showing **partial resistance to digestion/absorption/fermentation**. Interestingly, the **marked interpersonal differences** in the treatment study arms (particularly WPI) suggest that the amino acids derived from the protein products during digestion were indeed (to different extent) further converted into metabolites by the gut microbes. Specific findings were that **SPI** exhibited the **highest levels of phenylalanine**, while **WPI** exhibited the highest levels of the **other essential amino acids**. Finally, **all detected amino acids** were **efficiently consumed** when comparing the NSC samples at 24h with those collected at 0h (INO). Such **efficient conversion of amino acids is of interest** given the **potential resulting production of health-related metabolites**.



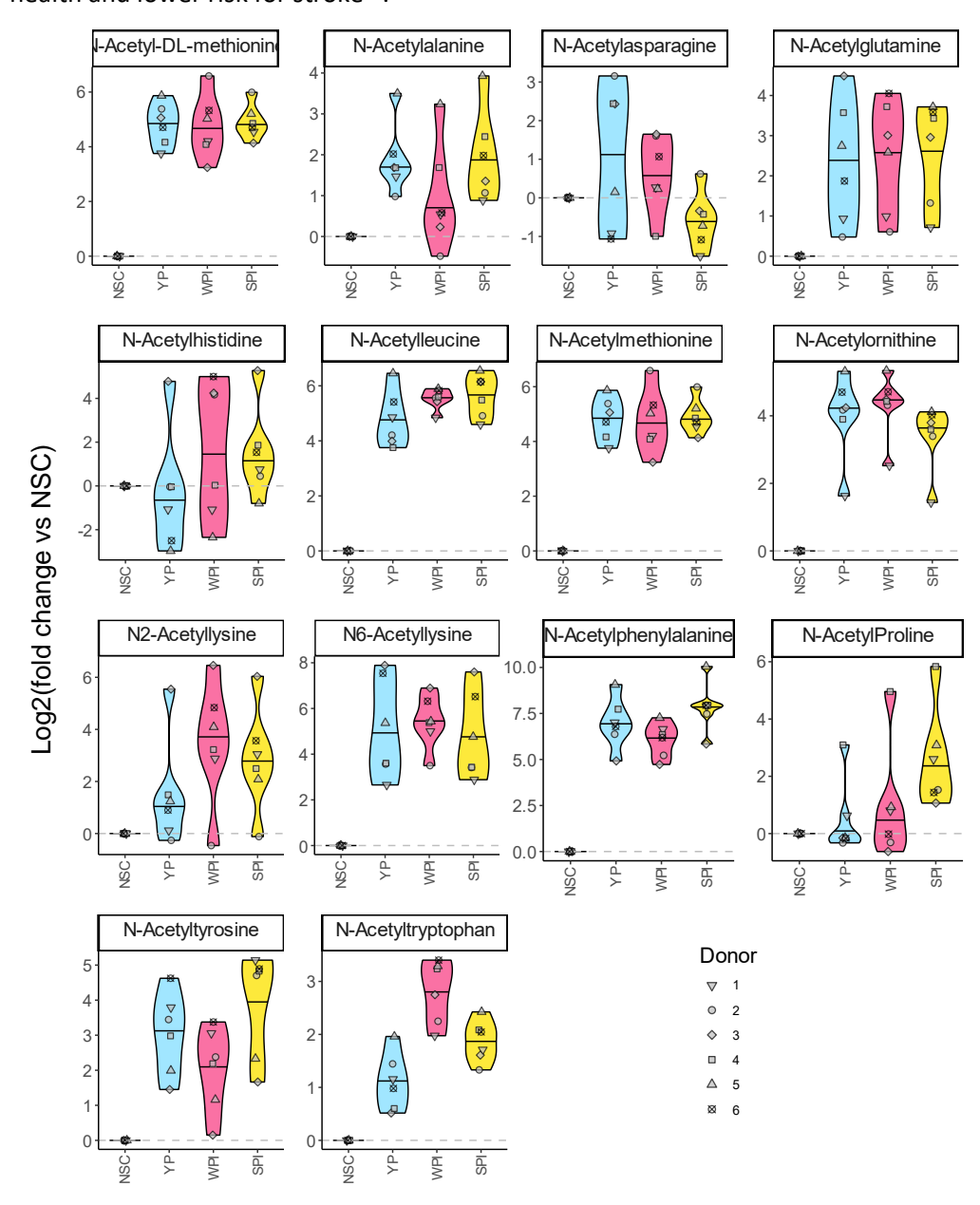
A prominent class of amino acid-derived metabolites that significantly stimulated by the protein products were **N-acetylated amino acids**. The strength of the stimulation also varied for different N-acetylated amino acids, depending on the test products. For example, **WPI** stimulated more **N-acetyltryptophan**, **N-acetylornithine** and **N2-acetyllysine** compared to YP/SPI, while **N-acetylhistidine**, **N-acetylphenylalanine**, **N-acetylproline** were the most enhanced by **SPI**. Further, the



levels of **N-acetylalanine**, **N-acetylasparagine**, **N-acetylornithine**, **N-acetylphenylalanine**, **N-acetyltyrosine** were higher for **YP**, compared to at least one of the other two products.

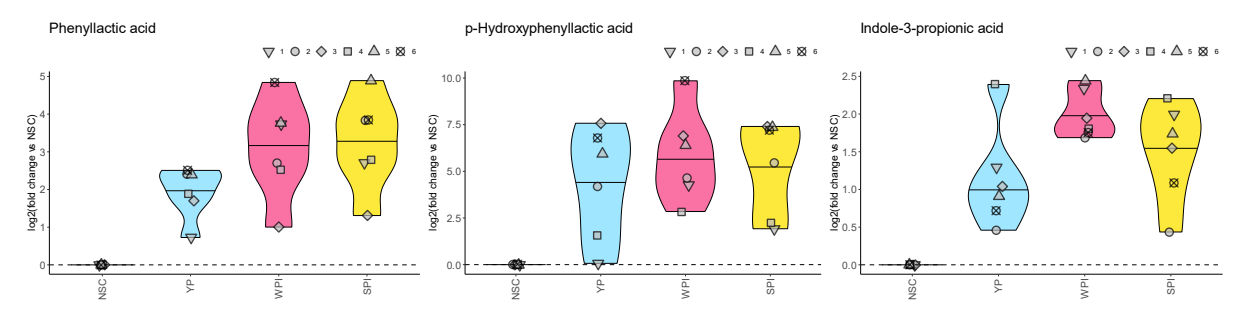
Stimulation of N-acetylation of amino acids has recently been observed upon treatment with human milk oligosaccharides and was suggested to contribute to **early-life immune development and a healthy gut barrier function**<sup>78</sup>. Further, other potential health-promoting effects have been implied for several N-acetylated amino acids:

- Treatment with **N-acetylleucine** showed neuroprotective effects, attenuates neuronal death and neuroinflammation in mice<sup>79,80</sup>
- In animal models, treatment with **N-acetyltyrosine** significantly increases the stress tolerance and potentially represses tumor growth<sup>81</sup>
- Higher plasma levels of **N-acetylornithine** have been associated with better cardiometabolic health and lower risk for stroke<sup>82</sup>.





<u>Two aromatic lactic acids</u> (3-phenyllactic acid, hydroxyphenyllactic acid) were boosted by all three protein products. While the third aromatic lactic acid (indole-3-lactic acid) was not detected in the metabolomics analysis, its downstream metabolite indole-3-propionic acid was also significantly increased by all three test products, especially by WPI.



Breastmilk-promoted *Bifidobacterium* species can convert **aromatic amino acids** (**tryptophan**, **phenylalanine and tyrosine**) into their respective **aromatic lactic acids** (**indole-3-lactic acid**, **3-phenyllactic acid and 4-hydroxyphenyllactic acid**) by aromatic lactate dehydrogenase (ALDH) via a reductive pathway (Figure 22) <sup>83</sup>. Metabolites in the reductive pathways that were stimulated in the current study are highlighted in red rectangles. It was also demonstrated that enhanced **indole-3-lactic acid** production were associated with activation of the aryl hydrocarbon receptor (AhR), a receptor important for controlling **intestinal homeostasis** and **immune responses**<sup>8</sup>. Further, its metabolite **indole-3-propionic acid** also exhibits strong anti-inflammatory effects and is linked to a wide range of health benefits such as neuroprotection, preventing liver fibrosis and kidney injury, promoting muscle growth, protecting the ling from bacterial and fungal infections as well as regulating cardiovascular health <sup>84</sup>. Overall, treatments with the protein products might thus exert health benefits via the production of **aromatic lactic acids**.

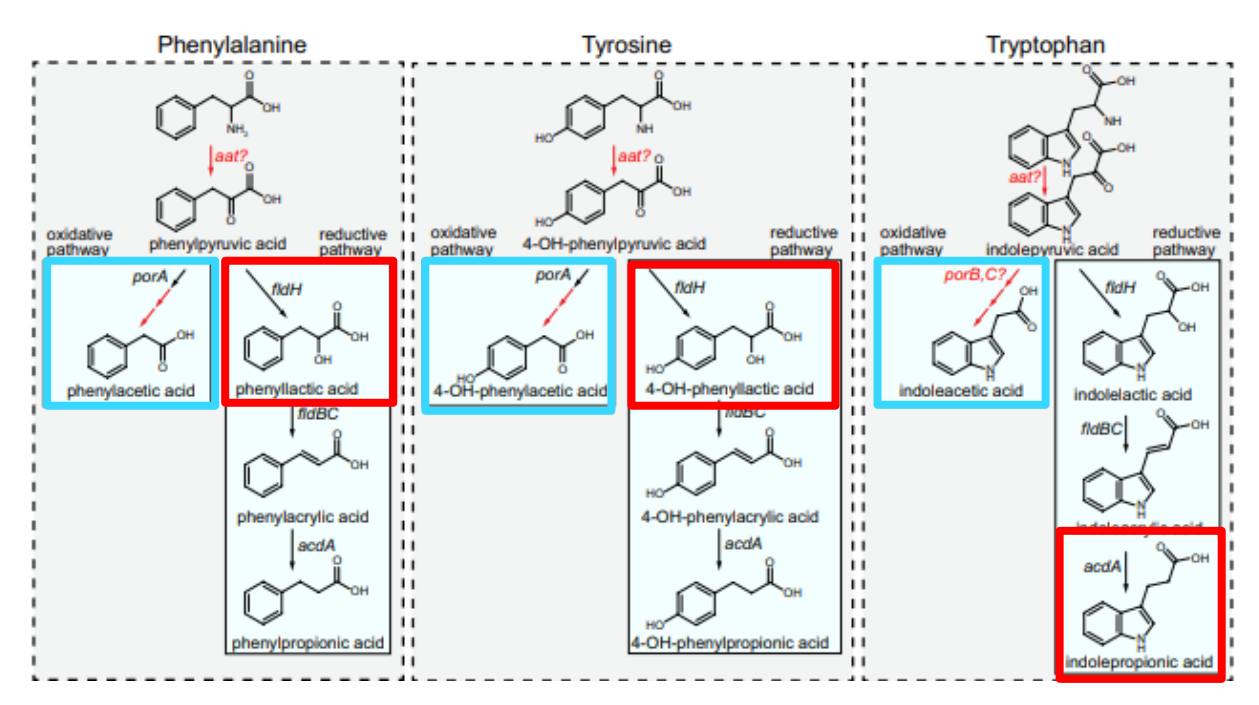
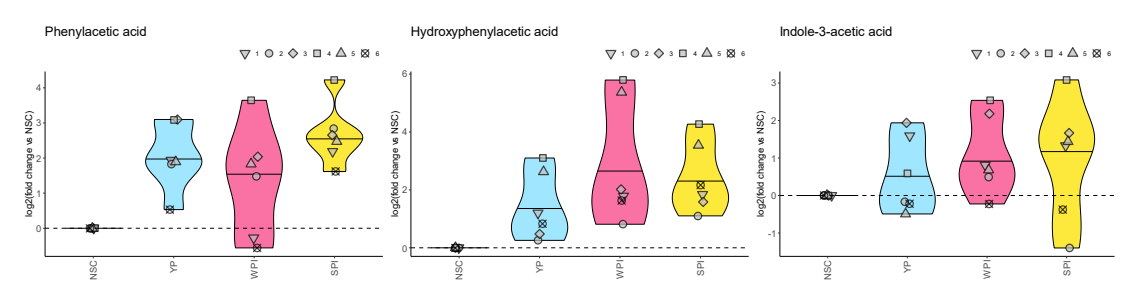


Figure 22. Pathways of microbial fermentation of aromatic lactic acids<sup>85</sup>, highlighting metabolites in the reductive pathways (red rectangles) and in the oxidative pathways (blue rectangles) that were increased by specific test products during the current project.



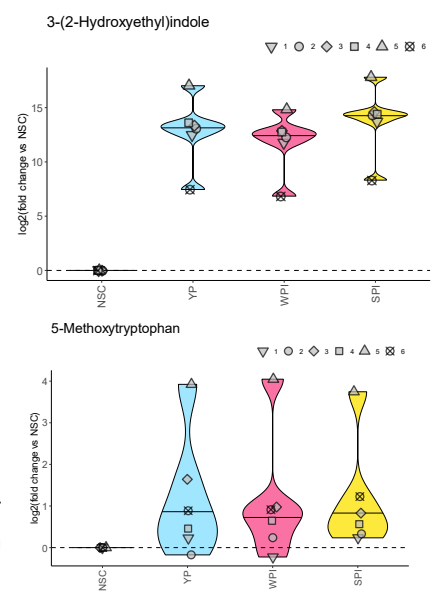
Besides the metabolites in the reductive pathways, the protein products also strongly promoted three metabolites produced from aromatic amino acids via the oxidative pathway (**phenylacetic acid**, **hydroxyphenylacetic acid and indole-3-acetic acid**) (Figure 22, blue rectangles). These metabolites have been implicated in both health and disease context:

- Indole-3-acetic acid (IAA): IAA was suggested to have both potential health-related effects and disease-related effects. Hendrikx *et al.* reviewed the mechanism of action of tryptophan catabolites and attribute following effects to IAA, i.e., activation of AhR, anti-oxidative and anti-inflammatory effects<sup>86</sup>. IAA was shown to alleviate ankylosing spondylitis<sup>87</sup> and attenuated hepatic lipogenesis in mice<sup>88</sup>. However, high IAA levels positively correlated with markers of oxidative stress and inflammation and with high mortality in chronic kidney disease<sup>89</sup>.
- Hydroxyphenylacetic acid (HPAA): HPAA exhibits antioxidant<sup>90</sup> and anti-microbial properties<sup>91</sup>, as well as hepato-protective activity<sup>92</sup> in animal model.
- **Phenylacetic acid:** a causal relation relationship between gut-derived PAA and hepatic steatosis (abnormal retention of fat in liver) has been established in mice model<sup>93</sup>.



Besides IPA and IAA, <u>multiple tryptophan metabolites</u> were also strongly upregulated by all three test products, indicating increased tryptophan metabolism:

- 3-(2-hydroxyethyl)indole (tryptophol): has been suggested as a functional analogue of the neurotransmitter melatonin and serotonin. Further, together with the tryptophan metabolites indole-3-pyruvic acid, indole-3-acetaldehyde, gut microbiota-derived tryptophol also potentially ameliorates the disease severity related to ulcerative colitis by reducing inflammation and attenuating intestinal permeability<sup>94</sup>.
- **5-Methoxytryptophan** (5-MTP) is an endothelial factor with antiinflammatory properties. 5-MTP protects endothelial barrier function and promotes endothelial repair<sup>95</sup>.



∇102♦3□4△5⊗6

V 1 O 2 O 3 D 4 A 5 8

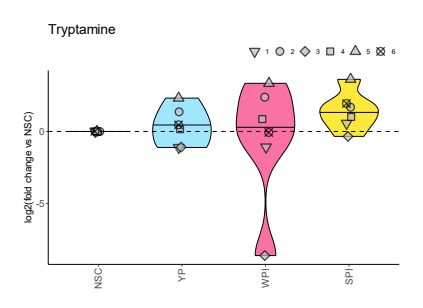
5-Methyltryptophan



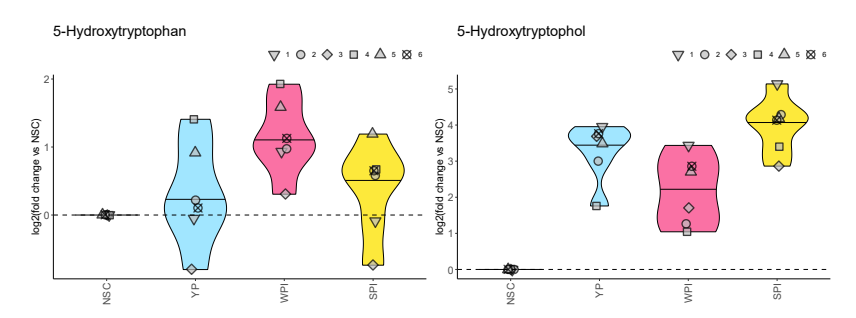
- 5-Methyltryptophan (5-MT): while 5-MT has not been associated with any potential health benefits, its isomer 1-methyltryptophan (1-MT) (identical molecular mass) have been shown to ameliorate high-fat diet-induced depression in mice<sup>96</sup>. Further, 1-MT also drives tryptophan catabolism toward the kynurenic acid pathway which mediate various immunomodulatory effects under inflammatory conditions<sup>97</sup>
- Indole Indole: synthesized exclusively through the action of the bacterial enzyme tryptophanase. Indole induces the expression of genes involved in the intestinal epithelial barrier function and mucin production, as well as increases expression of the regulatory cytokine IL-10 and decreases expression of the pro-inflammatory IL-898. Thus, indole potentially enhances gut barrier function as well as may exhibit some anti-inflammatory effects. However, excessive levels of indole could cause oxidative stress in colonocytes as well as the production of harmful metabolites after absorption such as the uremic toxin indoxyl sulfate which is produced in the liver<sup>98</sup>

Besides, other tryptophan-derived metabolites were boosted in a more product-specific manner:

Tryptamine: only significantly promoted by SPI. Tryptamine is a neurotransmitter and act as agonist of hTAAR1 receptor which is under investigation as a novel treatment for depression, addiction, and schizophrenia<sup>99</sup>. Further, tryptamine induces the release of serotonin (= 5-hydroxytryptamine (5-HT)) by enteric neuron, and thus stimulating gastrointestinal motility<sup>100</sup>. Further, 5-HT enhances intestinal epithelial proliferation, and decreased injury from intestinal inflammation<sup>101</sup>. Activation of serotonin signalling leads to neurogenesis and

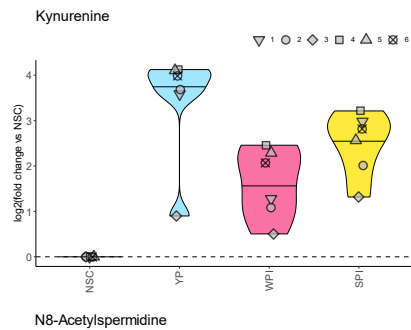


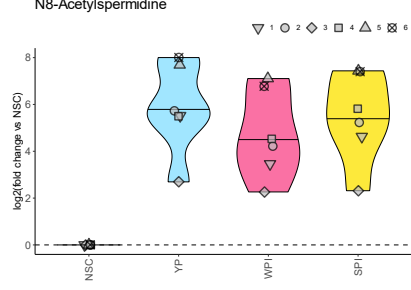
- neuroprotection in the setting of intestinal injury. Serotonin dysfunction is likely involved in the pathophysiology of a number of functional GI disorders, such as chronic constipation, irritable bowel syndrome and functional dyspepsia<sup>102</sup>.
- 5-hydroxytryptophan (5-HTP): only significantly increased for WPI. 5-hydroxytryptophan restores gut microbiota dysbiosis in a mouse model of depression<sup>103</sup>. Decarboxylation of 5-HTP would yield serotonin.
- Interestingly, the downstream metabolite of serotonin, 5-hydroxytryptophol (5-HTOL) was also identified. In contrast to the serotonin precursor 5-HTP which displayed higher levels for WPI, 5-HTOL exhibited higher levels for YP and SPI





- Kynurenine: most pronounced stimulation was observed for YP.
   The kynurenine pathway promotes immunosuppression in response to inflammation or infection. Alleviating the accumulation of kynurenine in the central nervous system can positively affect mental health, such as reducing stress-induced depressive symptoms<sup>104</sup>.
- **N8-acetylspermidine** is the acetylated form of spermidine a polyamine derived from arginine/agmatine. Dietary polyamine uptake correlates with reduced **cardiovascular** and cancer-related mortality<sup>105</sup>. In addition, **spermidine** preserves mitochondrial function, exhibits **anti-inflammatory** and reduces **blood pressure**<sup>105,106</sup>.

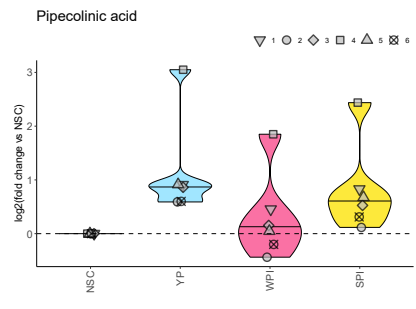




In addition to tryptophan, other amino acids were also converted into other health- and disease-related metabolites by the gut microbiota. <u>Several other amino acid-derived metabolites</u> that were stimulated by the protein products, and <u>especially enhanced by YP</u>:

Pipecolinic acid: PIPA is a metabolite of lysine and serves as a precursor of other health-related microbial secondary metabolites<sup>107</sup>. Gut microbes have been shown to alleviate constipation in both adults and children by increasing PIPA level in the gut<sup>108,109</sup>

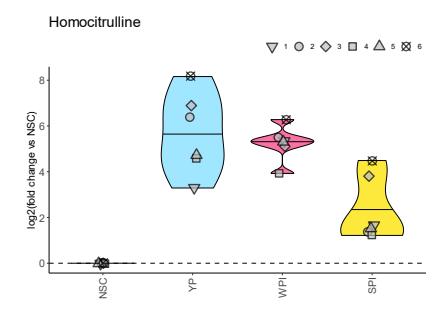
Homoarginine: a non-proteinogenic amino acids that have been studied for its protective effects on cardiovascular system (still debated) <sup>110–112</sup>. In mice, homoarginine supplementation exerted several beneficial effects such as preventing diabetic kidney damage<sup>113</sup> and improving blood glucose in diet-induced obese mice<sup>114</sup>



Homoarginine

\textstyle 1 \in 2 \in 3 \in 4 \in 5 \in 6 \in

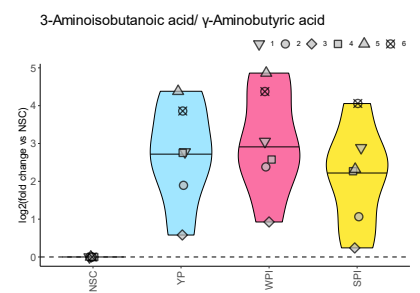
• **Homocitrulline**: elevated homocitrulline levels have been associated with several disease-related conditions such as uraemia and renal failure<sup>115</sup>, inflammation<sup>116</sup> and rheumatoid arthritis<sup>117</sup>





In addition, **YP** exhibited higher levels for <u>other amino acid-derived metabolites</u> compared to at least one of the other two other protein products:

3-aminoisobutanoic acid (BAIBA) or γ-aminobutyric acid (GABA):
GABA can be formed via decarboxylation of glutamate<sup>118</sup> is likely produced by *Bacteroides* and *Parabacteroides* species. GABA a major inhibitory neurotransmitter with relaxing, anti-anxiety, and anti-convulsive effects<sup>119</sup>. GABA increases the cell surface mucin MUC1 that prevents the adhesion of microorganisms <sup>120</sup>. Importantly, a recent human study found that transplant of fecal microbiome from

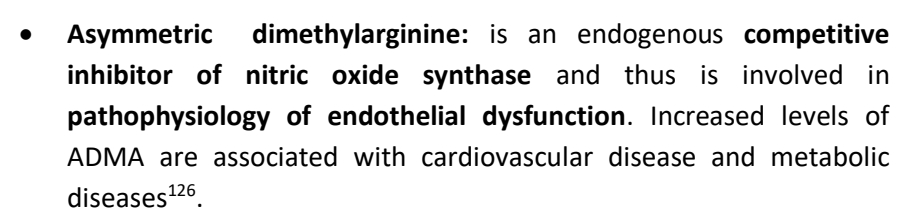


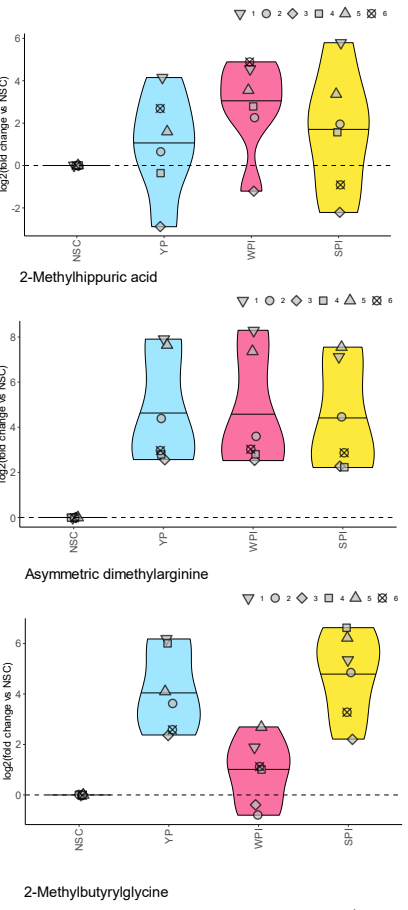
lean to obese individuals resulted in increased levels of GABA in plasma, demonstrating how host–microbial interactions are transmitted systemically<sup>121</sup>.

On the other hand, **BAIBA** is a breakdown product of the nucleobase thymine and can induces browning of white fat and hepatic  $\beta$ -oxidation and is inversely correlated with **cardiometabolic risk factors**<sup>122</sup>. Like GABA (mentioned above), it is reported to be elevated in Indian centenarians and thus associated with longevity <sup>123</sup>

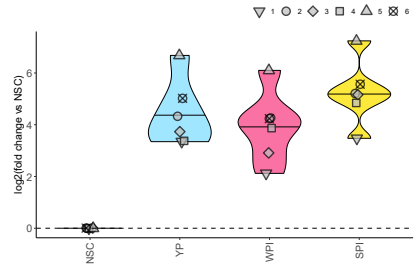
Acetylagmatine

- Acetylagmatine: an arginine metabolite that shows neuroprotective effect in varied types of neurological diseases, including acute attack (stroke and trauma brain injury) and chronic neurodegenerative diseases (Parkinson's disease, Alzheimer's disease). The potential mechanism of agmatine induced neuroprotection includes antioxidation, anti-apoptosis, anti-inflammation, brain blood barrier (BBB) protection and brain edema prevention 124
- **2-methylhippuric acid:** an acylated glycine. **Hippurate** has- been shown to be positively associated with microbial diversity and functional modules for microbial benzoate biosynthetic pathways<sup>125</sup>. Hippurate also potentially promotes cardiovascular and metabolic health, particularly by regulating blood sugar level<sup>125</sup>



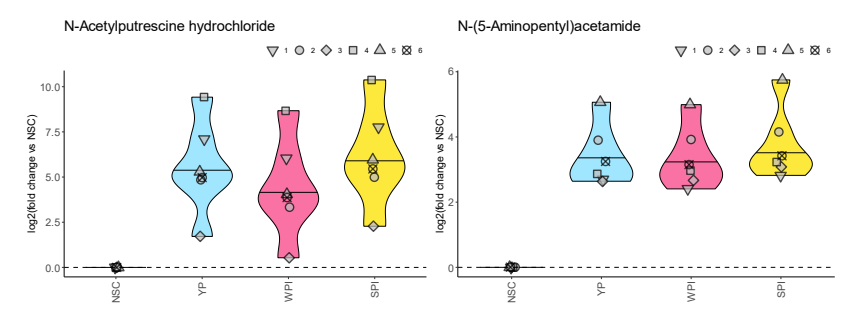


 2-methylbutyrylglycine (2-MBG): 2-MBG was previously shown to induce lipid oxidative damage and decreases antioxidant defences in rat brain<sup>127</sup>

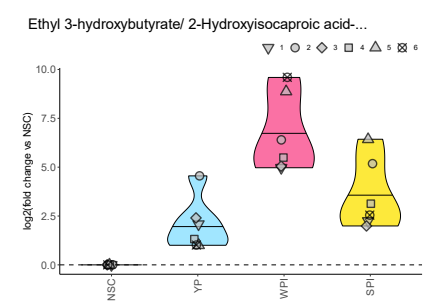




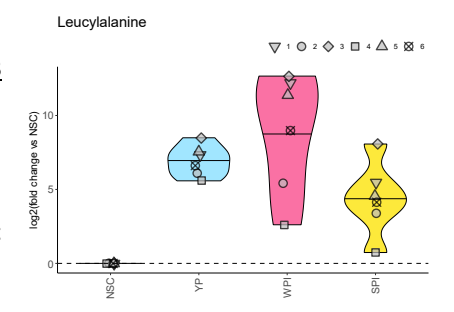
Two additional N-acetylated polyamines, N-acetylputrescine hydrochloride and N-(5-aminopentyl)acetamide (N-acetylcadaverine)



Another notable amino acid-derived metabolite is **2-hydroxyisocaproic acid (HICA)** which were stimulated by all three test products (WPI > SPI > YP). **HICA** is derived from leucine and exhibits both **antimicrobial**  $^{128-130}$  and **anti-inflammatory activity**  $^{131}$ . HICA can also improve **muscle recovery** by inducing an increase in protein synthesis through mTOR signalling  $^{132}$ , which also regulates the innate immune response to bacterial, fungal or parasitic infection.

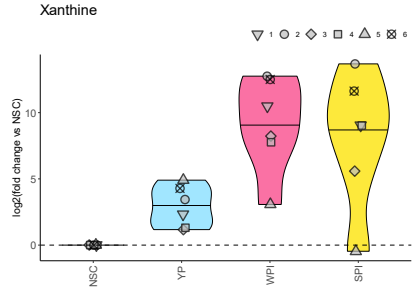


Further, the test products also increased <u>several (cyclic) dipeptides</u> (cyclo(Tyr\_Leu), glycylleucine, leucylalanine, phenylalaninephenylalanine) which could originate from microbial biosynthesis or from incomplete breakdown of proteins. Among these metabolites, preliminary data suggested **leucylalanine** has anticancer activity, however no mechanistic insights have been established<sup>133</sup>.

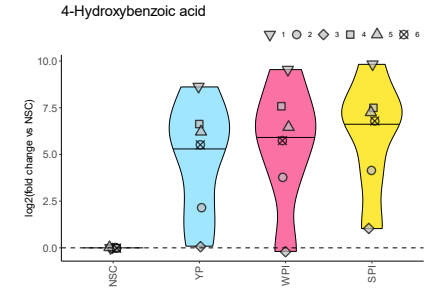


In addition to the amino acid-derived metabolites, other metabolites significantly stimulated by the test products were also noted:

 Xanthine: Gut microbiota-mediated xanthine metabolism is associated with resistance to high-fat diet-induced obesity<sup>134</sup>

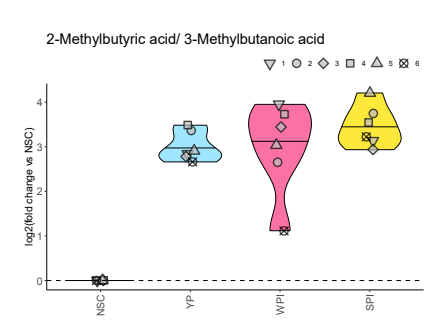


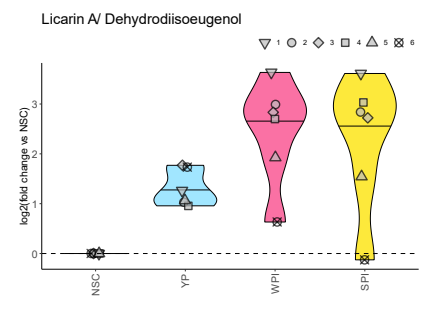
 4-hydroxybenzoic acid (p-hydroxybenzoic acid): a phenolic compound that has been shown to alleviate colitis-related inflammatory responses in mice by improving the mucosal barrier in a gut microbiota-dependent manner<sup>135,136</sup>



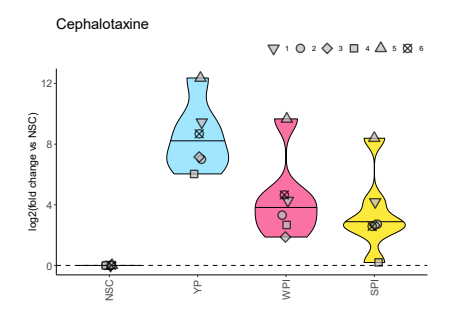


- 2-methylbutyric acid/3-methylbutanoic acid (or isovaleric acid):
   bCFA such as 2-methylbutyric acid and 3-methylbutanoic acid has been associated with both health-related effects such as anti-cancer, lipid lowering, anti-inflammatory and neuroprotective actions but are also potentially associated with disease-related conditions<sup>137</sup>. However, their mechanism of action still remains unknown
- Licarin A/Dehydrodiisoeugenol (DHIE): a neolignan compound found in plants and exhibits antimicrobial, anti-oxidant and anti-inflammatory properties<sup>138</sup>. Further, Licarin A/DHIE potentially exhibits neuroprotective activity<sup>139</sup> and may also have anticancer properties via activation of autophagy and apoptosis in cancer cells<sup>140</sup>.



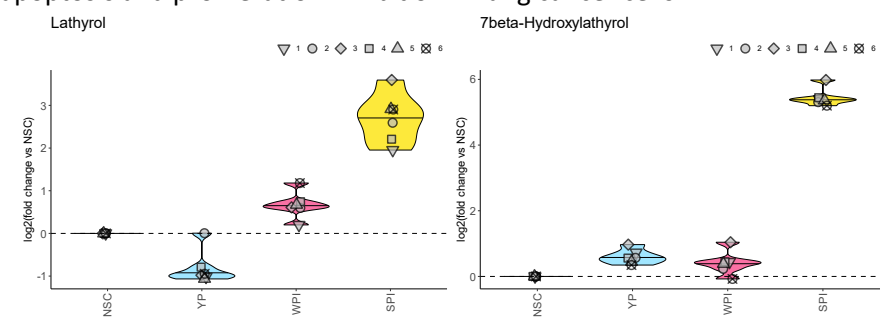


 Cephalotaxine: also increased for all three test products but especially for YP. Cephalotaxine is a natural alkaloid that potentially exhibit antileukemia effects via activation of mitochondrial apoptosis pathway in leukemia cells<sup>141</sup>

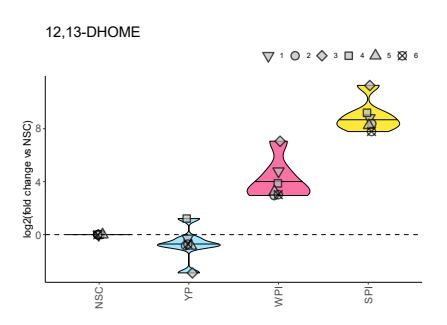


Further, three metabolites were especially strongly increased with SPI:

Lathyrol and its derivative 7-beta-hydroxylathyrol: Lathyrol is another natural compound that
potentially exhibits anti-tumor activity. Lathyrol was recently shown to promote ER stressinduced apoptosis and proliferation inhibition in lung cancer cells<sup>142</sup>



• 12,13-DiHOME: significantly increased with both SPI and WPI but not with YP. Elevated faecal 12,13-DiHOME levels have been shown to be produced by gut bacteria and impede immune tolerance in neonates at high risk for asthma<sup>143</sup>. 12,13-DiHOME is an exercise-induced lipokine that facilitate fatty acid uptake<sup>144,145</sup> and has been proposed as a new therapeutic target for prevention and treatment of obesity and metabolic diseases<sup>146</sup>.





#### 7 Results - Host-microbe interactions

### Background on the endpoints will be discussed below.

As reviewed by Chelakkot et al.<sup>147</sup>, the epithelial cell layer of the gut wall performs a pivotal role as the first physical barrier against external factors. The tight junction proteins, including, are crucial for the maintenance of <u>epithelial barrier integrity</u>. A compromised barrier integrity ('leaky gut') is considered to contribute to many pathological conditions including, amongst others, inflammatory bowel disease, obesity, and metabolic disorders. Measuring the trans-epithelial electrical resistance (TEER) is a widely accepted quantitative technique to measure the integrity of tight junction dynamics in cell culture models.

Following <u>cytokines/chemokines</u> were measured during the current project: IL-6, IL-10, IL-18, CXCL10, IL-8 and TNF- $\alpha$ . First, **IL-10** is an anti-inflammatory cytokine that inhibits both antigen presentation and subsequent release of pro-inflammatory cytokines, thereby attenuating mucosal inflammation<sup>148</sup>. Further, while **IL-6** can exert pro-inflammatory effects owing to its ability to prevent T cell apoptosis, it is also known to promote barrier function, survival of intestinal epithelial cells and antimicrobial defence<sup>149</sup>. In contrast, **TNF-** $\alpha$  is a driver of intestinal inflammation and weakens the epithelial barrier integrity by inducing apoptosis in intestinal epithelial cells<sup>149</sup>. Also **IL-16** exerts pro-inflammatory effects by e.g. promoting pathogenic T cell responses such as Th17 cell differentiation and IFN- $\gamma$  production<sup>150,151</sup>. Further, **CXCL10**, an 'inflammatory' chemokine, is also known to mediate immune responses through the activation and recruitment of leukocytes such as T cells, eosinophils, monocytes and NK cells<sup>152</sup>. **IL-8** is mainly a neutrophil chemoattractant that induces the migration of neutrophils from peripheral blood into inflamed tissue. It is well known that IL-8 production is increased in the tissue of IBD patients compared with that of normal controls <sup>153</sup>.

Finally, the **total levels** of **Nuclear factor kappa-light-chain-enhancer of activated B cells (NF-κB)** and the levels of **phosphorylated NF-κB** were also measured. **NF-κB** is a protein complex that functions as a transcription factor and plays a central in inflammation by regulating the expression of numerous genes involved in the inflammatory response<sup>154</sup>. Upon activation, **NF-κB** is phosphorylated and translocated to the nucleus where it induces the expression of cytokines and chemokines, especially pro-inflammatory ones. Thus, increased **NF-κB** and **phosphorylated NF-κB** level is an indicator for increased cellular activity related to inflammation and immune responses<sup>154</sup>.

Report reference: 0443/P0140 44



### 7.1 Gut barrier integrity

Following key findings were observed regarding the **effect of the protein products on gut barrier integrity** upon **24h** of interaction between colonic samples and the co-culture of epithelial and immune cells (Caco-2 and THP-1 differentiated macrophages) (Figure 23A):

- All test products significantly improved gut barrier integrity, i.e., the protein products increased TEER after 24h of interaction (= under non-stressed conditions, in absence of LPS)
- YP significantly outperformed WPI and SPI at enhancing epithelial integrity

After stimulation of THP-1 differentiated macrophages with LPS (= <u>stressed conditions</u>) over an additional 6h period (thus total of 30h) (Figure 23B), the **products continued to enhance gut barrier integrity** with notably stronger average effects for YP (albeit not significant).

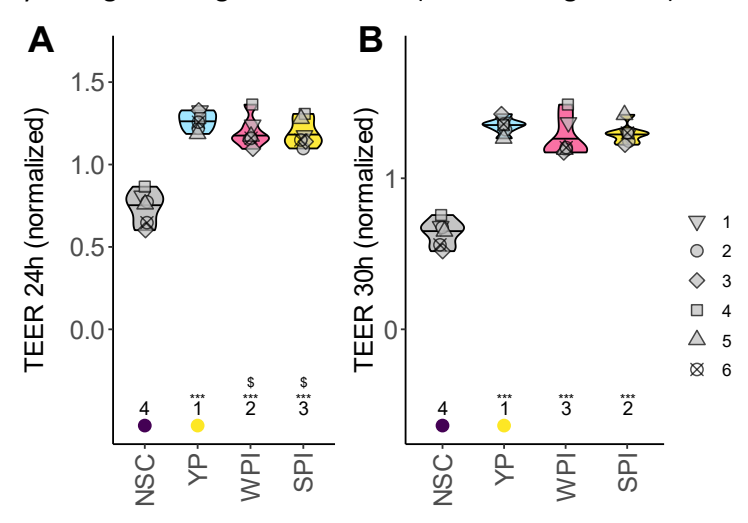


Figure 23. The impact of the test products compared to a no substrate control (NSC) on gut barrier integrity as measured by the TEER of the Caco-2 epithelial layer after (A) <u>24h treatment in absence of LPS and (B) 30h treatment (including 6h treatment with LPS)</u> in the basal compartment containing differentiated THP-1 cells) using the SIFR® technology. Samples exposed to the cells were collected from the SIFR® model after 24h of colonic incubation. Statistical differences between NSC and the individual treatments are visualized via \* (0.1 <  $p_{adjusted} < 0.2$ ), \*\* (0.05 <  $p_{adjusted} < 0.1$ ) or \*\*\* ( $p_{adjusted} < 0.05$ ). Significant differences between WPI/SPI vs. YP are indicated via \$/\$\$/\$\$\$, and between SPI vs. WPI via &/&&/&&&. The rank of the average values per treatment are indicated at the bottom of the figure, with the lowest average being indicated purple, and the highest value in yellow

To further establish potential **correlations** between **gut barrier integrity** and **SCFA** production, a correlation analysis was performed between the individual SCFA and TEER. This revealed that **acetate**, **propionate**, **butyrate** and **total SCFA** positively correlated with an increase in TEER at both 24h in the absence of LPS as well as after 6h of treatment with LPS (Figure 24). The data partially suggested a potential **role of SCFA** in maintaining a healthy gut barrier. Additionally, other microbial metabolites (including those reported in section 6) might also play a role in the modulation of gut barrier integrity.

Finally, a correlation between microbial composition (species level (Figure 28)) revealed the marked positive correlation between improved gut barrier integrity at 24/30h and presence of, amongst others, a *Coprococcus* species, an *Enterocloster* species, *Dorea* spp., propionate-producing *Bacteroides uniformis*, succinate-producing *Parabacteroides distasonis* and butyrate-producing *Eubacterium\_I ramulus*, *Roseburia hominis*, suggesting that these specific species might be involved in the beneficial effect of the treatments on barrier integrity.



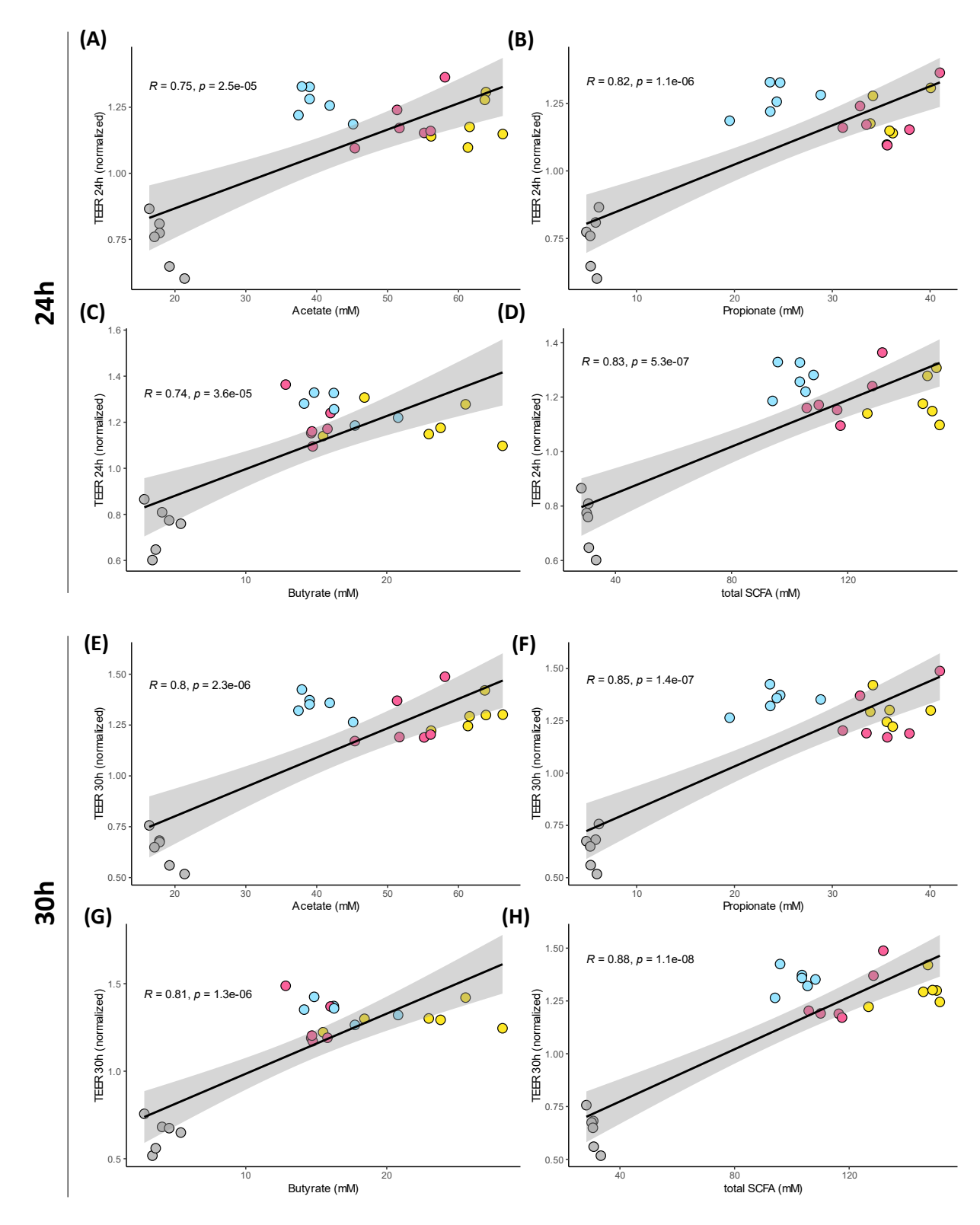


Figure 24. Pearson correlation analysis between <u>SCFA production and gut barrier integrity</u> as measured by the TEER of the Caco-2 epithelial layer after (A-D) 24h treatment in the absence of LPS and (E-H) 30h of treatment (= 24h in absence of LPS and 6h in presence of LPS in the basal compartment containing differentiated THP-1 cells).



#### 7.2 Immune modulation

Upon 24h of interaction between the colonic samples and the co-culture of epithelial and immune cells, macrophages were triggered with LPS to boost their cytokine/chemokine response. It is important to note that LPS was not administered apically of the epithelial cells but basolaterally (so in the compartment where immune cells are present). Doing so, immune cells are equally stimulated. The response of immune cells thus reflects a potential differential priming of immune cells in presence of the treatments, prior to the LPS trigger. Besides presenting the individual cytokines (Figure 25), an anti-inflammatory index (AI)<sup>m</sup> was calculated based on levels of pro-inflammatory markers (IL-1 $\beta$ , CXCL10, IL-8 and TNF- $\alpha$ ) (Figure 26)<sup>n</sup>. Following observations were made:

- The test products, especially SPI, strongly and significantly reduced the production of 3 out of 4 pro-inflammatory markers (TNF-α, IL1-β and CXCL10).
- The levels of pro-inflammatory IL-8 increased only with WPI, and not with SPI/YP
- The anti-inflammatory IL-10 significantly increased with all three test products (YP/WPI > SPI). Similarly, the test products also increased the levels of the pleiotropic cytokine IL-6 (YP > WPI/SPI) which exhibits both pro-inflammatory and anti-inflammatory properties
- The anti-inflammatory index suggested overall anti-inflammatory effects for all three protein products (SPI/YP > WPI)

In addition, the levels of total and phosphorylated NF-κB were also measured as proxy for cellular activity related to inflammation. In contrast to the aforementioned cytokines/chemokines, the levels of (phosphorylated) **NF-κB** were **unaffected by the protein products**, suggesting that the fermentation of the protein products rather affected signalling events downstream of **NF-κB**.

Further, a correlation analysis was performed between the individual SCFAs and the anti-inflammatory markers. This revealed that acetate, propionate, butyrate positively correlated with the anti-inflammatory marker IL-10 as well as IL-6 (which displays both anti- and pro-inflammatory properties) across all study arms (Figure 27). In contrast, significant negative correlations were established between all three SCFAs and the pro-inflammatory markers CXCL10, TNF- $\alpha$  and IL1- $\beta$ . These correlations confirmed the role of SCFA in reducing inflammation in the intestine when exposed to inflammatory triggers.

Finally, correlation between cytokine/chemokine responses with microbial composition were established. The anti-inflammatory marker IL-10 positively correlated with a *Copromonas* species, *Dorea* spp., propionate-producing *B. uniformis*, succinate-producing *Parabacteroides distasonis*, butyrate-producing *Eubacterium\_i ramulus*, *Roseburia hominis*. In contrast, the pro-inflammatory TNF-α, IL1-β and CXCL10 tended to negatively correlate with these species and additionally, propionate-producing *Phascolarctobacterium faecium* and butyrate-producing *Dysosmobacter welbionis*, *Flavonifractor plautii*.

\_

<sup>&</sup>lt;sup>m</sup> The results were first normalized by dividing the levels within a marker by those of the corresponding NSC (of a given donor). Subsequently, within each pro-inflammatory marker, values were converted by subtracting the lowest detected value of that marker across all samples and dividing by the range that values of a certain marker covered (e.g. 0.75 in case the normalized changes vs. the NSC ranged from 0.80 up to 1.55). Doing so, all values were reduced to the same scale from 0 to 1. The values of pro-inflammatory markers were multiplied with -1. Finally, the obtained values of the NSC were subtracted from the values (within a given donor) so the NSC results in an anti-inflammatory index of 0, while test products with anti- and pro-inflammatory effects respectively increase and decrease index values.



Overall, fibres and fibre mixes such as **IN, C, CXP** and **XP** potentially exert anti-inflammatory effects by decreasing **pro-inflammatory** cytokines/chemokines and increasing anti-inflammatory cytokines/chemokines.

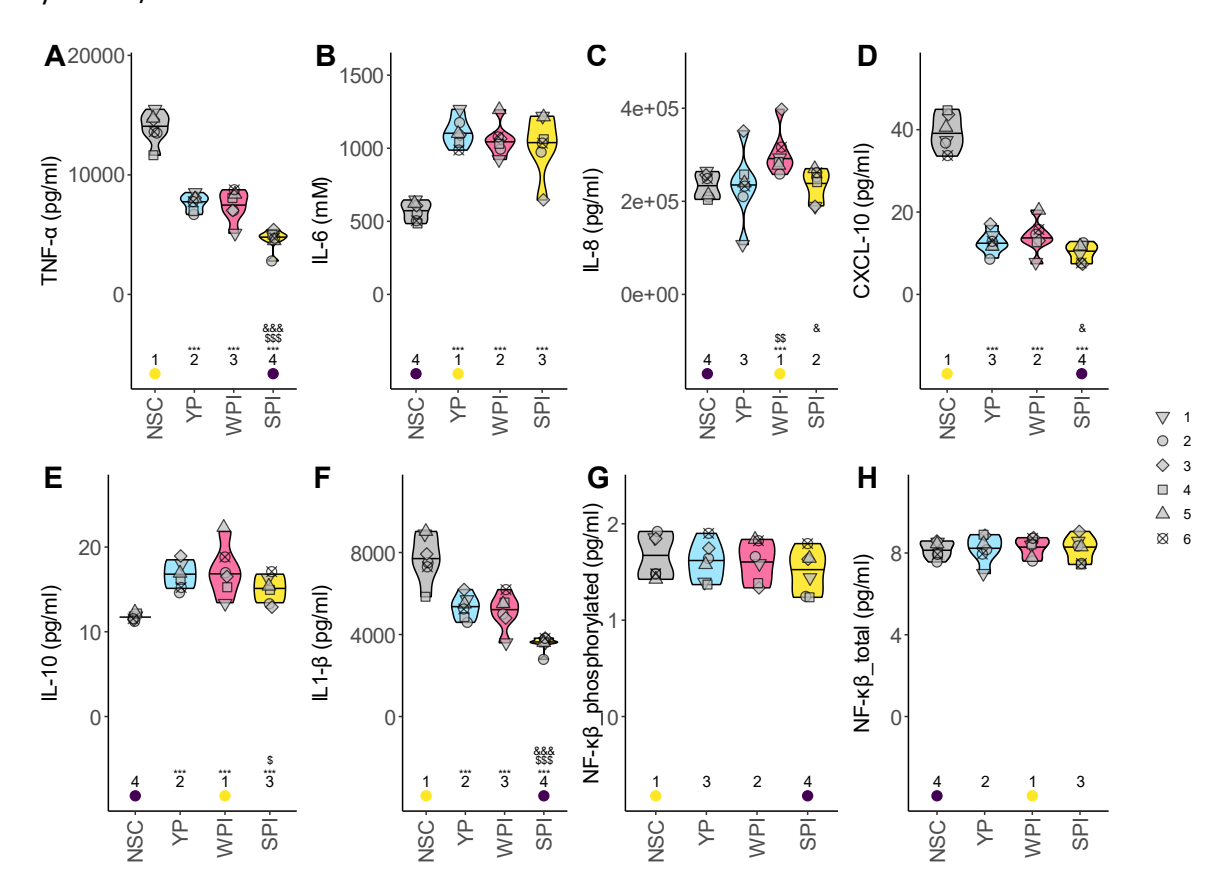


Figure 25. The impact of the test products compared to a no substrate control (NSC), on immune modulation as measured by the levels of immune markers (A)TNF- $\alpha$ , (B) IL-6, (C) IL-8, (D) CXCL-10, (E) IL-10, (F) IL1- $\beta$ , (G) phosphorylated NF-κB and (H) total NF-κB. Statistical differences between NSC and the individual treatments are visualized via \* (0.1 <  $p_{adjusted}$  < 0.2), \*\* (0.05 <  $p_{adjusted}$  < 0.1) or \*\*\* ( $p_{adjusted}$  < 0.05). Significant differences between WPI/SPI vs. YP are indicated via \$/\$\$/\$\$\$, and between SPI vs. WPI via &/&&/&&&. The rank of the average values per treatment are indicated at the bottom of the figure, with the lowest average being indicated purple, and the highest value in yellow.

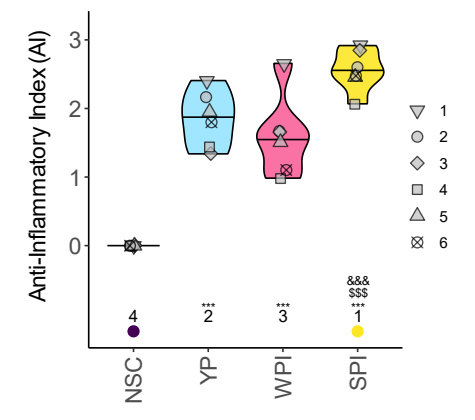


Figure 26. 'Anti-inflammatory index' based on the cytokine production by THP-1 differentiated macrophages. Statistically significant differences compared to the NSC are visualized via \*  $(0.1 < p_{adjusted} < 0.2)$ , \*\*  $(0.05 < p_{adjusted} < 0.1)$  or \*\*\*  $(p_{adjusted} < 0.05)$ , while differences compared to IN are indicated with \$/\$\$/\$\$\$. The potential significance of 18 additional comparisons of interest is shown in matrices at the right side. Values in each matrix represent the difference between the product on the horizontal axis compared to the one on the vertical axis (expressed as  $log_2FC$ ), with significant differences  $(p_{adjusted} < 0.20)$  being indicated in bold.



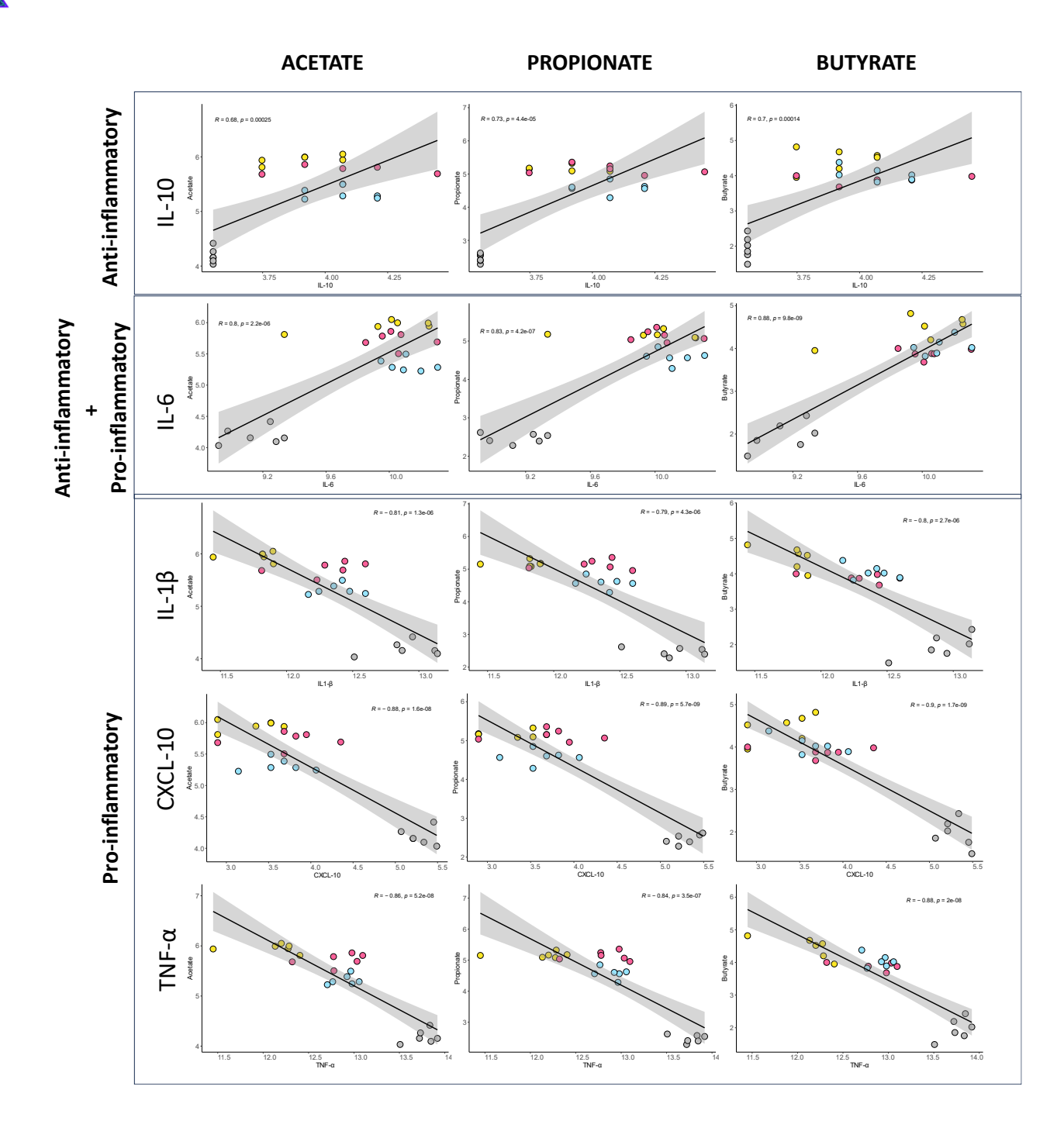


Figure 27. Pearson correlation analysis between <u>SCFA production and gut barrier integrity</u> as measured by the TEER of the Caco-2 epithelial layer after (A-D) 24h treatment in the absence of LPS and (E-H) 30h of treatment (= 24h in absence of LPS and 6h in presence of LPS in the basal compartment containing differentiated THP-1 cells).



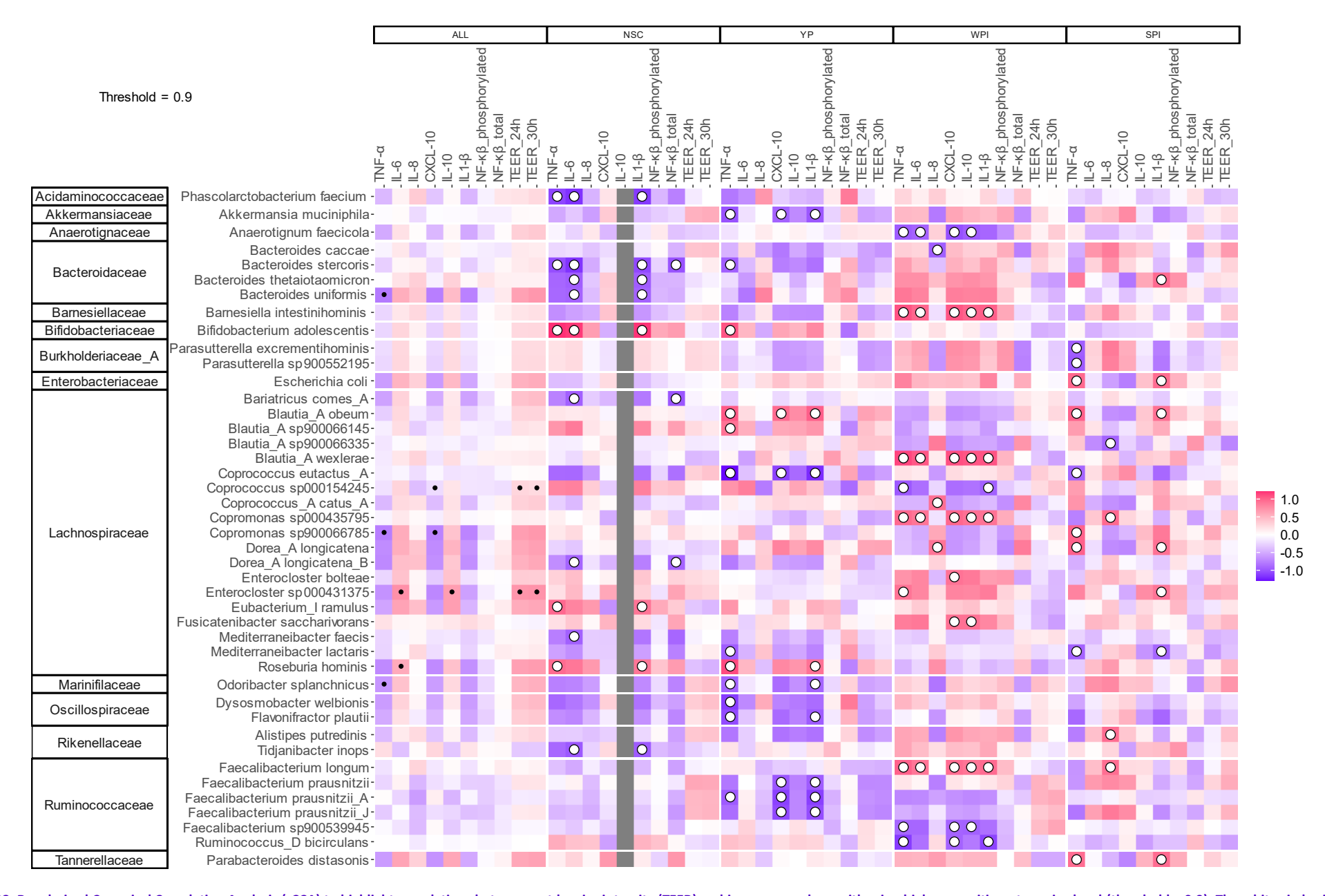


Figure 28. Regularized Canonical Correlation Analysis (rCCA) to highlight correlations between gut barrier integrity (TEER) and immune markers with microbial composition at species level (threshold > 0.9). The white circles indicate values larger than the threshold and black dots indicate statistical significance (p < 0.05) in the individual correlations between the SCFA and the families based on Kendall rank correlation coefficient.

Report reference: 0443/P0140 50



### 8 Discussion and conclusions

The research objective of the study was to characterise the impact of **three protein products** (yeast protein (YP), whey protein isolate (WPI) and soy protein isolate (SPI)) on the gut microbiota of **50-65y male human adults**. Using the *ex vivo* SIFR® technology, the impact on **metabolite production** (key fermentation parameters (pH, gas, SCFA, bCFA), untargeted metabolomics (LC-MS)), **microbial composition** (deep shotgun sequencing) and **host-microbiota interaction** was assessed **at 24h** after introduction of the test products in the **colonic environment**, as simulated with the *ex vivo* SIFR® **technology**.

The **high technical reproducibility** of the SIFR® technology was demonstrated by the minor variation observed across technical replicates, i.e., the coefficient of variation (= SD/AVG) was on average **0.89%** for analysis of key fermentation parameters. This very high technical reproducibility renders the **SIFR®** technology very sensitive to decipher changes in the human gut microbiome.

**Six test subjects** were included in the study design as it has been established that there are marked interpersonal differences among the human population<sup>1</sup>. Analysis of microbial composition at baseline indeed revealed that the test subjects **covered a broad spectrum of microbial composition that occurs in vivo**, in line with the so-called **enterotypes**, thus **ensuring representative findings**.

Upon simulation of a single intake, all three protein products remarkably stimulated metabolic activity of the gut microbiota, decreasing pH and increasing the production of gases, acetate, propionate, butyrate (thus, total SCFA), valerate as well as isobutyrate and isovalerate (thus, total bCFA). At the same doses of 40 g/L, the effects were the most pronounced for SPI which stimulated the most SCFA and bCFA production. When compared WPI and YP, WPI performed better at stimulating acetate/propionate (thus, total SCFA), while YP was superior at promoting butyrate/valerate/bCFA. The stimulation of SCFA production could be explained by the impact of the test products on the microbial composition:

- Bifidogenic effects (mainly on acetate/lactate-producing B. adolescentis, B. pseudocatenulatum) were stronger for SPI > WPI > YP → highest acetate and butyrate production (via cross-feeding) for SPI
- Stimulatory effects on different acetate/propionate producers in the phylum Bacteroidota (especially in the family *Bacteroidaceae*) as well as in the phylum *Bacillota\_C*. Key propionogenic species that SPI and WPI stimulated the most was respectively *Bacteroides uniformis* and *Phocaeicola vulgatus*, respectively, which were the two most abundant species in *Bacteroidaceae*. → higher propionate production for SPI and WPI
- YP also specifically promoted other less prominent propionate producers including Bacteroides thetaiotaomicron, while also promoting B. uniformis and P. vulgatus, albeit more mildly compared to SPI/WPI → milder propionate production for YP
- The protein products also stimulated succinate-producing *Parabacteroides spp*. and succinate-converting propionate producers *Phascolarctobacterium faecium* and *Acidaminococcus intestini* → promoting their cross-feeding to further boost overall propionate production
- The protein products promoted different butyrate producers in the phylum Bacillota\_A. Key butyrogenic species stimulated by SPI were Faecalibacterium and Agathobaculum spp. which were very prevalent in the microbiota, thus explaining the highest butyrate production



for **SPI.** In addition, the effects of **YP** were generally also stronger on most butyrate producers (except *F. longum*), correlating with higher butyrate levels for **YP** compared to **WPI** 

Besides species with known SCFA-producing capacity, the protein isolates also stimulated species within the phylum **Pseudomonadota** – another evidence for increased proteolytic activity in the gut microbiota.

The combined community modulation score recently developed by Cryptobiotix confirmed that the test products, **especially SPI/YP**, exerted a **positive impact on the microbial diversity** of the human gut microbiota, in line with the stimulation of the broad range of aforementioned taxa.

Overall, treatment with **YP** resulted in **remarkably low gas production** compared to the other treatments. Indeed, when the gas production was normalized against the amount of total SCFA, it was noted that YP fermentation produced **27.2% and 19.4% less gases per mol of total SCFA** compared to **WPI** and **SPI**, respectively (Figure 29). Therefore, to promote the same amount of total SCFA, YP is more efficient at maintaining lower gas production. **Excessive gas production** can lead to **bloating and abdominal discomfort** <sup>155</sup>. This suggests that among the three protein products, **YP** may have the highest tolerability for human consumption.

SCFAs are known to promote the integrity of the gut barrier by increasing the expression tight junction proteins such as claudin-1, occluding, zonula occludens-1 as well as strengthen the mucus layer by increasing the expression of Mucin 2. Indeed, host-microbiota interaction assays demonstrated an enhancing effect of the protein isolates, especially YP, on the epithelial barrier before and after exposing to the potent inflammation inducer LPS. Importantly, this effect positively correlated

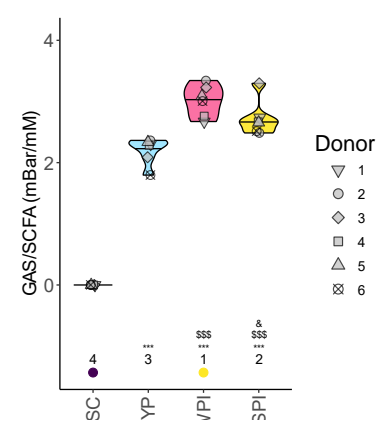


Figure 29. The impact of the test products on (D) gas production per mM of total produced SCFA for the gut microbiota of human adults.

with all the increased production of all three main SCFAs across all study arms. In addition, the assays also suggested an important role of SCFAs in modulating inflammatory responses, since their increased production positively correlated with increased levels of anti-inflammatory cytokine IL-10 and negatively correlated with decreased levels of pro-inflammatory markers IL-1 $\beta$ , TNF- $\alpha$ , CXCL10 and phosphorylated NF- $\kappa$ B (no significant effects for NF- $\kappa$ B). In addition, unlike WPI, YP and SPI did not increase the level of the pro-inflammatory cytokine IL-8. Overall, this resulted in a positive anti-inflammatory index for all three protein isolates (higher for SPI > YP > WPI), thus suggesting their anti-inflammatory effect in the intestine.

In addition to **SCFA**, metabolomics analysis also revealed a series of other health-related metabolites that were promoted by the protein isolates. Among these, several metabolites with anti-inflammatory effects and/or enhancing gut barrier function were noted, i.e., **N-acetylated amino acids**, **phenyllactic acid** and **p-hydroxyphenyllactic** acid, **2-hydroxyisocaproic acid**, the tryptophan metabolites **tryptophol**, **5-methoxytryptophan**, **indole** and especially **indole-3-propionic acid** (**IPA**) – a derivative of **indole-3-lactic acid** that has garnered attention for its benefits in various organs in the host, thus helping maintaining systemic homeostatis<sup>84,156</sup>. Further, each protein product specifically exhibited stronger stimulation of some metabolites compared to the other two test products:

YP: kynurenine (~ neuroprotective), N8-acetylspermidine (~ anti-inflammatory, cardiovascular health), homoarginine (~ preventing diabetic kidney damage, improving blood glucose), pipecolinic acid (~ anti-constipation), cephalotaxine (~ anticancer)



- WPI: IPA, 2-hydroxyisocaproic acid, p-hydroxyphenyllactic as well as hydroxyphenylacetic acid (~ antioxidant, anti-microbial, hepato-protective), acetylagmatine (~neuroprotective), 3-aminoisobutanoic acid (BAIBA)/γ-aminobutyric acid (GABA) (~ neurotransmitter, gut barrier function, cardioprotective), Licarin A (~ antimicrobial, antioxidant, anti-inflammatory, neuroprotective)
- SPI: phenyllactic acid as well as the acetylated polyamines N-acetylputrescine hydrochloride and N-acetylcadaverine, indole-3-acetic acid (anti-oxidative and anti-inflammatory), tryptamine (~ neurotransmitter, gut barrier function), p-hydroxybenzoic acid (~ gut barrier function), 2-methylbutyric acid (~ anti-cancer, anti-inflammatory and neuroprotective).

Overall, the increased production of additional metabolites beyond SCFAs could imply other health benefits of the supplementation of the protein products in human host. Protein supplements are increasingly used by older people to increase protein intake as a strategy to maintain/improve muscle function. The findings in this study suggest that protein supplements may exert other health-related effects on the host via their pronounced impact on the gut microbiota.

In summary, colonic fermentation of the protein products resulted in pronounced changes in microbial composition that correlated with increased production of SCFA and led to stimulation of additional health-related metabolites. This stimulated production of health-related metabolites likely explains the observed enhanced gut barrier function as well as anti-inflammatory effects. In addition, the protein products also displayed a positive impact on microbial diversity. Altogether, the findings in the study suggested a series of potential health benefits for the host upon supplementation with the protein products.



#### 9 References

- 1. Lavelle, A. *et al.* Spatial variation of the colonic microbiota in patients with ulcerative colitis and control volunteers. *Gut* **64**, 1553–1561 (2015).
- 2. Healey, G. R., Murphy, R., Brough, L., Butts, C. A. & Coad, J. Interindividual variability in gut microbiota and host response to dietary interventions. *Nutr Rev* **75**, 1059–1080 (2017).
- 3. Van den Abbeele, P. *et al.* Bridging preclinical and clinical gut microbiota research using the ex vivo SIFR technology. *Front Microbiol* (2023) doi: 10.3389/fmicb.2023.1131662.
- 4. Van den Abbeele, P. *et al.* Microbial community development in a dynamic gut model is reproducible, colon region specific, and selective for Bacteroidetes and Clostridium cluster IX. *Appl Environ Microbiol* **76**, 5237–5246 (2010).
- 5. Rajilić-Stojanović, M. *et al.* Evaluating the microbial diversity of an in vitro model of the human large intestine by phylogenetic microarray analysis. *Microbiology (Reading)* **156**, 3270–3281 (2010).
- 6. Berner, A. Z. *et al.* Novel Polyfermentor Intestinal Model (PolyFermS) for Controlled Ecological Studies: Validation and Effect of pH. *PLOS ONE* **8**, e77772 (2013).
- 7. Wiese, M. *et al.* CoMiniGut-a small volume in vitro colon model for the screening of gut microbial fermentation processes. *PeerJ* **6**, e4268 (2018).
- 8. Biagini, F. et al. A novel 3D in vitro model of the human gut microbiota. Sci Rep 10, 21499 (2020).
- 9. O'Donnell, M. M., Rea, M. C., Shanahan, F. & Ross, R. P. The Use of a Mini-Bioreactor Fermentation System as a Reproducible, High-Throughput ex vivo Batch Model of the Distal Colon. *Front. Microbiol.* **9**, 1844 (2018).
- 10. Gaisawat, M. B. *et al.* Probiotic Supplementation in a Clostridium difficile-Infected Gastrointestinal Model Is Associated with Restoring Metabolic Function of Microbiota. *Microorganisms* **8**, E60 (2019).
- 11. Flint, H. J., Scott, K. P., Louis, P. & Duncan, S. H. The role of the gut microbiota in nutrition and health. *Nat Rev Gastroenterol Hepatol* **9**, 577–589 (2012).
- 12. Rivière, A., Selak, M., Lantin, D., Leroy, F. & De Vuyst, L. Bifidobacteria and Butyrate-Producing Colon Bacteria: Importance and Strategies for Their Stimulation in the Human Gut. *Frontiers in Microbiology* **7**, 979 (2016).
- 13. Koh, A., De Vadder, F., Kovatcheva-Datchary, P. & Bäckhed, F. From Dietary Fiber to Host Physiology: Short-Chain Fatty Acids as Key Bacterial Metabolites. *Cell* **165**, 1332–1345 (2016).
- 14. Gonçalves, P., Araújo, J. R. & Di Santo, J. P. A Cross-Talk Between Microbiota-Derived Short-Chain Fatty Acids and the Host Mucosal Immune System Regulates Intestinal Homeostasis and Inflammatory Bowel Disease. *Inflamm Bowel Dis* 24, 558–572 (2018).
- 15. van der Hee, B. & Wells, J. M. Microbial Regulation of Host Physiology by Short-chain Fatty Acids. *Trends Microbiol* **29**, 700–712 (2021).
- 16. Boets, E. *et al.* Quantification of in Vivo Colonic Short Chain Fatty Acid Production from Inulin. *Nutrients* **7**, 8916–8929 (2015).



- 17. Vandeputte, D. *et al.* Prebiotic inulin-type fructans induce specific changes in the human gut microbiota. *Gut* **66**, 1968–1974 (2017).
- 18. Iribarren, C. *et al.* Human milk oligosaccharide supplementation in irritable bowel syndrome patients: A parallel, randomized, double-blind, placebo-controlled study. *Neurogastroenterol Motil* **32**, e13920 (2020).
- 19. Elison, E. *et al.* Oral supplementation of healthy adults with 2'-O-fucosyllactose and lacto-N-neotetraose is well tolerated and shifts the intestinal microbiota. *Br J Nutr* **116**, 1356–1368 (2016).
- 20. Thirion, F. *et al.* Diet Supplementation with NUTRIOSE, a Resistant Dextrin, Increases the Abundance of Parabacteroides distasonis in the Human Gut. *Molecular Nutrition & Food Research* n/a, 2101091.
- 21. Van den Abbeele, P. et al. Lacticaseibacillus rhamnosus ATCC 53103 and Limosilactobacillus reuteri ATCC 53608 Synergistically Boost Butyrate Levels upon Tributyrin Administration Ex Vivo. *International Journal of Molecular Sciences* **24**, 5859 (2023).
- 22. Van den Abbeele, P. *et al.* Serum-Derived Bovine Immunoglobulin Stimulates SCFA Production by Specific Microbes in the Ex Vivo SIFR® Technology. *Microorganisms* **11**, 659 (2023).
- 23. Bajic, D. *et al.* HMOs Exert Marked Bifidogenic Effects on Children's Gut Microbiota Ex Vivo, Due to Age-Related Bifidobacterium Species Composition. *Nutrients* **15**, 1701 (2023).
- 24. Van den Abbeele, P., Deyaert, S., Albers, R., Baudot, A. & Mercenier, A. Carrot RG-I Reduces Interindividual Differences between 24 Adults through Consistent Effects on Gut Microbiota Composition and Function Ex Vivo. *Nutrients* **15**, 2090 (2023).
- 25. Jansma, J. *et al.* Dynamic effects of probiotic formula ecologic®825 on human small intestinal ileostoma microbiota: a network theory approach. *Gut Microbes* **15**, 2232506.
- 26. Van den Abbeele, P. *et al.* A Comparison of the In Vitro Effects of 2'Fucosyllactose and Lactose on the Composition and Activity of Gut Microbiota from Infants and Toddlers. *Nutrients* **13**, (2021).
- 27. Brodkorb, A. *et al.* INFOGEST static in vitro simulation of gastrointestinal food digestion. *Nature Protocols* **14**, 991–1014 (2019).
- 28. Minekus, M. *et al.* A standardised static in vitro digestion method suitable for food an international consensus. *Food Funct* **5**, 1113–1124 (2014).
- 29. Vandeputte, D. *et al.* Quantitative microbiome profiling links gut community variation to microbial load. *Nature* **551**, 507–511 (2017).
- 30. Doneanu, C. E. UPLC/MS Monitoring of Water-Soluble Vitamin Bs in Cell Culture Media in Minutes. 7 (2011).
- 31. Adams, K. J. *et al.* Skyline for Small Molecules: A Unifying Software Package for Quantitative Metabolomics. *J Proteome Res* **19**, 1447–1458 (2020).
- 32. Lee, S. & Lee, D. K. What is the proper way to apply the multiple comparison test? *Korean J Anesthesiol* **71**, 353–360 (2018).
- 33. Rohart, F., Gautier, B., Singh, A. & Cao, K.-A. L. mixOmics: An R package for 'omics feature selection and multiple data integration. *PLOS Comput Biol* **13**, e1005752 (2017).



- 34. Hinnebusch, B. F., Meng, S., Wu, J. T., Archer, S. Y. & Hodin, R. A. The effects of short-chain fatty acids on human colon cancer cell phenotype are associated with histone hyperacetylation. *J Nutr* **132**, 1012–1017 (2002).
- 35. McDonald, J. A. K. *et al.* Inhibiting Growth of Clostridioides difficile by Restoring Valerate, Produced by the Intestinal Microbiota. *Gastroenterology* **155**, 1495-1507.e15 (2018).
- 36. Davila, A.-M. *et al.* Intestinal luminal nitrogen metabolism: role of the gut microbiota and consequences for the host. *Pharmacol Res* **68**, 95–107 (2013).
- 37. Nowak, A. & Libudzisz, Z. Influence of phenol, p-cresol and indole on growth and survival of intestinal lactic acid bacteria. *Anaerobe* **12**, 80–84 (2006).
- 38. Kikugawa, K. & Kato, T. Formation of a mutagenic diazoquinone by interaction of phenol with nitrite. *Food Chem Toxicol* **26**, 209–214 (1988).
- 39. Blachier, F., Mariotti, F., Huneau, J. F. & Tomé, D. Effects of amino acid-derived luminal metabolites on the colonic epithelium and physiopathological consequences. *Amino Acids* **33**, 547–562 (2007).
- 40. Boudry, G. *et al.* Dietary protein excess during neonatal life alters colonic microbiota and mucosal response to inflammatory mediators later in life in female pigs. *J Nutr* **143**, 1225–1232 (2013).
- 41. Nair, A. B. & Jacob, S. A simple practice guide for dose conversion between animals and human. *J Basic Clin Pharm* **7**, 27–31 (2016).
- 42. McNeil, N. I. The contribution of the large intestine to energy supplies in man. *Am J Clin Nutr* **39**, 338–342 (1984).
- 43. Stephen, A. M. *et al.* Dietary fibre in Europe: current state of knowledge on definitions, sources, recommendations, intakes and relationships to health. *Nutrition Research Reviews* **30**, 149–190 (2017).
- 44. Jiao, A. R. *et al.* Oral administration of short chain fatty acids could attenuate fat deposition of pigs. *PLOS ONE* **13**, e0196867 (2018).
- 45. Fang, C. L., Sun, H., Wu, J., Niu, H. H. & Feng, J. Effects of sodium butyrate on growth performance, haematological and immunological characteristics of weanling piglets. *J Anim Physiol Anim Nutr* **98**, 680–685 (2014).
- 46. De Vuyst, L., Moens, F., Selak, M., Rivière, A. & Leroy, F. Summer Meeting 2013: growth and physiology of bifidobacteria. *J Appl Microbiol* **116**, 477–491 (2014).
- 47. Louis, P. & Flint, H. J. Formation of propionate and butyrate by the human colonic microbiota. *Environmental Microbiology* **19**, 29–41 (2017).
- 48. Wu, F. *et al.* Phascolarctobacterium faecium abundant colonization in human gastrointestinal tract. *Exp Ther Med* **14**, 3122–3126 (2017).
- 49. Dot, T., Osawa, R. & Stackebrandt, E. Phascolarctobacterium faecium gen. nov, spec. nov., a Novel Taxon of the Sporomusa Group of Bacteria. *Syst. Appl. Microbiol.* **16**, 380–384 (1993).



- 50. Shetty, S. A. *et al.* Reclassification of Eubacterium hallii as Anaerobutyricum hallii gen. nov., comb. nov., and description of Anaerobutyricum soehngenii sp. nov., a butyrate and propionate-producing bacterium from infant faeces. *Int J Syst Evol Microbiol* **68**, 3741–3746 (2018).
- Allen-Vercoe, E. et al. Anaerostipes hadrus comb. nov., a dominant species within the human colonic microbiota; reclassification of Eubacterium hadrum Moore et al. 1976. Anaerobe 18, 523– 529 (2012).
- 52. Tannock, G. W. *et al.* Comparison of the compositions of the stool microbiotas of infants fed goat milk formula, cow milk-based formula, or breast milk. *Applied and Environmental Microbiology* **79**, 3040–3048 (2013).
- 53. Saulnier, D. M. *et al.* Gastrointestinal microbiome signatures of pediatric patients with irritable bowel syndrome. *Gastroenterology* **141**, 1782–1791 (2011).
- 54. Gossling, J. & Moore, W. E. C. Gemmiger formicilis, n.gen., n.sp., an Anaerobic Budding Bacterium from Intestines. *International Journal of Systematic Bacteriology* **25**, 202–207 (1975).
- 55. Sokol, H., Dr. *et al.* Specificities of the Fecal Microbiota in Inflammatory Bowel Disease. *Inflammatory Bowel Diseases* **12**, 106–111 (2006).
- 56. Arumugam, M. et al. Enterotypes of the human gut microbiome. Nature 473, 174–180 (2011).
- 57. Wu, G. D. *et al.* Linking long-term dietary patterns with gut microbial enterotypes. *Science* **334**, 105–108 (2011).
- 58. Steenackers, N. *et al.* Specific contributions of segmental transit times to gut microbiota composition. *Gut* (2021) doi:10.1136/gutjnl-2021-325916.
- 59. Van den Abbeele, P. et al. A Novel Non-Digestible, Carrot-Derived Polysaccharide (cRG-I) Selectively Modulates the Human Gut Microbiota while Promoting Gut Barrier Integrity: An Integrated in Vitro Approach. *Nutrients* **12**, 1917 (2020).
- 60. Van den Abbeele, P. *et al.* Butyrate-producing Clostridium cluster XIVa species specifically colonize mucins in an in vitro gut model. *ISME J* **7**, 949–961 (2013).
- 61. Tintoré, M. *et al.* A Long-Chain Dextran Produced by Weissella cibaria Boosts the Diversity of Health-Related Gut Microbes Ex Vivo. *Biology* **13**, 51 (2024).
- 62. Parker, B. J., Wearsch, P. A., Veloo, A. C. M. & Rodriguez-Palacios, A. The Genus Alistipes: Gut Bacteria With Emerging Implications to Inflammation, Cancer, and Mental Health. *Frontiers in Immunology* **11**, (2020).
- 63. Lei, Y. *et al.* Parabacteroides produces acetate to alleviate heparanase-exacerbated acute pancreatitis through reducing neutrophil infiltration. *Microbiome* **9**, 115 (2021).
- 64. Göker, M. *et al.* Complete genome sequence of Odoribacter splanchnicus type strain (1651/6). *Stand Genomic Sci* **4**, 200–209 (2011).
- 65. Fernández-Veledo, S. & Vendrell, J. Gut microbiota-derived succinate: Friend or foe in human metabolic diseases? *Rev Endocr Metab Disord* **20**, 439–447 (2019).
- 66. Jeong, H., Chang, D. & Kim, B. *Agathobaculum*. in *Bergey's Manual of Systematics of Archaea and Bacteria* (ed. Whitman, W. B.) 1–10 (Wiley, 2024). doi:10.1002/9781118960608.gbm01657.



- 67. Rodriguez-Castaño, G. P. *et al.* Bacteroides thetaiotaomicron Starch Utilization Promotes Quercetin Degradation and Butyrate Production by Eubacterium ramulus. *Front. Microbiol.* **10**, 1145 (2019).
- 68. Bunesova, V., Lacroix, C. & Schwab, C. Mucin Cross-Feeding of Infant Bifidobacteria and Eubacterium hallii. *Microb Ecol* **75**, 228–238 (2018).
- 69. Falony, G., Vlachou, A., Verbrugghe, K. & Vuyst, L. D. Cross-Feeding between Bifidobacterium longum BB536 and Acetate-Converting, Butyrate-Producing Colon Bacteria during Growth on Oligofructose. *Appl Environ Microbiol* **72**, 7835–7841 (2006).
- 70. Diether, N. E. & Willing, B. P. Microbial Fermentation of Dietary Protein: An Important Factor in Diet<sup>-</sup>Microbe<sup>-</sup>Host Interaction. *Microorganisms* **7**, 19 (2019).
- 71. Wang, K. *et al.* Parabacteroides distasonis Alleviates Obesity and Metabolic Dysfunctions via Production of Succinate and Secondary Bile Acids. *Cell Rep* **26**, 222-235.e5 (2019).
- 72. Ahn, S. *et al.* Agathobaculum butyriciproducens gen. nov. sp. nov., a strict anaerobic, butyrate-producing gut bacterium isolated from human faeces and reclassification of Eubacterium desmolans as Agathobaculum desmolans comb. nov. *Int J Syst Evol Microbiol* **66**, 3656–3661 (2016).
- 73. Le Roy, T. *et al.* Dysosmobacter welbionis is a newly isolated human commensal bacterium preventing diet-induced obesity and metabolic disorders in mice. *Gut* **71**, 534–543 (2022).
- 74. Rodriguez-Castaño, G. P., Rey, F. E., Caro-Quintero, A. & Acosta-González, A. Gut-derived Flavonifractor species variants are differentially enriched during in vitro incubation with quercetin. *PLoS ONE* **15**, e0227724 (2020).
- 75. Zou, Y. *et al.* Characterization and description of Faecalibacterium butyricigenerans sp. nov. and F. longum sp. nov., isolated from human faeces. *Sci Rep* **11**, 11340 (2021).
- 76. Choi, S.-H. *et al.* Anaerotignum faecicola sp. nov., isolated from human faeces. *J Microbiol.* **57**, 1073–1078 (2019).
- 77. Ueki, A., Goto, K., Ohtaki, Y., Kaku, N. & Ueki, K. Y. Description of Anaerotignum aminivorans gen. nov., sp. nov., a strictly anaerobic, amino-acid-decomposing bacterium isolated from a methanogenic reactor, and reclassification of Clostridium propionicum, Clostridium neopropionicum and Clostridium lactatifermentans as species of the genus Anaerotignum. *International Journal of Systematic and Evolutionary Microbiology* **67**, 4146–4153 (2017).
- 78. Martin, F.-P. *et al.* Host-microbial co-metabolites modulated by human milk oligosaccharides relate to reduced risk of respiratory tract infections. *Frontiers in Nutrition* **9**, 935711 (2022).
- 79. Sarkar, C. & Lipinski, M. N-acetyl-L-leucine: a promising treatment option for traumatic brain injury. *Neural Regen Res* **17**, 1957 (2022).
- 80. Hegdekar, N., Lipinski, M. M. & Sarkar, C. N-Acetyl-l-leucine improves functional recovery and attenuates cortical cell death and neuroinflammation after traumatic brain injury in mice. *Sci Rep* **11**, 9249 (2021).
- 81. Matsumura, T. *et al.* N-acetyl-L-tyrosine is an intrinsic triggering factor of mitohormesis in stressed animals. *EMBO Reports* **21**, e49211 (2020).



- 82. Smith, E. *et al.* Ergothioneine is associated with reduced mortality and decreased risk of cardiovascular disease. *Heart* **106**, 691–697 (2020).
- 83. Laursen, M. F. *et al.* Bifidobacterium species associated with breastfeeding produce aromatic lactic acids in the infant gut. *Nature Microbiology* **6**, 1367–1382 (2021).
- 84. Jiang, H., Chen, C. & Gao, J. Extensive Summary of the Important Roles of Indole Propionic Acid, a Gut Microbial Metabolite in Host Health and Disease. *Nutrients* **15**, 151 (2022).
- 85. Dodd, D. *et al.* A gut bacterial pathway metabolizes aromatic amino acids into nine circulating metabolites. *Nature* **551**, 648–652 (2017).
- 86. Hendrikx, T. & Schnabl, B. Indoles: metabolites produced by intestinal bacteria capable of controlling liver disease manifestation. *Journal of Internal Medicine* **286**, 32–40 (2019).
- 87. Shen, J. *et al.* Indole-3-Acetic Acid Alters Intestinal Microbiota and Alleviates Ankylosing Spondylitis in Mice. *Front. Immunol.* **13**, 762580 (2022).
- 88. Ji, Y., Gao, Y., Chen, H., Yin, Y. & Zhang, W. Indole-3-Acetic Acid Alleviates Nonalcoholic Fatty Liver Disease in Mice via Attenuation of Hepatic Lipogenesis, and Oxidative and Inflammatory Stress. *Nutrients* 11, 2062 (2019).
- 89. Dou, L. *et al.* The Cardiovascular Effect of the Uremic Solute Indole-3 Acetic Acid. *Journal of the American Society of Nephrology* **26**, 876–887 (2015).
- 90. Sari, M., Chung, Y., Agatha, F. & Kim, H. K. Evaluation of antioxidant and antimicrobial activity of phenolic lipids produced by the transesterification of 4-hydroxyphenylacetic acid and triglycerides. *Appl Biol Chem* **62**, 5 (2019).
- 91. YujiaLiu *et al.* Antimicrobial mechanism of 4-hydroxyphenylacetic acid on Listeria monocytogenes membrane and virulence. *Biochemical and Biophysical Research Communications* **572**, 145–150 (2021).
- 92. Zhao, H. *et al.* 4-Hydroxyphenylacetic Acid Prevents Acute APAP-Induced Liver Injury by Increasing Phase II and Antioxidant Enzymes in Mice. *Front. Pharmacol.* **9**, 653 (2018).
- 93. Hoyles, L. *et al.* Molecular phenomics and metagenomics of hepatic steatosis in non-diabetic obese women. *Nat Med* **24**, 1070–1080 (2018).
- 94. Scott, S. A., Fu, J. & Chang, P. V. Microbial tryptophan metabolites regulate gut barrier function via the aryl hydrocarbon receptor. *Proceedings of the National Academy of Sciences* **117**, 19376–19387 (2020).
- 95. Wu, K. K., Kuo, C.-C., Yet, S.-F., Lee, C.-M. & Liou, J.-Y. 5-methoxytryptophan: an arsenal against vascular injury and inflammation. *Journal of Biomedical Science* **27**, 79 (2020).
- 96. Hu, J. *et al.* 1-Methyltryptophan treatment ameliorates high-fat diet-induced depression in mice through reversing changes in perineuronal nets. *Transl Psychiatry* **14**, 228 (2024).
- 97. Wirthgen, E., Leonard, A. K., Scharf, C. & Domanska, G. The Immunomodulator 1-Methyltryptophan Drives Tryptophan Catabolism Toward the Kynurenic Acid Branch. *Front. Immunol.* **11**, 313 (2020).



- 98. Tennoune, N., Andriamihaja, M. & Blachier, F. Production of Indole and Indole-Related Compounds by the Intestinal Microbiota and Consequences for the Host: The Good, the Bad, and the Ugly. *Microorganisms* **10**, 930 (2022).
- 99. Dodd, S. *et al.* Trace Amine-Associated Receptor 1 (TAAR1): A new drug target for psychiatry? *Neuroscience & Biobehavioral Reviews* **120**, 537–541 (2021).
- 100. Benech, N., Rolhion, N. & Sokol, H. Tryptophan metabolites get the gut moving. *Cell Host & Microbe* **29**, 145–147 (2021).
- 101. Shah, P. A., Park, C. J., Shaughnessy, M. P. & Cowles, R. A. Serotonin as a Mitogen in the Gastrointestinal Tract: Revisiting a Familiar Molecule in a New Role. *Cellular and Molecular Gastroenterology and Hepatology* **12**, 1093–1104 (2021).
- 102. Beattie, D. T. & Smith, J. A. M. Serotonin pharmacology in the gastrointestinal tract: a review. *Naunyn-Schmied Arch Pharmacol* **377**, 181–203 (2008).
- 103. Wu, L. *et al.* Oral Administration of 5-Hydroxytryptophan Restores Gut Microbiota Dysbiosis in a Mouse Model of Depression. *Frontiers in Microbiology* **13**, (2022).
- 104. Cervenka, I., Agudelo, L. Z. & Ruas, J. L. Kynurenines: Tryptophan's metabolites in exercise, inflammation, and mental health. *Science* **357**, eaaf9794 (2017).
- 105. Madeo, F., Eisenberg, T., Pietrocola, F. & Kroemer, G. Spermidine in health and disease. *Science* **359**, eaan2788 (2018).
- 106. Eisenberg, T. *et al.* Cardioprotection and lifespan extension by the natural polyamine spermidine. *Nat Med* **22**, 1428–1438 (2016).
- 107. He, M. Pipecolic acid in microbes: biosynthetic routes and enzymes. *J IND MICROBIOL BIOTECHNOL* **33**, 401–407 (2006).
- 108. Li, H. *et al.* Protective effect of L-pipecolic acid on constipation in C57BL/6 mice based on gut microbiome and serum metabolomic. *BMC Microbiol* **23**, 144 (2023).
- 109. Ou, Y. *et al.* Lactobacillus casei Strain Shirota Alleviates Constipation in Adults by Increasing the Pipecolinic Acid Level in the Gut. *Front. Microbiol.* **10**, 324 (2019).
- 110. Karetnikova, E. S. *et al.* Is Homoarginine a Protective Cardiovascular Risk Factor? *ATVB* **39**, 869–875 (2019).
- 111. Mokhaneli, M. C. *et al.* Homoarginine and blood pressure: a 10-year prospective relationship in normotensives. *J Hum Hypertens* **36**, 135–143 (2022).
- 112. März, W. *et al.* Homoarginine, Cardiovascular Risk, and Mortality. *Circulation* **122**, 967–975 (2010).
- 113. Wetzel, M. D., Gao, T., Venkatachalam, M., Morris, S. M. & Awad, A. S. L. -Homoarginine supplementation prevents diabetic kidney damage. *Physiol Rep* **7**, (2019).
- 114. Stockebrand, M. *et al.* Homoarginine supplementation improves blood glucose in dietinduced obese mice. *Amino Acids* **47**, 1921–1929 (2015).
- 115. Pieniazek, A., Bernasinska-Slomczewska, J. & Gwozdzinski, L. Uremic Toxins and Their Relation with Oxidative Stress Induced in Patients with CKD. *IJMS* **22**, 6196 (2021).



- 116. Delanghe, S., Delanghe, J. R., Speeckaert, R., Van Biesen, W. & Speeckaert, M. M. Mechanisms and consequences of carbamoylation. *Nat Rev Nephrol* **13**, 580–593 (2017).
- 117. Turunen, S. *et al.* Rheumatoid arthritis antigens homocitrulline and citrulline are generated by local myeloperoxidase and peptidyl arginine deiminases 2, 3 and 4 in rheumatoid nodule and synovial tissue. *Arthritis Res Ther* **18**, 239 (2016).
- 118. Otaru, N. *et al.* GABA Production by Human Intestinal Bacteroides spp.: Prevalence, Regulation, and Role in Acid Stress Tolerance. *Frontiers in Microbiology* **12**, (2021).
- 119. Foster, A. C. & Kemp, J. A. Glutamate- and GABA-based CNS therapeutics. *Current Opinion in Pharmacology* **6**, 7–17 (2006).
- 120. Braun, H.-S., Sponder, G., Pieper, R., Aschenbach, J. R. & Deiner, C. GABA selectively increases mucin-1 expression in isolated pig jejunum. *Genes Nutr* **10**, 47 (2015).
- 121. Kootte, R. S. *et al.* Improvement of Insulin Sensitivity after Lean Donor Feces in Metabolic Syndrome Is Driven by Baseline Intestinal Microbiota Composition. *Cell Metab* **26**, 611-619.e6 (2017).
- 122. Roberts, L. D. *et al.*  $\beta$ -Aminoisobutyric Acid Induces Browning of White Fat and Hepatic  $\beta$ -Oxidation and Is Inversely Correlated with Cardiometabolic Risk Factors. *Cell Metabolism* **19**, 96–108 (2014).
- 123. Tuikhar, N. *et al.* Comparative analysis of the gut microbiota in centenarians and young adults shows a common signature across genotypically non-related populations. *Mechanisms of Ageing and Development* **179**, 23–35 (2019).
- 124. Xu, W., Gao, L., Li, T., Shao, A. & Zhang, J. Neuroprotective Role of Agmatine in Neurological Diseases. *Curr Neuropharmacol* **16**, 1296–1305 (2018).
- 125. Brial, F. *et al.* Human and preclinical studies of the host–gut microbiome co-metabolite hippurate as a marker and mediator of metabolic health. *Gut* **70**, 2105–2114 (2021).
- 126. Tousoulis, D. *et al.* Asymmetric Dimethylarginine: Clinical Significance and Novel Therapeutic Approaches. *CMC* **22**, 2871–2901 (2015).
- 127. Knebel, L. A. *et al.* 2-Methylbutyrylglycine induces lipid oxidative damage and decreases the antioxidant defenses in rat brain. *Brain Research* **1478**, 74–82 (2012).
- 128. Sakko, M. *et al.* 2-Hydroxyisocaproic acid (HICA): a new potential topical antibacterial agent. *International Journal of Antimicrobial Agents* **39**, 539–540 (2012).
- 129. Sakko, M., Tjäderhane, L., Sorsa, T., Hietala, P. & Rautemaa, R. 2-Hydroxyisocaproic acid is bactericidal in human dental root canals ex vivo. *International Endodontic Journal* **50**, 455–463 (2017).
- 130. 2-hydroxyisocaproic acid is fungicidal for Candida and Aspergillus species Sakko 2014 Mycoses Wiley Online Library. https://onlinelibrary.wiley.com/doi/10.1111/myc.12145.
- 131. Nieminen, M. T. *et al.* dl-2-Hydroxyisocaproic Acid Attenuates Inflammatory Responses in a Murine Candida albicans Biofilm Model. *Clinical and Vaccine Immunology* (2014).



- 132. Lang, C. H. *et al.* Chronic α-hydroxyisocaproic acid treatment improves muscle recovery after immobilization-induced atrophy. *American Journal of Physiology-Endocrinology and Metabolism* **305**, E416–E428 (2013).
- 133. Feng, Y. et al. Causal effects of genetically determined metabolites on cancers included lung, breast, ovarian cancer, and glioma: a Mendelian randomization study. Transl Lung Cancer Res 11, 1302–1314 (2022).
- 134. Wei, B. *et al.* Gut microbiota-mediated xanthine metabolism is associated with resistance to high-fat diet-induced obesity. *The Journal of Nutritional Biochemistry* **88**, 108533 (2021).
- 135. Xu, X. *et al.* p-Hydroxybenzoic acid alleviates inflammatory responses and intestinal mucosal damage in DSS-induced colitis by activating ERβ signaling. *Journal of Functional Foods* **87**, 104835 (2021).
- 136. Han, X. *et al.* p-Hydroxybenzoic Acid Ameliorates Colitis by Improving the Mucosal Barrier in a Gut Microbiota-Dependent Manner. *Nutrients* **14**, 5383 (2022).
- 137. Gozdzik, P., Magkos, F., Sledzinski, T. & Mika, A. Monomethyl branched-chain fatty acids: Health effects and biological mechanisms. *Progress in Lipid Research* **90**, 101226 (2023).
- 138. Alvarenga, D. J. *et al.* Natural and Semi-synthetic Licarins: Neolignans with Multi-functional Biological Properties. *Rev. Bras. Farmacogn.* **31**, 257–271 (2021).
- 139. Abourashed, E. A. & El-Alfy, A. T. Chemical diversity and pharmacological significance of the secondary metabolites of nutmeg (Myristica fragrans Houtt.). *Phytochem Rev* **15**, 1035–1056 (2016).
- 140. Maheswari, U., Ghosh, K. & Sadras, S. R. Licarin A induces cell death by activation of autophagy and apoptosis in non-small cell lung cancer cells. *Apoptosis* **23**, 210–225 (2018).
- 141. Liu, T. *et al.* Cephalotaxine Inhibits the Survival of Leukemia Cells by Activating Mitochondrial Apoptosis Pathway and Inhibiting Autophagy Flow. *Molecules* **26**, 2996 (2021).
- 142. Chen, P., Li, Y., Zhou, Z., Pan, C. & Zeng, L. Lathyrol promotes ER stress-induced apoptosis and proliferation inhibition in lung cancer cells by targeting SERCA2. *Biomedicine & Pharmacotherapy* **158**, 114123 (2023).
- 143. Levan, S. R. *et al.* Elevated faecal 12,13-diHOME concentration in neonates at high risk for asthma is produced by gut bacteria and impedes immune tolerance. *Nat Microbiol* **4**, 1851–1861 (2019).
- 144. Lynes, M. D. *et al.* The cold-induced lipokine 12,13-diHOME promotes fatty acid transport into brown adipose tissue. *Nat Med* 23, 631–637 (2017).
- 145. Stanford, K. I. *et al.* 12,13-diHOME: An Exercise-Induced Lipokine that Increases Skeletal Muscle Fatty Acid Uptake. *Cell Metabolism* 27, 1111-1120.e3 (2018).
- 146. Macêdo, A. P. A., Muñoz, V. R., Cintra, D. E. & Pauli, J. R. 12,13-diHOME as a new therapeutic target for metabolic diseases. *Life Sciences* **290**, 120229 (2022).
- 147. Chelakkot, C., Ghim, J. & Ryu, S. H. Mechanisms regulating intestinal barrier integrity and its pathological implications. *Exp Mol Med* **50**, 1–9 (2018).



- 148. Sanchez-Muñoz, F., Dominguez-Lopez, A. & Yamamoto-Furusho, J. K. Role of cytokines in inflammatory bowel disease. *World J Gastroenterol* **14**, 4280–4288 (2008).
- 149. Friedrich, M., Pohin, M. & Powrie, F. Cytokine Networks in the Pathophysiology of Inflammatory Bowel Disease. *Immunity* **50**, 992–1006 (2019).
- 150. Zielinski, C. E. *et al.* Pathogen-induced human TH17 cells produce IFN-γ or IL-10 and are regulated by IL-1β. *Nature* **484**, 514–518 (2012).
- 151. Coccia, M. *et al.* IL-1β mediates chronic intestinal inflammation by promoting the accumulation of IL-17A secreting innate lymphoid cells and CD4+ Th17 cells. *Journal of Experimental Medicine* **209**, 1595–1609 (2012).
- 152. Vazirinejad, R., Ahmadi, Z., Arababadi, M. K., Hassanshahi, G. & Kennedy, D. The Biological Functions, Structure and Sources of CXCL10 and Its Outstanding Part in the Pathophysiology of Multiple Sclerosis. *NIM* **21**, 322–330 (2014).
- 153. Lee, S. H., Kwon, J. E. & Cho, M.-L. Immunological pathogenesis of inflammatory bowel disease. *Intest Res* **16**, 26–42 (2018).
- 154. Liu, T., Zhang, L., Joo, D. & Sun, S.-C. NF-κB signaling in inflammation. *Sig Transduct Target Ther* **2**, 17023 (2017).
- 155. Kalantar-Zadeh, K., Berean, K. J., Burgell, R. E., Muir, J. G. & Gibson, P. R. Intestinal gases: influence on gut disorders and the role of dietary manipulations. *Nat Rev Gastroenterol Hepatol* **16**, 733–747 (2019).
- 156. Konopelski, P. & Mogilnicka, I. Biological Effects of Indole-3-Propionic Acid, a Gut Microbiota-Derived Metabolite, and Its Precursor Tryptophan in Mammals' Health and Disease. *IJMS* **23**, 1222 (2022).
- 157. Rinninella, E. *et al.* What is the Healthy Gut Microbiota Composition? A Changing Ecosystem across Age, Environment, Diet, and Diseases. *Microorganisms* **7**, 14 (2019).
- 158. Vandeputte, D. *et al.* Quantitative microbiome profiling links gut community variation to microbial load. *Nature* **551**, 507–511 (2017).
- 159. Van den Abbeele, P. et al. Bridging preclinical and clinical gut microbiota research using the ex vivo SIFR® technology. Frontiers Microbiol 14, (2023).
- 160. Hughes, J. B., Hellmann, J. J., Ricketts, T. H. & Bohannan, B. J. M. Counting the Uncountable: Statistical Approaches to Estimating Microbial Diversity. *Applied and Environmental Microbiology* **67**, 4399–4406 (2001).



# 10 Appendix

# 10.1 Supplementary files

**Supplementary File 1.** The absolute abundances (cells/mL) of the most abundant bacterial families in the dataset

**Supplementary File 2.** The absolute abundances (cells/mL) of the most abundant species in the dataset.

**Supplementary File 3** – Absolute levels (peak area) of the significantly affected metabolites



## 10.2 New diversity score: community modulation score (CMS)

#### 10.2.1 Diversity indices: problem statement

When assessing the impact of interventions on the gut microbiota,  $\alpha$ -diversity indices are often used to obtain insights into community structure <sup>157</sup>. Results of diversity indices should however be interpreted with caution. First,  $\alpha$ -diversity indices can be based on **species richness** [e.g., observed number of species/OTUs and the Chao1 diversity index] **and/or evenness** [e.g., reciprocal Simpson diversity and Shannon diversity index], **two fundamentally different concepts**:

- Species richness = higher as more taxa are present
- **Evenness** = higher as the dominant microbes are more evenly distributed (e.g. when dominant microbes are present at similar levels = high index value <-> when specific microbes are highly abundant = low index value)
  - → Results obtained with one index cannot necessarily be compared with another index!!

Further, while **differences in cell density** among microbial samples is **key to obtain accurate insights into the gut microbiota** (both *in vivo* <sup>158</sup> and *ex vivo* <sup>159</sup>), current diversity indices largely ignore such differences<sup>15</sup>. The resulting inaccuracy is illustrated for two main scenarios (Figure 30):

- Prebiotics that increase cell density (~ larger community circle area in Figure 30)
- Antibiotics that lower cell density (~ smaller community circle area in Figure 30)

Given the **similar sequencing depth among samples** (illustrated by similar area of analysed community fractions in Figure 30, <sup>(2)</sup>), when products modulate cell density, they alter proportional sampling depth impact, and cause **inaccurate insights into microbial diversity**:

- Prebiotic lowers proportional sequencing depth → underestimation of diversity
- Antibiotic increases proportional sequencing depth → overestimation of diversity

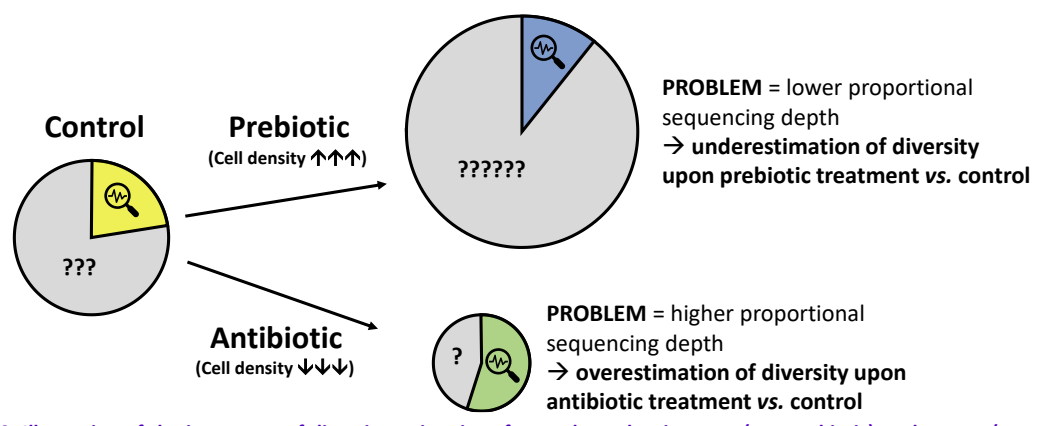


Figure 30. Illustration of the inaccuracy of diversity estimations for products that increase (e.g. prebiotic) or decrease (e.g. antibiotic) total cell density of the gut microbiome

Summary: moving away from relative composition analysis towards quantitative taxonomic analysis exposes limitations of traditional  $\alpha$ -diversity indices. Variations in cell density are often overlooked, leading to an underestimated diversity in high-biomass samples.

<sup>&</sup>lt;sup>15</sup> To deal with the resulting inaccuracy, the Chao1 diversity index for instance attempts to estimate the number of missing species, and thus "count the uncountable" <sup>160</sup>.



### 10.2.2 CMS: towards more accurate diversity estimations

Cryptobiotix recently introduced a new diversity index, the Community Modulation Score (CMS), which better captures the impact on diversity of test products that impact cell density<sup>61</sup>. The CMS, rooted in quantitative sequencing, reflects the number of gut microbes that is supported (positive CMS (CMS+)) or suppressed (negative CMS (CMS-)) upon treatment. The sum of both values (overall CMS) reflects the nett number of species that increasingly grew upon treatment:

- CMS > 0 → product increased overall diversity
- CMS < 0 → product lowered overall diversity</li>

Upon its introduction, Tintoré *et al.* (2024)<sup>61</sup> demonstrated the potential of this new approach to discriminate between prebiotics. First, both the **positive CMS** and **negative CMS** were **higher** for **dextran** compared to inulin (IN), suggesting that more species are stimulated/less species are inhibited for dextran compared to inulin. As a result, the **combined CMS was positive for dextran** (average = 13.8) and **negative for inulin** (average = -12.7). In other words, inulin specifically increased a limited number of species that outcompeted a larger number of other gut microbes.

### → Dextran increased microbial diversity, while inulin decreased microbial diversity

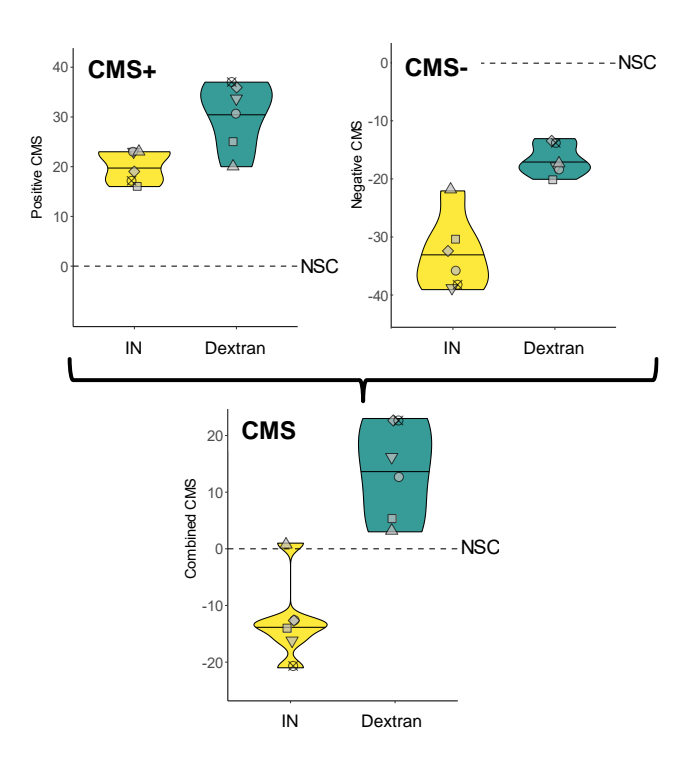


Figure 31. Dextran supported a high microbial diversity of the human adult gut microbiota *ex vivo*. The impact of dextran and IN on the novel community modulation scores (CMS), presented as a positive (increased OTUs), negative (decreased OTUs) and combined score.



# 10.3 Supplementary Tables

Table 4. List of level 1/2a metabolites identified in the metabolomics analysis; Level 1: identification by retention times (compare d against in-house authentic standards), accurate mass (accepted deviation of 3ppm), and MS/MS spectra, Level 2a: identification by retention times (compared against in-house authentic standards), accurate mass (accepted deviation of 3ppm).

Compound class	Compound name	Annotation level
Acylated amino acid	N-Acetylarginine	1
Acylated amino acid	N-Acetylleucine	1
Acylated amino acid	N-Acetylmethionine	1
Acylated amino acid	N-Acetylphenylalanine	1
Acylated amino acid	N-Acetyltryptophan	1
Acylated amino acid	N-Isovalerylglycine	1
Acylated amino acid	N6-Acetyllysine	1
Acylated amino acid	O-Acetylserine	1
Acylated amino acid	N-Acetyl-DL-methionine	2a
Acylated amino acid	N-AcetylProline	2a
Acylated amino acid	N-Acetylalanine	2a
Acylated amino acid	N-Acetylasparagine	2a
Acylated amino acid	N-Acetylglutamine	2a
Acylated amino acid	N-Acetylhistidine	2a
Acylated amino acid	N-Acetylornithine	2a
Acylated amino acid	N-Acetylserine	2a
Acylated amino acid	N-Acetyltyrosine	2a
Acylated amino acid	N2-Acetyllysine	2a
Amino acid	Isoleucine	1
Amino acid	Leucine	1
Amino acid	Lysine	1
Amino acid	Methionine	1
Amino acid	Phenylalanine	1
Amino acid	Tryptophan	1
Amino acid	Valine	1
Amino acid	Aspartic acid	2a
Amino acid	Proline	2a
Amino acid-related	2-Hydroxy-3-methylbutyric acid	1
Amino acid-related	4-Guanidinobutyric acid	1
Amino acid-related	Acetylagmatine	1
Amino acid-related	Asymmetric dimethylarginine	1
Amino acid-related	Carnosine	1
Amino acid-related	Cyclo(L-Phe-L-Pro)	1
Amino acid-related	Cyclo(Tyr-Leu)	1
Amino acid-related	Cyclo-(Pro-Gly)	1
Amino acid-related	Glutaric acid	1
Amino acid-related	Glycylleucine	1
Amino acid-related	Indole-3-acetic acid	1
Amino acid-related	Indole-3-propionic acid	1
Amino acid-related	Leucylalanine	1
Amino acid-related	N-(5-Aminopentyl)acetamide	1
Amino acid-related	N8-Acetylspermidine	1
	2-Hydroxybutyric acid/ 3-Hydroxybutyric acid/ β-	
Amino acid-related	hydroxyisobutyric acid	2a
	2-Hydroxyphenylacetic acid/ 3-Hydroxyphenylacetic	
Amino acid-related	acid	2a
Amino acid-related	2-Methylbutyrylglycine	2a
Amino acid-related	2-Methylhippuric acid	2a
Amino acid-related	3-(2-Hydroxyethyl)indole	2a



Amino acid-related	3-Aminoisobutanoic acid/ γ-Aminobutyric acid	2a
Amino acid-related	5-Hydroxytryptophan	2a
Amino acid-related	5-Hydroxytryptophol	2a
Amino acid-related	5-Methoxytryptophan	2a
Amino acid-related	5-Methyltryptophan	2a
Amino acid-related	Creatine	2a
Amino acid-related	Creatinine	2a
Amino acid-related	Diaminopimelic acid	2a
	Ethyl 3-hydroxybutyrate/ 2-Hydroxyisocaproic acid/	
Amino acid-related	2-Ethyl-2-hydroxybutyric acid	2a
Amino acid-related	Glycylvaline 	2a
Amino acid-related	Homoarginine	2a
Amino acid-related	Homocitrulline	2a
Amino acid-related	Indole	2a
Amino acid-related	Kynurenine	2a
Amino acid-related	Kyotorphine	2a
Amino acid-related	Methylguanidine	2a
Amino acid-related	N-Acetylputrescine hydrochloride	2a
Amino acid-related	N-Methyltyramine	2a
Amino acid-related	Norleucine	2a
Amino acid-related	Phenylacetic acid	2a
Amino acid-related	Phenylacetylglutamine	2a
Amino acid-related	Phenylalanylphenylalanine	2a
Amino acid-related	Pipecolinic acid	2a
Amino acid-related	Pyroglutamic acid	2a
Amino acid-related	Stachydrine	2a
Amino acid-related	Tryptamine	2a
Amino acid-related	Valylglycine	2a
Amino acid-related	Phenyllactic acid	2a
Amino acid-related	p-Hydroxyphenyllactic acid	2a
Bile acid	Glycocholic acid	2a
Bile acid	Taurocholic acid	2a
Glycolysis/TCA	Hexose trimer	2a
Glycolysis/TCA	Isocitric acid	2a
Nucleic acid(-related)	7-Methylguanine	1
Nucleic acid(-related)	Cytidine	1
Nucleic acid(-related)	Inosine	1
Nucleic acid(-related)	3-Ureidopropionic acid	2a
Nucleic acid(-related)	5,6-Dihydrothymine	2a
Nucleic acid(-related)	5-Methylcytosine	2a
Nucleic acid(-related)	Adenine	2a
Nucleic acid(-related)	Guanine	2a
Nucleic acid(-related)	Theophylline	2a
Nucleic acid(-related)	Xanthine	2a
Other	Betaine	1
Other	Choline	1
Other	Crotonoside	1
Other	Maculosin	1
Other	N-Acetylgalactosamine	1
Other	Trimethylamine N-Oxide	1
Other	Urobilin	1
Other	12,13-DHOME	2a
Other	2-Deoxyglucose	2a
Other	2-Methylbutyric acid/ 3-Methylbutanoic acid	2a
Other	3-Hydroxy-2-methyl-4-pyrone	<b>2</b> a
Other	4-Hydroxybenzoic acid	2a



Other	7beta-Hydroxylathyrol	<b>2</b> a
Other	Allopurinol	2a
Other	Artemisinine	2a
Other	Butylated hydroxyanisole	2a
Other	Carnitine	2a
Other	Cephalotaxine	2a
Other	Dihydroartemisinin	2a
Other	Dihydrocoumarin	2a
Other	Ergolide	2a
Other	Gigantol	2a
Other	Hexamethylene bisacetamide	2a
Other	Hydroquinidine	2a
Other	Lathyrol	2a
Other	Licarin A/ Dehydrodiisoeugenol	2a
Other	Metformin	2a
Other	Prostaglandin E2	2a
Other	Quinine	2a
Other	Rhodojaponin III	2a
Other	Traumatic acid	2a
Other	Wighteone	2a
Other	alpha-Asarone	2a
Other	cis-Aconitic acid	2a
Other	α-Solanine	2a
Vitamin	Biotin	1
Vitamin	Pantothenic acid	1
Vitamin	Nicotine amide	2a
Vitamin	Nicotinic acid	2a
Vitamin	Pyridoxamine	2a
Vitamin	Thiamine	2a
Vitamin	Trigonelline	2a



# 10.4 Supplementary Figures

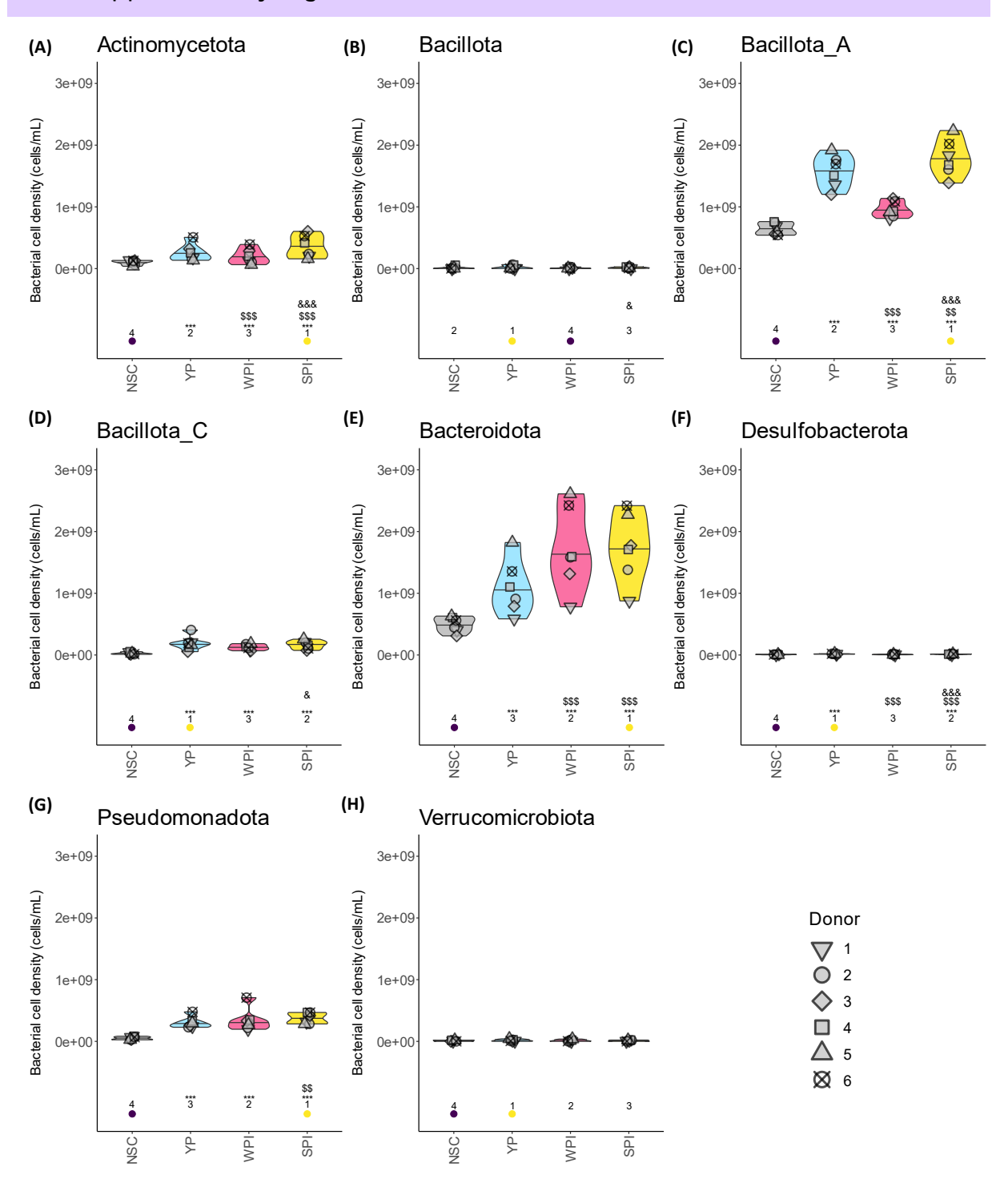


Figure 32. (1/2) The impact of the test products on the most abundant phyla in the microbiota of human adults (n=6), compared to a no-substrate control (NSC). Statistical differences between NSC and the individual treatments are visualized via \* (0.1 <  $p_{adjusted} < 0.2$ ), \*\* (0.05 <  $p_{adjusted} < 0.1$ ) or \*\*\* ( $p_{adjusted} < 0.05$ ). Significant differences between WPI/SPI vs. YP are indicated via \$/\$\$/\$\$, and between SPI vs. WPI via &/&&/&&. The rank of the average values per treatment are indicated at the bottom of the figure, with the lowest average being indicated purple, and the highest value in yellow.



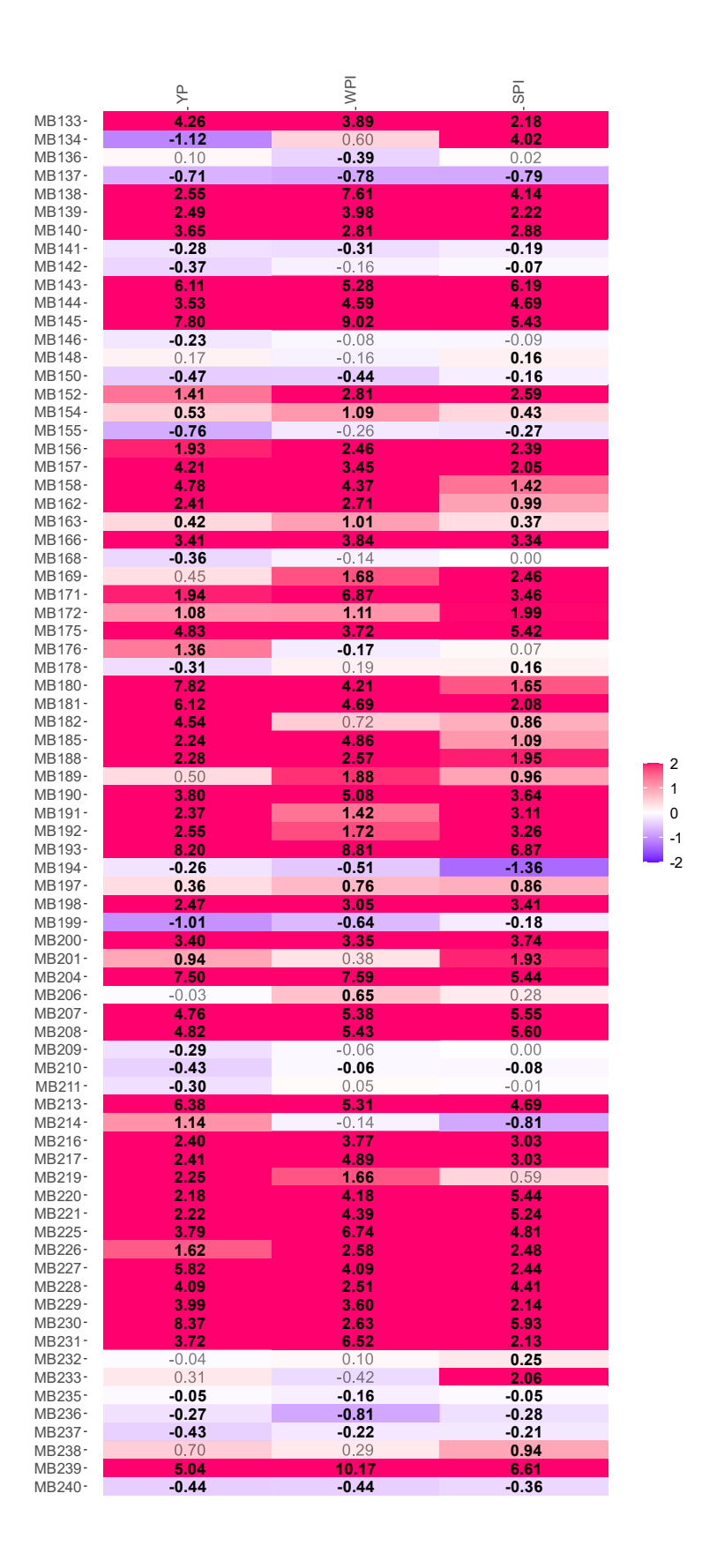


Figure 33. The impact of all test products compared to a no substrate control (NSC) on <u>metabolites annotated at level 2b</u> as quantified via untargeted LC-MS after 24h of incubation, tested via the SIFR® technology for <u>human adults (n = 6)</u>, expressed as <u>the log2 transformation of the geometric mean of treatment/NSC or NSC\* ratios.</u> The metabolites were <u>significantly affected</u> by any of the treatments (FDR = 0.20), indicated in bold.



Supplementary Table for Figure 33. Full name of the compounds in the figure.

Identifier	Suggested compound name
MB133	(2S,5aS,8aR)-2-[3-(4-Hydroxy-1-piperidinyl)-3-oxopropyl]-1-methyl-6-[4- (trifluoromethyl)benzyl]octahydropyrrolo[3,2-E][1,4]diazepin-5(2H)-one
MB134	(±)13-HpODE
MB136	1,3,7-trimethyl-2,3,6,7-tetrahydro-1H-purine-2,6-dione
MB137	1,3-diazaspiro[4.5]decane-2,4-dione
MB138	1,5-Naphthalenediamine
MB139	1,5-dimethyl-N-(4-morpholinobenzyl)-1H-pyrazole-3-carboxamide
MB140	1,7-Dimethyluric acid
MB141	1-(3,4-dimethoxyphenyl)ethan-1-one oxime
MB142	1-(3,4-dimethoxyphenyl)ethan-1-one oxime
MB143	1-Methylhistidine
MB144	1-Vinylimidazole
MB145	2-(2-amino-3-methylbutanamido)-3-phenylpropanoic acid
MB146	2-(cyclopropylcarbonyl)-3-(methylthio)-3-morpholinoacrylonitrile
MB148	2-[4-(3-Amino-2-hydroxypropoxy)phenyl]acetamide
MB150	2-phenyl[1,3]oxazolo[5,4-d]pyrimidin-7-amine
MB152	3,3',5,5'-Tetramethyldiphenoquinone
MB154	3-(1-hydroxyethyl)-2,3,6,7,8,8a-hexahydropyrrolo[1,2-a]pyrazine-1,4-dione
MB155	3-(propan-2-yl)-octahydropyrrolo[1,2-a]pyrazine-1,4-dione
MB156	3-Methylcrotonylglycine
MB157	3-Morpholino-4-tetrahydro-1H-pyrrol-1-ylcyclobut-3-ene-1,2-dione
MB158	3-Morpholino-4-tetrahydro-1H-pyrrol-1-ylcyclobut-3-ene-1,2-dione
MB162	3-ethyl-4-hydroxy-1-methyl-1,2-dihydroquinolin-2-one
MB163	3-hydroxyquinuclidine-3-carbonitrile hydrochloride
MB166	4-Coumaric acid
MB168	5-amino-2-(dimethylamino)benzoic acid
MB169	6-Methyl[1,2,4]triazolo[4,3-b]pyridazin-8-ol
MB171	8-HYDROXYQUINOLINE
MB172	Acetophenone
MB175	Caprolactam
MB176	Carbendazim
MB178	Cyclo(leucylprolyl)
MB180	DLK
MB181	DLK DLK
MB182 MB185	ILK
MB188	
MB189	Isoamylamine Isoquinoline
	·
MB190	LPK
MB191	Lauramidopropyl betaine
MB192	Lauramidopropyl betaine
MB193	Leucylproline  Mathylimida a la sastia a sid
MB194	Methylimidazoleacetic acid
MB197	N-(5-acetamidopentyl)acetamide
MB198	N-Acetylhistamine
MB199	N-Acetyltyramine
MB200	N-Methylcaprolactam
MB201	N-[2-(1,5-dimethyl-4-nitro-1H-pyrazol-3-yl)vinyl]-N,N-dimethylamine
MB204	NP-016455
MB206	NP-021074
MB207	Nikethamide 1-oxide
MB208	PD 0200347



MB210	PEG n7
MB211	PEG n8
MB213	PPK
MB214	Pilocarpine
MB216	Piperidine
MB217	Piperidine
MB219	Prolinamide
MB220	Prolylleucine
MB221	Prolylleucine
MB225	Tiglic acid
MB226	Tiglic acid
MB227	Tolycaine
MB228	Tropine
MB229	VLH
MB230	VLK
MB231	VLK
MB232	Valsartan
MB233	Valylproline
MB235	[5-(2-thienyl)-3-isoxazolyl]methanol
MB236	[5-(2-thienyl)-3-isoxazolyl]methanol
MB237	ethyl 3-amino-4-(methylamino)benzoate
MB239	trans-3-Indoleacrylic acid
MB240	trans-Zeatin
•	<u> </u>



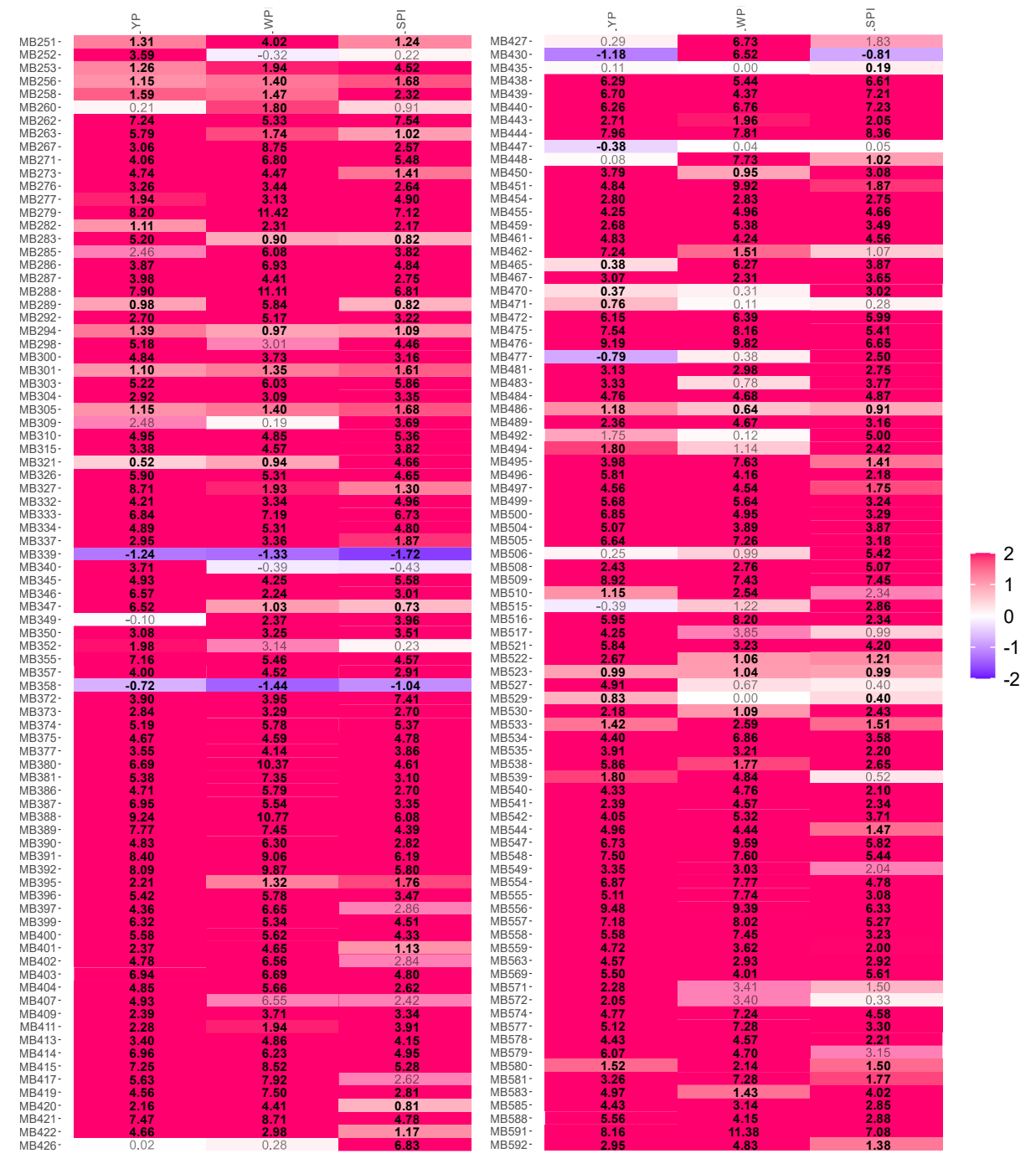


Figure 34. The impact of all test products compared to a no substrate control (NSC) on <u>metabolites annotated at level 3</u> as quantified via untargeted LC-MS after 24h of incubation, tested via the SIFR® technology for <u>human adults (n = 6)</u>, expressed as <u>the log2 transformation of the geometric mean of treatment/NSC or NSC\* ratios.</u> The metabolites were <u>significantly affected</u> by any of the treatments (FDR = 0.20), indicated in bold.



Supplementary Table for Figure 34. Full name of the compounds in the figure.

Identifier	Suggested compound name
MB241	(+)-Mometasone
MB246	(2S,3R,4E)-2-[(17Z)-17-Hexacosenoylamino]-3-hydroxy-4-icosen-1-yl dihydrogen phosphate
MB247	(3R,4S,5S,6S)-6-Carboxy-N-[2-(diphenylmethoxy)ethyl]-3,4,5-trihydroxy-N,N-dimethyltetrahydro-2H-
WID247	pyran-2-aminium (non-preferred name)
MB248	(3Z,6Z,9Z,12Z,21R)-27-Amino-24-hydroxy-24-oxido-18-oxo-19,23,25-trioxa-24lambda~5~- phosphaheptacosa-3,6,9,12-tetraen-21-yl (4Z,7Z,10Z,13Z,16Z,19Z)-4,7,10,13,16,19-docosahexaenoate
MB251	(4R)-O~15~-Acetyl-4-(alpha-L-talopyranuronosyloxy)retinol
MB252	(5E)-2,10-Diamino-5-{[(5-amino-5-carboxypentyl)amino]methyl}-5-undecenedioic acid (non-preferred name)
MB253	(6alpha,8xi,11beta,14xi,16alpha,17alpha)-6,9-Difluoro-11,17-dihydroxy-16-methyl-3-oxoandrosta-1,4- diene-17-carboxylic acid
MB256	(±)-Equol
MB258	1-Methyl-1,2,3,4-tetrahydro-β-carboline-3-carboxylic acid
MB260	1-Methyladenine
MB261	1-Methylimidazoleacetic acid
MB262	1-[(4E)-4-(4-Methyl-5-oxo-2(5H)-furanylidene)butyl]-2-pyrrolidinone
MB263	11-beta-Hydroxyandrosterone-3-glucuronide
MB267	2,3,8,9-Tetrahydroxybenzo[b][1]benzofuro[2,3-f][1]benzofuran-6,12-dione
MB270	2-(2-Carboxyethyl)-4-methyl-5-pentyl-3-furoic acid
MB271	2-(3,4-Dimethoxyphenyl)-5,6,7,8-tetramethoxy-2,3-dihydro-4H-chromen-4-one
MB273	2-Acetamidohexanedioic acid
MB276	2-Ethyl-4,5-dimethylthiazole
MB277	2-Hexenoylcarnitine
MB279	2-Methylthiazolidine
MB281	2-Pyrrolidone
MB282	2-[(2E)-3,7-Dimethyl-2,6-octadien-1-yl]-5-hydroxy-6-methoxy-3-methyl-1,4-benzoquinone
MB283	2-{(E)-2-[3,5-Dihydroxy-4-(3-methyl-2-buten-1-yl)phenyl]vinyl}-5-hydroxyphenyl hexopyranosiduronic
MB284	3,4a,5-Trimethyl-6-{[(2E)-3-(methylsulfanyl)-2-propenoyl]oxy}-4,4a,5,6,7,8,8a,9-octahydronaphtho[2,3-b]furan-4-yl (2E)-2-methyl-2-butenoate
MB285	3-(Sulfooxy)-L-tyrosine
MB286	3-(Sulfooxy)-L-tyrosine
MB287	3-Benzyl-6-isobutyl-2,5-piperazinedione
MB288	3-Methylsulfolene
MB289	3-O-{[(3S,3aS,10E,11aS)-3,10-Dimethyl-2-oxo-2,3,3a,4,5,8,9,11a-octahydrocyclodeca[b]furan-6- yl]carbonyl}-beta-D-glucopyranose
MB290	3-hydroxy-3-methyloxindole
MB291	4-(METHYLNITROSAMINO)-1-(3-PYRIDYL-N-OXIDE)-1-BUTANOL
MB292	4-Amino-1-piperidinecarboxylic acid
MB294	4-Hydroxyprolylleucine
MB298	5-Hydroxy-DL-tryptophan
MB300	6,7-Dihydro-7-methyl-5H-benzo[g]-1,3-benzodioxolo[6,5,4-de]quinoline
MB301	6,7-Dimethoxy-3-(2-methyl-3-buten-2-yl)-2H-chromen-2-one
MB302	8-Amino-7-oxononanoic acid
MB303	8-Amino-7-oxononanoic acid
MB304	8-Azabicyclo[3.2.1]octan-3-ol
MB305	8-[(3,3-Dimethyl-2-oxiranyl)methyl]-7-methoxy-2H-chromen-2-one
MB309	Acetohydroxamic acid
MB310	Acetyl benzoyl
MB315	Aminocaproic acid
MB320	Arg-pro
MB321	Arg-pro
MB326	Aspartame
MB327	Biocytin
MB332	Carbofuran
אככטואו	Calputuali



MB333	Chromone
MB334	Coumarone
MB335	D-Tyrosyl-L-alloisoleucyl-D-leucine
MB337	DL-Alanylglycine
MB339	Dambonitol
MB340	Deanol
MB345	FB9500000
MB346	FC6D57000M
MB347	Fluocinolone Acetonide
MB349	GLYCERYL 2-PENTADECANOATE
MB350	GW7340000
MB352	Glu-Gly
MB355	Gly-DL-Phe
MB357	Glycyl-L-asparaginyl-D-leucine
MB358	Guanadrel
MB359	Guanadrel
MB367	Homoanserine
MB369	Hostmaniane
MB372	Isoniazid alpha-ketoglutaric acid
MB373	Isopelletierine
MB374	Isopelletierine
MB375	Isophorone
MB376	Kahweofuran
MB377	L-Alloisoleucine
MB380	L-gamma-Glutamyl-L-leucine
MB381	L-gamma-Glutamyl-L-leucine
MB384	L-gamma-Glutamyl-L-valine
MB386	L-gamma-Glutamyl-L-valine
MB387	L-gamma-Glutamyl-L-valine
MB388	Leu-Leu
MB389	Leu-Leu
MB390	Leu-Leu
MB391	Leu-Val
MB392	Leu-Val
MB395	Leu-pro
MB396	Leucylasparagine
MB397	Leucylasparagine
MB399	Leucylasparagine
MB400	Leucylasparagine
MB401	Leucylglycine
MB402	Leucylglycine
MB403	Leucylglycine
MB404	Leucyltryptophan
MB407	Leucyltyrosine
MB409	Lysylvaline
MB410	MEGX
MB411	MFCD00025555
MB412	MFCD00025555
MB413	MFCD00025555
MB414	MFCD00025555
MB415	MFCD00025555
MB417	MFCD02728197
MB419	Marimastat
MB420	Marimastat
MB421	Methionylleucine



MB422	Methionylphenylalanine
MB424	Methylol Dimethylhydantoin
MB426	Midodrine
<b>MB427</b>	N(2)-succinyl-L-ornithine
VIB430	N,N-Dimethylisoleucyl-N-[(10Z)-7-benzyl-5,8-dioxo-3-phenyl-2-oxa-6,9-diazabicyclo[10.2.2]hexadeca-1(14),10,12,15-tetraen-4-yl]prolinamide
MB434	N-(Carboxymethyl)norleucine
<b>MB435</b>	N-Acetylvaline
ИВ436	N-Benzoylaspartic acid
<b>∕</b> 1B438	N-Nonanoylglycine
ИВ439	N-Pentanoylphenylalanine
MB440	N-Propionylmethionine
<b>MB443</b>	N-formylkynurenine
<b>VIB444</b>	N-{3-[(4-Acetamidobutyl)amino]propyl}acetamide
MB446	Nalpha-{(2R)-2-Benzyl-3-[(2-methyl-2-propanyl)sulfonyl]propanoyl}-N-[(2R,3S,4R)-1-cyclohexyl-4- cyclopropyl-3,4-dihydroxy-2-butanyl]-L-histidinamide
MB447	Netilmicin
MB448	Niflumic acid
ИВ449	Nirvanol
MB450	N~6~,N~6~-Dimethyllysine
MB451	Oglufanide
MB454	Penicillamine
MB455	Penicillamine
MB459	Piperidine
MB461	Pro-tyr
MB462	Procaine
MB464	Prolylvaline
MB465	Pyridinoline
MB467	Pyrrolidine
MB468	Pyrrolidine
MB469	Rivastigmine
MB470 MB471	S-Propylcysteine
MB471 MB472	SL4506500
	Salicylaldehyde
MB475	Spermic acid Spermic acid
MB476 MB477	Stearidonic acid
VIB477 VIB478	Steamdonic acid Styrene
VIB478 VIB480	T00110000
VIB480 VIB481	T00127900
VIB481 VIB482	T00127900
VIB482 VIB483	T00127900
VIB483 VIB484	T00127900
VIB484 VIB486	Tetraacetylethylenediamine
VIB480 VIB489	Tetrahydrofuran
VIB483 VIB492	Tolbutamide
VIB492 VIB494	Toluene
MB495	Tryptophyl-tyrosine
VIB493 VIB496	Tyr-Phe
VIB490 VIB497	Tyrosyltyrosine
VIB497 VIB499	Val-Met
VIB499 VIB500	Val-Met
MB504	Val-Net Val-Ser
MB505	Val-Trp
MB506	Valyl-4-hydroxyproline
MB508	Valyl-4-hydroxyproline



MB509	Valylvaline
MB510	Verimol F
MB512	Zalcitabine
MB515	[1-(5-phosphoribosyl)imidazol-4-yl]acetic acid
MB516	ala-met
MB517	ala-ser
MB518	alliin
MB520	asn-phe
MB521	asn-phe
MB522	asn-pro
MB523	asn-pro
MB526	bacimethrin
MB527	balenine
MB528	benzylsuccinic acid
MB529	butalbital
MB530	butalbital
MB533	entecavir
MB534	epsilon-(gamma-Glutamyl)-lysine
MB535	felbamate
MB538	gamma-Glutamyl-N~5~-acetylornithine
MB539	gamma-Glutamyl-N°5~-acetylornithine
MB540	gamma-L-glutamyl-L-tyrosine
MB541	gancaonin G
MB542	gln-ser
MB544	gln-trp
MB545	glu-thr
MB547	leu-gin
MB548	leu-gin
MB549	leu-gin
MB554	meprobamate
MB555	meprobamate
MB556	meprobamate
MB557	meprobamate
	· · · · · · · · · · · · · · · · · · ·
MB558	met-thr
MB559	met-tyr
MB561	methylxanthine
MB563	phe-gln 
MB566	prilocaine 
MB569	procainamide
MB571	pyr-gln-OH
MB572	pyroglutamylglycine
MB574	tert-Butyl 3-amino-1-methyl-2,3-dioxopropylcarbamate
MB575	thiodiglycol
MB577	thr-trp
MB578	threonylphenylalanine
MB579	threonylphenylalanine
MB580	tolnaftate
MB581	trp-lys
MB583	trp-pro
MB585	trp-ser
MB588	tyr-thr
MB589	tyramine sulfate
MB591	vinyl sulfide
	{4-[(1E)-4-Chloro-1,2-diphenyl-1-buten-1-yl]phenoxy}acetaldehyde